DEVELOPMENT OF SOME NOVEL APPLICATIONS OF ULTRASONIC AND CAPACITIVE TECHNIQUES IN THE FIELD OF INSTRUMENTATION

THESIS

SUBMITTED IN PARTIAL FULFILMENT OF THE REQUIREMENTS
FOR THE AWARD OF THE DEGREE OF

Doctor of Philosophy

IN

Electronics Engineering

BY

EISA BASHIER MOHAMMED

Under the Supervision of

PROF. MAHFOOZUR REHMAN

DEPARTMENT OF ELECTRONICS ENGINEERING
Z. H. COLLEGE OF ENGINEERING & TECHNOLOGY
ALIGARH MUSLIM UNIVERSITY
ALIGARH (INDIA)

2003

Professor Mahfoozur Rehman
BSc Engg, MSc Engg, PhD (IIT-M), FIETE,
Principal Investgator,
CSIR Project, AICTE Project
Head of Instrumentation and Control Group

Tel: (O) +91 0571 701845
(R)+91 0571 700729
e-mail: mahfoozur_rehman@hotmail.com

DEPARTMENT OF ELECTRONICS ENGINEERING

Z. H. College of Engineering and Technology
Aligarh Muslim University, Aligarh-202002

Date: 22nd April 2003

CERTIFICATE

Certified that this work entitled "**DEVELOPMENT OF SOME NOVEL APPLICATIONS OF ULTRASONIC AND CAPACITIVE TECHNIQUES IN THE FIELD OF INSTRUMENTATION**" which is being submitted by Mr. EISA BASHIER MOHAMMED, in partial fulfillment of the requirements for the award of the degree of doctor of Philosophy in Electronics Engineering from Aligarh Muslim University, Aligarh - India. This is a record of candidate's own work under my supervision and guidance. The matter embodied in this thesis has not been submitted for the award of any other degree or diploma.

(Prof. Mahfoozur Rehman)

ACKNOWLEDGEMENTS

I am very much indebted and have great pleasure in expressing my deep sense of gratitude to my supervisor Prof. Mahfoozur Rehman Department of Electronics Engineering, Aligarh Muslim University, Aligarh, for his creative ideas, instructive guidance, expert advise and sparing his time. Without him, this work would have not been completed. He was always at hand for his valuable suggestions, stimulating discussions and critical evaluations of theories and results. He provided the necessary facilities for conducting the experimental work smoothly. Indeed, he has been a constant source of inspiration throughout this work. For this and much more, I am deeply grateful to him.

I record my sincere thanks to Prof. V. G. K. Murti for his valuable comments, assessments and help in beautifying some of the applications.

I utilize this opportunity to thank the University Grants Commission UGC-India for their support in the form of awarding a Junior Research Fellowship (JRF), the authorities of Sudan University of Science & Technology, Sudan and Electronics Engineering Department, Aligarh Muslim University for the facilities provided for carrying out the research work reported in this thesis.

Last but not the least, I would like to express my gratitude to my parents and loving family members, for their support and encouragement not only during this work but throughout my carrier. Great thanks for my wife, Mss. Ehssan, for her endurance, patience and preparation of special environment throughout the period of the research work.

6.5.03

(Eisa Bashier Mohammed)

CONTENTS

Page No.

ABSTRACT

DEVELOPMENT OF SOME NOVEL APPLICATIONS OF ULTRASONIC AND CAPACITIVE TECHNIQUES IN THE FIELD OF INSTRUMENTATION

This thesis presents development of some novel applications in the field of electronic instrumentation. It is broadly divided into two major sections, the first section treats in details some selected applications of capacitive techniques while the second covers some of the ultrasonic techniques.

A capacitive angular-position sensor has been developed which is capable of covering the complete 360° angle. It is based on four quadrants of parallel plate capacitors, which are having common lower potential plate. A grounded semi-circular plate, whose angular position is to be measured, moves in between the plates of these capacitors. The shape of the plates has been designed, based on intensive simulation, to achieve linear relationship, which has been done in the light of rigorous experimentation. The phase of the output voltage is then measured digitally and it is found to be linear in relation to the angular-position of the semi-circular plate. The electronic circuit used is simple and is prepared at low cost.

Second application deals with the design and realization of a novel high-performance capacitive rotation-speed transducer. The transducer mainly consists of two equal parallel plate

capacitors, which are connected in an active bridge circuit. The capacitance of one of the capacitor changes periodically with the increase of stray capacitance due to the presence of conducting tooth of a rotating plate having a number of teeth, which rotates with the member whose rotational-speed we want to measure. This gives a periodic signal whose frequency, after demodulation, depends upon the speed of rotation of the device under test. Main potential of the application lies in the fact that rotating plate is outside the active area of the capacitor and is not grounded. This idea is original as well as it has clear-cut advantages. Accuracy and precision of the method depends upon the number of conducting slots in the rotating plate. A simple proto-type model based upon a simple and cheap electronics gives experimental results that comply with the simulated results completely.

Third application deals with the design, fabrication and testing of a new digital capacitive-encoder whose advantages includes simplicity, high response speed, insensitiveness to dirt and can be made compact. The resolution of this capacitive-encoder can be easily adjusted by adjusting the effective areas of its plates. Acheavable precision is not limited and it can be designed for any number of bits in compact form. It provides direct digital output signal for linear or rotary displacement. It can be used in a variety of applications such as in automatic control of machine tools, robotics and in the measurement of level, pressure, etc. A proto-type model, of five bits, has been developed and tested. This also gives very good results when used for liquid-level measurement.

The second section deals with the ultrasonic applications. The first application is the implementation of Piezoceramic Lead Zirconate Titanate (PZT) disk-type transducer for the measurement of liquid viscosity in kHz frequency range. The natural resonance frequency of the unloaded PZT transducer and its higher harmonics are used in the experiments. The properties of the liquid are reflected on the resonance resistance of the transducer when it is in complete contact with the liquid sample. The experimental results show straightforward relationship between the resonance resistance and the square root of the viscosity. This method can be very useful in the monitoring of the viscosity during production of materials such as plastic, polymers, and petrochemicals to ensure consistent quality.

The second application of the second section deals with the development of a device for the measurement of very low vacuum pressure. Ultrasonic wave gets attenuated while it is traveling through mediums and the attenuation depends upon the physical properties of these mediums. The effect of decreasing the pressure below atmospheric upon the transducer output has been studied to form a base for low vacuum pressure measurement using ultrasonic transducers (in a transmitter-receiver pair) with a continuous ultrasonic wave. The measurement was successfully carried with high sensitivity.

Conclusions drawn from the theoretical, simulated and practical investigations conducted on the proto-type modules have been presented. This is terminated with the future scope for continuation in the directions of the covered and proposed works in this thesis.

LIST OF PUBLICATIONS

The author has jointly published the following papers, which are related to the research work reported in this thesis:

1- A Novel Capacitive Rotation-Speed Transducer, *Institute Of Physics Publishing, Meas. Sci. Technol.(UK), Vol. 13, November 2002, pp 2027-2031.*

2- Digital Capacitive angular-Position Sensor, *IEE Proc.-Sci. Meas. Technol.(UK), Vol. 150, No 1, January 2003, pp 15-18.*

3- Digital Capacitive-Encoder, *Proceedings of the International Conference on Robotics, Vision, Information and Signal Processing, January 2003, Penang-Malaysia, pp 723-727.*

4- A Novel Method for Liquid Viscosity Measurement Using Piezoelectric (PZT) Transducer, *Proceedings of the International Conference on Robotics, Vision, Information and Signal Processing, January 2003, Penang-Malaysia, pp 767-770.*

5- Low-Pressure Measurements Using Ultrasonic Technique, *National Seminar on Advanced Instrumentation, January-2001, CSIO Chandigarh - India.*

6- Precise Displacement Measurement using Ultrasonic Technique, *All India Seminar on Instrumentation Engineering -Practices, Teaching and Research, July-2001, Hyderabad - India, pp 4.20-4.23.*

7- Measurements of Vacuum Pressure Using Ultrasonic Transmitter-Receiver Pair, *(Under communication for Publication).*

CHAPTER ONE

INTRODUCTION

CHAPTER I

INTRODUCTION

1.1 A SURVEY OF PREVIOUS WORK

Science and technology are so intertwined with measurement as to be totally inseparable from it. It is true that measuring instruments are one of the fruits of science, but it is equally true that without the ability to measure, there would be no science. When Lord Kelvin warned that knowledge not expressible in numbers was 'of meager and unsatisfactory kind' he was not expressing a fetish; he was identifying an essential aspect of scientific knowledge. The laws of physics are quantitative laws, and their validity can only be established by precise measurement. Extension of electrical techniques and systems for measuring various non-electrical quantities necessitated the development of devices known as 'sensors' and 'transducers'. These are the first in a sequence chain of instrumentation. Obviously the development of sensors and transducers, their application and advisory services in the area of relevant electronics required to be considered as one of the major thrust area. This development involves close cooperation between area specialists in material science, electronics, mechanical engineering, biology, chemistry, various physical-based technology and even economic services. Instrumentation is a branch of engineering that serves not only science but all branches of engineering and medicine as well

1.1.1 Capacitive Transducers

The capacitor is one of the oldest electrical devices; it consists of at least two electric conductors separated by dielectric material as defined by Maxwell in 1873. Among passive devices it can be fabricated in pure form i.e without residuals, at nominal cost. However, its small values have prominent effect of earth admittances and fringing effects. Their measurements have been posing a lot of difficulties to research works [1,10-12, 21]. Even then, the absolute standard capacitors are constructed so that their capacitances can be calculated from accurately measured dimensions and they are said to be calculable. Therefore, they have to be of some simple geometrical shape and dielectric should be air or preferably a vacuum.

Capacitive transducers are increasingly being used as sensing elements, because of their negligible energy consumption, low cost, small size, simple structure and high order of accuracy and precision [1-6]. Their limitations have been contained due to the development of new high quality electronic devices. Moreover, these transducers can be developed in integrated form also. Generally, three configurations have been used in the preparation of different grades of transducers. Parallel plate capacitors, co-axial cylinder capacitors and cylindrical cross-capacitors. Cylindrical cross-capacitors have been used in the development of standards devices but these require transformer ratio-arm bridges and associated circuits [3,7-9]. Their values are very small, and size is big and interfac-

ing circuits are costly. Co-axial cylinder capacitors are also used in the development of capacitive sensors and these can be used together with the latest electronic circuits. However, parallel plate capacitors, in different configurations, have been used in the development of different types of transducers. Main problems with reduced sizes are the effects of stray capacitances. These effects can be taken care of with the help of new electronic circuits effectively [10,12]. Although the capacitor is among the simplest type of the transducers it involves at least two conducting electrodes supported on insulator. If it's to be used as a transducer of mechanical movement, at least one of the electrodes must be free to move with minimal constraint on it in the direction of movement. The resulting requirement is an assembly of metallic and insulating components, both are individually rigid and should be held rigidly together, with either flexible or sliding linkage which will permit the relative motion that to be transduced, but that may prohibit any movement due to undesired causes. Among these causes are 'creep' in electrodes and insulators, vibration, thermal expansion, changes in atmospheric pressure and humidity, geometrical distortion of the transducer supports, and change in direction of weight forces if the transducer is tilted. All these undesired causes should be taken care of, by complete removal or at least by keeping them as minimum as possible to allow the transducer to perform the role of transduction with perfection.

Capacitive transducers have been employed intensively in the measurement of non-electrical quantities. As the position or

displacement is a basic variable whose measurement is involved in many other physical quantities, its accurate and precise measurement has been the focus of many studies [13-17]. Also capacitive transduction techniques have been involved in the precise and accurate measurement of angular speed [18]. In the light of rigorous research work, many commercial instruments are developed based on the capacitive transducers for the measurements of other non-electrical quantities such as level, force, pressure velocity, acceleration etc. [7,8,18-20]. The present work is in the line with this trend. The objective is to develop new capacitive transducers for the precision measurement of displacement, rotation speed and angular displacement. Some novel transducers based upon new configurations and electronic circuits are successfully developed and tested.

1.1.2 Piezoelectricity and Ultrasonic Transducers

Electricity might be produced by pressure application was first theoretically said by Coulomb (1815). But the actual discovery of piezoelectric phenomena was made by P. Cruie and J. Cruie (1880) and they wrote their experimental results and comments.

In (1881), Hankel suggested using the term "piezoelectricity" which later became the accepted term for this phenomenon. In the same year (1881), Lippman suggested that the reverse effect should also exist. Curie brothers (1882) verified exp-

erimentally this assumption by showing the coefficient for both the direct and reverse effects were identical [Ballato 1996]. After a series of investigations done by: Neumann (1890), Kelvin (1893), Voigt (1894), Langevin (1914), Born (1920 & 1933-1934), Cady's (1921), and finally Mason (1940) who explained and extended Kelvin model. Langevin and French co-workers during Word War-I came up with the practical ultrasonic submarine detector. The following two decades produced a variety of inventions such as microphones, accelerators, ultrasonic transducers, and signal filters. From the year 1940-1965 Barium Titanate and Lead Zirconate Titanate (PZT) families of piezoceramics were the materials of research [22,23]. Followed by introduction of new PZT instruments by Japanese researchers, a lot of interest has been developed in this field [24 - 38].

Many contemporary applications of piezoelectricity use piezoelectric ceramics instead of natural piezoelectric crystals. These piezoelectric ceramics are more versatile; their physical, chemical and piezoelectric characteristics can be tailored to specific applications. The mechanical and electrical axes of these ceramics can be precisely oriented in relation to the shape of the ceramic. These axes are set during "poling" the process that includes the piezoelectric properties in the ceramics. The orientation of the D.C. poling field determines the orientation of the mechanical and electrical axes. Other properties of the piezoelectric ceramics such as aging rate and time stability, temperature stability, voltage and stress limitations all are dependent mainly on the ceramic

composition and the way the ceramic is processed during manufacturing and production [39].

The transducer based on PZT converts mechanical energy into electrical energy and vice versa. One of the most important applications of these transducers is their use in examination or inspection of materials to provide information that cannot be obtained so easily or some times at all by other means of measurements. These results may prove to be highly profitable, if any other means cannot achieve it or the simplicity of this technique greatly exceeds that of any alternative. Also they have a wide range of applications in research, domestic, commercial, industrial, aerospace, sea and medical fields and many more. Now days there are a remarkable array of applications for piezoelectric, it is hard to imagine an area in which these products cannot make a positive difference in design and functionality [40 - 45].

1.2 LAYOUT OF THE THESIS

Majority of the literature available on the transducers and sensors subject has followed a measurand-specific classification like transducers for displacement, acceleration, force, temperature, etc. This work has rather, ventured to follow the second classification of transducers and sensors, which may be called a principal variable-specific approach to their classification like resistive, inductive, capacitive, ultrasonic transducers, etc.

The work in this thesis is broadly divided into two main sections. Section one comprising chapters 2, 3 and 4, which deals with some novel circuits and simulations along with practical designs and developments of some capacitive transducers. The applications involved in this section are angular position measurement, speed of rotation and capacitive encoder for direct digital signal output. Section two containing chapters 5 and 6, treating some applications of ultrasonic transducers in the field of instrumentation and measurements. The goal, in each, has been achieved with full theoretical and practical investigations. In the last chapter, conclusions drawn from theoretical, simulated and experimental investigations conducted in this work have been presented and terminated with the suggestions for future scope and continuations in the direction of the work covered in this thesis.

A technique based on a grounded semi-circular rotor that moves between the plates of four quadrant capacitors with the mechanical arrangement permits coverage of the full-circle range of 360 degrees. This arrangement, which featured as a digital capacitive angular-position sensor, has been developed in chapter 2. The electronic circuit, which has been designed and practically implemented, when tested experimentally give a linear relationship between the mechanical angle and the output of the circuit after it has been fed through digital frequency meter.

Chapter 3 describes a novel high performance capacitive rotational speed, which has been tested practically and simulation

results help in achieving the optimum design. The transducer mainly consists of two equal capacitors the first is used as reference while the second changes with the increase of stray capacitances due to the presence of a tooth of rotating conducting plate that rotates with the member whose rotation-speed is to be measured. Arranging the two capacitors in a bridge circuit, the speed of rotation is then deduced from the periodic unbalance performed by the capacitance changes.

A new digital encoder that is based on capacitive transduction technique is presented in the chapter 4. It is an absolute, non-contact type digital displacement transducer. Although, due to the ease and versatility provided by digital signal processing circuits and digital computers now days, digital transducers that gives the output signals in direct digital form are preferable over the analog ones. Absolute type digital transducers for displacement measurement are termed as encoders. These are far better than hybrid digital transducers. The needs for direct digital output signals necessitate the development of digital encoders. The developed new digital capacitive-encoder is discussed with complete details. A simulated model of the presented encoder, comprising five bits, has been developed including smart electronic signal processing circuit with digital display unit.

In chapter 5, the natural resonance frequency of the unloaded Lead Zirconate Titanate (PZT) disk-type transducer and its harmonics are used for the determination of viscosity of liquids. The viscous properties of the liquid affects the

radiation resistance of the transducer that was immersed and becomes in complete contact with the liquid whose viscosity is to be determined. Among the advantages of acoustic waves is that, at low intensities they are not dangerous to personnel over a wide frequency range and transparency has no bearing on the measurements. The method based on contact radiation resistance of the (PZT) element provides continuous viscosity monitoring and hence ensures automatic process control in liquid type materials. The measurement was carried at a frequency ranged from 75 KHz to 420 KHz, which is very high in comparison to what was reported in this field.

Measurement of pressure is of considerable importance in all stages of scientific and engineering measurements. Low vacuum pressure has been measured using ultrasonic principles. Ultrasonic wave get attenuated as it is traveling through any medium. This attenuation depends upon the physical properties of the medium. A continuous ultrasonic signal, produced by the transmitter, is passed through the medium whose pressure is varying then received by a receiver. The output voltage of the receiver is found to be proportional to the pressure of the medium. With these principles low vacuum pressure (from atmospheric down to 40 K Pascal) has been measured in chapter 6 using piezoelectric transducers as a transmitter-receiver pair. The measurement was carried with a sensitivity of 0.124 mV/ Pascal.

The last chapter concludes the theoretical, simulated and the experimental results carried out along with the recommendations for future work in the same direction of the thesis.

CHAPTER TWO

Development Of A New Digital Capacitive Angular-Position Sensor

CHAPTER II

DEVELOPMENT OF A NEW DIGITAL CAPACITIVE ANGULAR-POSITION SENSOR

2.1 INTRODUCTION

Position or displacement is a fundamental variable whose measurement is involved in many other physical quantities (e.g. force, velocity, acceleration and torque etc). Different techniques have been used in the measurement of angular displacement. Due to its advantages over the others, the capacitive technique is becoming more and more popular. Some of the advantages are the low power consumption, simple structure, small size, low cost and simple electronic circuitry that can easily be constructed. Many methods have been introduced to convert the capacitance values into a convenient form of electrical quantity, which can easily be measured [13,14,19,16]. This necessitates introduction of methods, which deal with the conversion of displacement changes into corresponding changes of capacitance [6,15,17]. Some of these, for instance [6] and [17] using the modified Martin oscillator with micro-controller or with switched-capacitor interface, are not capable of handling capacitance changes at frequencies higher than 10 Hz [4]. Another method [15] based on virtual rotor grounding is not capable of covering complete 360° range. Compared with the inductive displacement sensors, the developed sensor geometries

are simple in structures and design, low in weight and may easily be fabricated according to requirements. In addition, the frequency range for inductive is generally, much smaller than of the capacitive sensors. If it is compared with differenttypes of encoders, it is free from the disadvantages of brushes (wear & tear and friction). It is better than optical type, which suffers mainly from dusty environments in addition to that any misalignment in the axial or radial direction in the optical measurement system will lead to high errors or some times data will be completely missing

In the presented technique, the capacitive angular-position sensor contains four quadrant capacitors, each of which consists of a parallel plate capacitor whose higher potential plate has a specific shape. The grounded semi-circular rotor, whose angular-position is to be measured, shields part of the active area of the capacitor plates during its angular movement, depending upon its position. This changes the values of the four capacitors alternatively. The mechanical arrangement used permits coverage of the full-circle range of 360 degrees (i.e. angular displacement for one complete mechanical revolution of the rotor). When these capacitors are supplied with sinusoidal voltages of mutually shifted phases in a bridge system, the phase of output voltage of the bridge changes with the mechanical angle. This change was found to be containing some non-linearity, but the simulation results show that this relationship can be linearized if the shapes of the higher potential plates (H.P.P.) are modified. A simple prototype has been developed in which shaping of the H.P.P. gives satisfactory, improved and linear results. The phase of the output voltage

is measured digitally and the relationship between the angular-position and the digital output is found to be linear with an error of ± 0.5% and has a resolution of 3 arc minutes. This digital output can be interfaced with a personal computer as well as it can be used in connection with micro-controller to control an angle within 360° range. With all the above advantages the designed sensor can be featured as novel capacitive sensor.

2.2 THEORETICAL ASPECTS OF THE DESIGN

Capacitors used in the development of different types of capacitive transducers may be, parallel plate capacitors, coaxial capacitors or cylindrical cross-capacitor. Precise capacitors are usually completely enclosed by a conducting screen in order to make inter-electrode capacitance more definite. When the screen is not connected to either of the electrodes, the unit is said to be a 3-terminal capacitor. In such type of capacitor the direct capacitance between electrodes is effective and quite definite in value. Generally, in the development of capacitive transducers, capacitance involved are of very small values and when provided with shield can be represented by a 3-terminal only for precise and accurate measurements.

The equivalent circuit of the 3-Terminal capacitor is shown in figure 2.1. C_{12} represents the designed capacitance while C_{13} & C_{23} are undesirable capacitances. C_{12} can be changed by extending third terminal through the active area of the capacitor, as shown by dotted lines. Practically, C_{12} becomes zero when extended portion of shield completely covers the active area of the plates. However, in this arrangement we have to device the capacitance

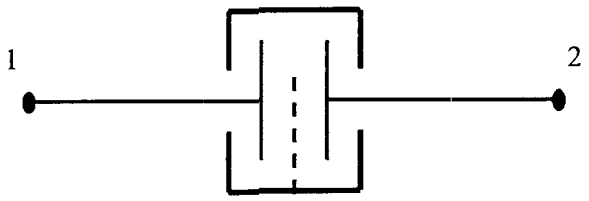

(a) 3-Terminal Capacitor

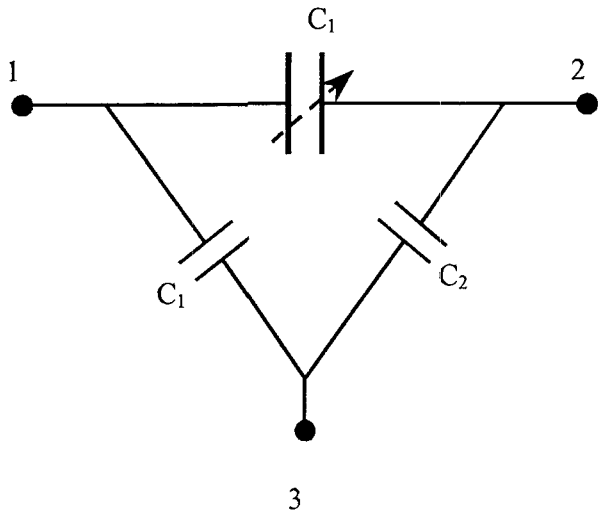

(b) Equivalent Circuit

Figure 2.1:

The 3-Terminal Capacitor and it's Equivalent Circuit

measuring techniques, which does not have the effect of C_{13} & C_{23} while measuring C_{12}.

A simple form of capacitive transducer for angular displacement measurement is the capacitor with semicircular plates of variable area type. Its capacitance is proportional to the common area and hence the angle of movement. The disadvantage of this arrangement is that; it can measure the angles is limited to less than 180 degrees only. The improved version of the above configuration is here employed in the measurement of angular position up to 360 degrees. The active plates are two circular conducting, parallel plates of the same radii and they are fixed while the third is a semicircular plate free to rotate. These plates are shown in figure 2.2 and they are defined as below:

(a) Higher potential plate (H.P.P):

It is a fixed circular disc that contains three annular rings; the inner and outer are grounded to serve as guards. The middle one is divided into four equal segments (S_1,.. S_4), each covering 90 degrees and insulated from each other. These segments are connected to electronic circuits, which supply them sinusoidal signals having the same amplitudes. However, the signals of each pair of adjacent segments have a phase difference of 90 degrees [46]. These segments are supplied with their appropriate signals through a wire having grounded-shield as shown in Figure 2.3.

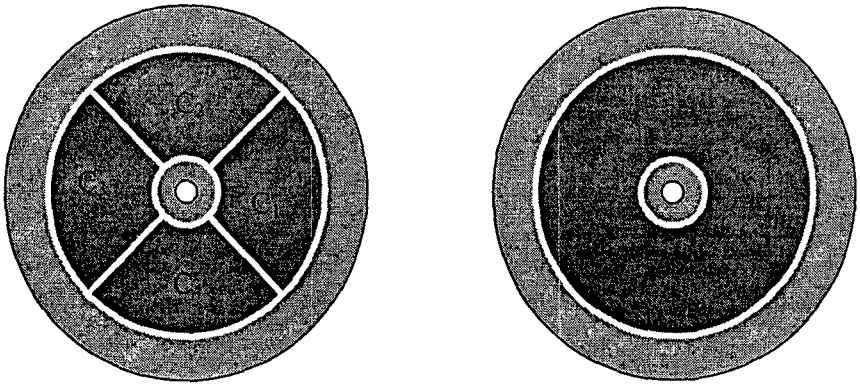

(a) Higher-potential plate (H.P.P) *(b) Lower potential plate (L.P.P)*

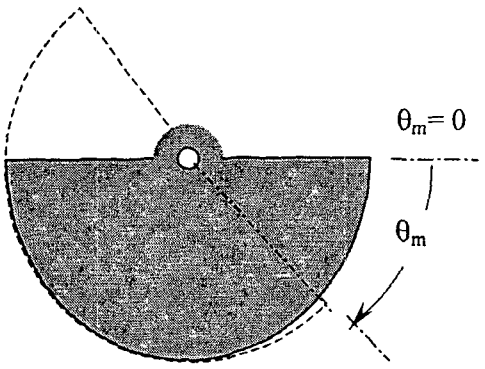

(c) Semi-circular shielding plate

(θ_m : mechanical angle of movement)

Figure 2.2: Details of the Designed Sensor plates

(b) Lower potential plate (L.P.P):

This plate is similar to the (H.P.P) except that its middle circle is conducting plate. This plate works as a common plate for the four segments of the (H.P.P). In this way four capacitances (C_1, C_2, C_3 & C_4) are present between H.P.P and L.P.P. A thin-shielded wire is attached to the common plate of the (L.P.P) to pass the corresponding currents (i_1, i_2, i_3, & i_4). These currents will be present when the segments are supplied with their specified signals (see Figure 2.3), and they are summed up to give the output signal.

(c) Shielding (Rotating) plate:

It is a semi-circular, grounded plate fixed on a shaft. The shaft passes through the centers of all the three plates. This grounded plate is kept between the lower and higher potential plates and allowed to rotate freely. While rotating at any instant, it covers an active area equal to half the total area of the segments, thereby varying the values of the capacitors and modifying the currents passing to the lower potential plates. The position of the shielding plate thus decides the currents to be summed up and so the output voltage V_o, which is the product of the sum of the currents and a pure resistor R (see Figure 2.3).

Each of the capacitors (C_1.... C_4) has a capacitance determined by its effective area that is in complete communication with the lower potential plate. This can be described through the well-known parallel plate capacitance equation: -

$$C = \varepsilon A / d \qquad \ldots(2.1)$$

where C is the capacitance in farad, ε is the permittivity of the material filling the capacitor in farad per meter, A is the effective area of the plates in square meters, d is the distance between the two plates (i.e. H.P.P and L.P.P) in meter.

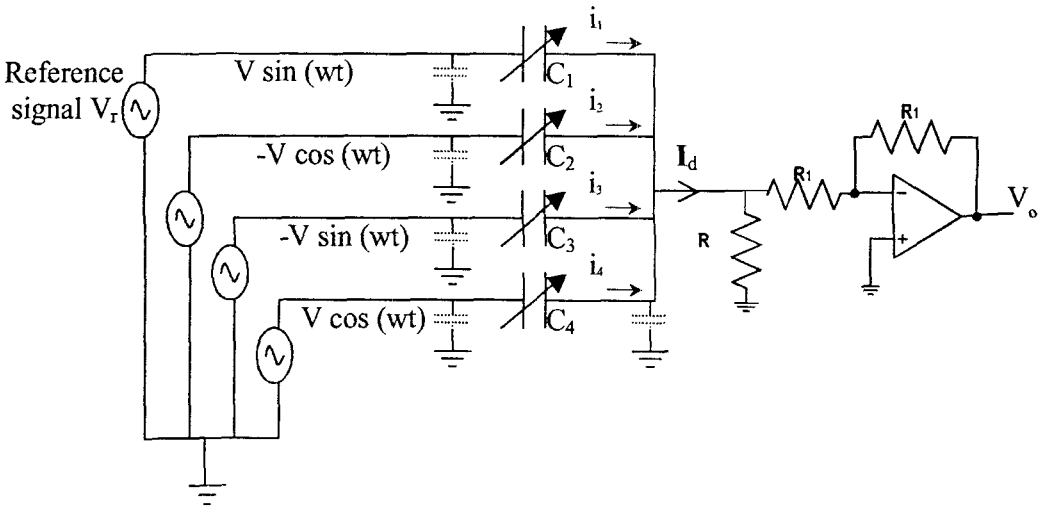

Figure 2.3: Electrical Representation Relates the Plate's Capacitances to Their Signals as well as the Reference and the Output Signals.

Since A, in this case, is the area of a sector, it can be expressed by:

$$A = (r_1^2 - r_2^2)\theta/2 \qquad \ldots(2.2)$$

where r_2, r_1 are the radii of the outer and inner circles respectively, and θ is the central mechanical angle (in radians) covered by the segment. Therefore, any change in the angular position of the shielding plate will change the effective area of some sectors and so the value of their capacitances. This change takes place in an alternate pattern following the change in the mechanical angle. Figure 2.4 shows the variation of these capacitors with respect to the mechanical angle of the movement.

These changes in the capacitors cause the phase of the output signal to change. The grounded semi-circular moving plate shields an area equal to half of the total area of the plates, but at least one segment from the H.P.P will have its effective area unaltered for movement over a range of 90°. This depends on the position of the semi-circular moving plate. As the moving plate is used as a shield, its misalignment, tilt, etc will not affect the operation of the system, because its position with slight tilt will not affect the shielding process. Also, the grounded moving plate, which is at ground potential and controls the effective area of the sensor capacitances, its axial component, due to vibrations will not affect the value of the effective capacitance. Stray capacitances will appear either across the supply or the detector and hence become ineffective. Shield as well as guard electrodes were properly designed to keep the fringing effects well defined as well as low, and the system free from grounding noise and pick-

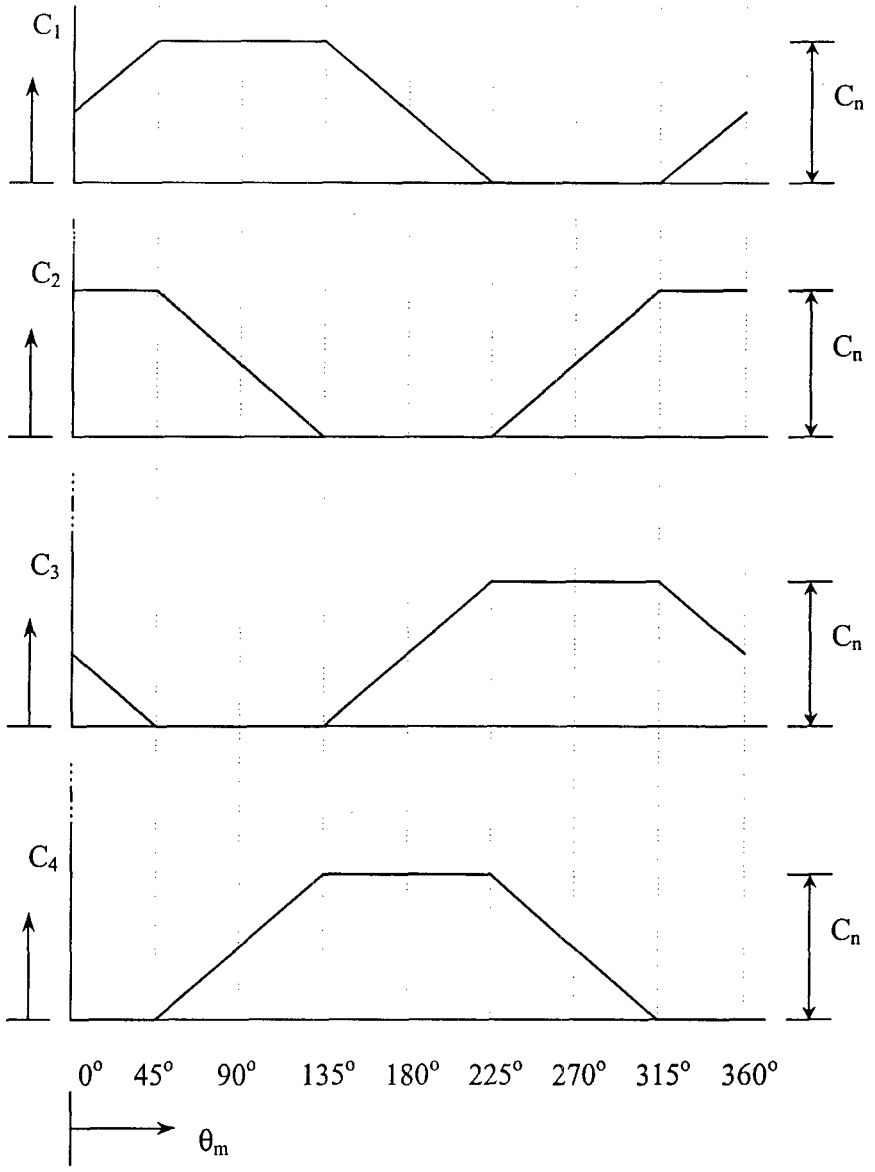

Figure 2.4: The Four Capacitors Variations During One Complete Revolution of The Rotor.

up. The electrical phase of the output voltage in the circuit of Figure 2.3 changes over 360 degrees when the moving plate completes one full mechanical revolution. During the complete revolution the output voltage V_o of this arrangement, after being passed through current to voltage converter, can be expressed by:

$$V_o = RI_d = R\sum_{i=1}^{4} I_i = RV\omega\{(C_2 - C_4)Sin(\omega t) + (C_1 - C_3)Cos(\omega t)\} \quad ...(2.3)$$

$$= K_1\{(C_2 - C_1)Sin(\omega t) + (C_1 - C_3)Cos(\omega t)\}$$

$$= K_1 K_2 Sin(\omega t + \phi) \quad ...(2.4)$$

where $K_1 = RV\omega$

$$= K_1\{(C_2 - C_1)Sin(\omega t) + (C_1 - C_3)Cos(\omega t)\}$$

$$K_2 = \{(C_2 - C_4)^2 + (C_1 - C_3)^2\}^{1/2}$$

and $\phi = \arctan\{\{(C_1 - C_3)/(C_2 - C_4)\}$

Due to the alternate changes in these capacitances (from maximum to minimum & vice versa), the above argument changes over a range of 90° degrees for each quarter of the complete cycle. This argument carries the complete output phase information. Let the capacitance of the segment that is in complete communication with the L.P.P. for 90 degrees; be denoted by C_n (see figure 2.4). The electrical and mechanical phase angles with respect to the reference electrical supply signal and reference mechanical angle are ϕ_n, θ_n respectively, and then the argument of the electrical output

signal ϕ_p can be given by:

$$\phi_p = \phi + \phi_n + 90 \qquad \ldots(2.5)$$

where $\phi = \arctan\{(C_{n-1} - C_{n+1})/C_n\}$, n =1,..4 over the complete circle range and C_0 taken as C_4 , C_5 is taken as C_1. The complete details of this arrangement are shown in table (2.1). While due to the symmetry of the electrical and the mechanical system, in this case the mechanical angle θ_m is given by:

$$\theta_m = \theta + \theta_n + 90 \qquad \ldots(2.6)$$

Plate in full Communication (C_i)	Electrical phase angle ϕ_p (degrees)	Range of ϕ_p (degrees)
C_1	$90 + \tan^{-1}\{(C_4 - C_2)/C_n\}$	$45 - 135^o$
C_4	$180 + \tan^{-1}\{(C_3 - C_1)/C_n\}$	$135 - 225^o$
C_3	$270 + \tan^{-1}\{(C_2 - C_4)/C_n\}$	$225 - 315^o$
C_2	$360 + \tan^{-1}\{(C_1 - C_3)/C_n\}$	$315 - 45^o$

Table (2.1): Plate In Full Communication with the L.P.P and the Corresponding Electrical Phase Angle ϕ_p.

This sensor works on the principle of comparing the phase of the electrical output signal V_o, which depends on the position of the grounded semi-circular plate, with the phase of the reference electrical signal V_r.

2.3 SIMULATIONS AND DESIGN OF THE PROTOTYPE SENSOR

2.3.1 Initial Studies

Moving the shielding plate (clockwise) from the position shown in Figure 2.5-a to that in Figure 2.5-b, the phase difference between the reference and the output signals changes over 90 degrees as shown in the attached waveforms of figure 2.5-c & d. This change takes place following the pattern shown by the continuous line of Figure 2.5-e, which is non-linear. Table 2.2 shows the ideal and the simulated out a long with the errors associated with it.

With the above arrangement, the phase of the output signal is found to be completely dependent on the tangent formula, which is a well-known non-linear quantity. The shape of each segment of the H.P.P can be modified in order to minimize this non-linearity. The modification has been done by introduction a design factor for linear output.

2.3.2 Choice and Optimization of the Design Factor

To compensate for the condition that the output is higher in value than the required (as in the range from 0 - 45° of Figure 2.5-e), the radii difference r of C_{n-1} (which is C_1 in this case) will be decreased by a factor f (i.e. r becomes r(1-f), or f is per-unit

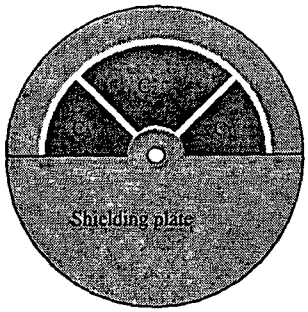

(a)

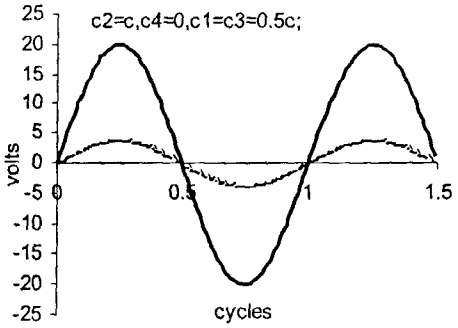

(c)

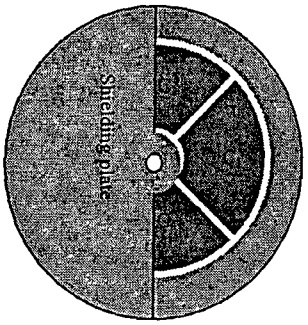

(b)

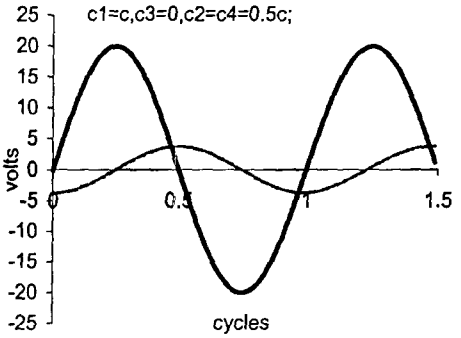

(d)

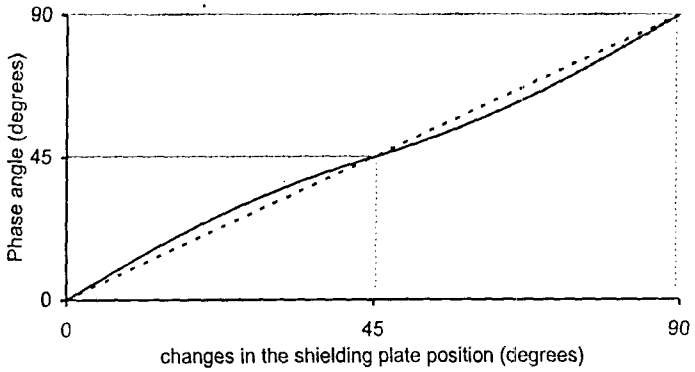

(e)

Figure 2.5:
The Simulated Shielding Plate Position Versus The Angle.

Ideal output	Practical output	Error	Ideal output	Practical output	Error
0.0	0.0	0.0	46	45.6	-0.4
1.0	1.3	0.3	47	46.3	-0.7
2.0	2.5	0.5	48	47.0	-1.0
3.0	3.8	0.8	49	47.7	-1.3
4.0	5.1	1.1	50	48.4	-1.6
5.0	6.3	1.3	51	49.1	-1.9
6.0	7.6	1.6	52	49.8	-2.2
7.0	8.8	1.8	53	50.6	-2.4
8.0	10.1	2.1	54	51.3	-2.7
9.0	11.3	2.3	55	52.1	-2.9
10.	12.5	2.5	56	52.9	-3.1
11.0	13.7	2.7	57	53.7	-3.3
12.0	14.9	2.9	58	54.6	-3.4
13.0	16.1	3.1	59	55.4	-3.6
14.0	17.3	3.3	60	56.3	-3.7
15.0	18.4	3.4	61	57.2	-3.8
16.0	19.6	3.6	62	58.1	-3.9
17.0	20.7	3.7	63	59.0	-4.0
18.0	21.8	3.8	64	60.0	-4.0
19.0	22.9	3.9	65	60.9	-4.1
20.0	24.0	4.0	66	61.9	-4.1
21.0	25.0	4.0	67	62.9	-4.1
22.0	26.1	4.1	68	63.9	-4.1
23.0	27.1	4.1	69	65.0	-4.0
24.0	28.1	4.1	70	66.0	-4.0
25.0	29.1	4.1	71	67.1	-3.9
26.0	30.0	4.0	72	68.2	-3.8
27.0	31.0	4.0	73	69.3	-3.7
28.0	31.9	3.9	74	70.4	-3.6
29.0	32.8	3.8	75	71.6	-3.4
30.0	33.7	3.7	76	72.7	-3.3
31.0	34.6	3.6	77	73.9	-3.1
32.0	35.4	3.4	78	75.1	-2.9
33.0	36.3	3.3	79	76.3	-2.7
34.0	37.1	3.1	80	77.5	-2.5
35.0	37.9	2.9	81	78.7	-2.3
36.0	38.7	2.7	82	79.9	-2.1
37.0	39.4	2.4	83	81.2	-1.8
38.0	40.2	2.2	84	82.4	-1.6
39.0	40.9	1.9	85	83.7	-1.3
40.0	41.6	1.6	86	84.9	-1.1
41.0	42.3	1.3	87	86.2	-0.8
42.0	43.0	1.0	88	87.5	-0.5-
43.0	43.7	0.7	89	88.7	0.3
44.0	44.4	0.4	90	90.0	0.0
45.	45.0	0.0			

Table (2.2): Simulated Outputs Without Design Factor

decrease of radii difference) and of C_{n+1} increased by the same factor to become $r(1 + f)$. At the same time the radius of the lower potential plate's middle circle was increased to $r(1 + f)$. This factor f, takes the value $f = 0$ (when $\phi = 0,45,90...$) since the repetition of the output at these extreme values lies on a linear straight line.

From 0 to 45 degrees, the design factor should not introduce any change in the output exactly at 0 and 45, while it's required to introduce the maximum change around the mid point between these extreme ends. Therefore, the equation for this design factor can be written in the form of:

$$f = k\phi(\phi - 45) \qquad \ldots(2.7)$$

where k is a weighting factor the choice of which is based on simulations. The practical significance of the above equation is to have concave and convex ends for each of the H.P.P segments each 45 degrees as shown in approximated practical shape of Figure 2.6.

Based on the fact that the design factor takes the value of zero every 45 degrees, the basic equation for this design factor f can be rewritten as:

$$f = k(\phi - N)(N + 45 - \phi) \qquad \ldots(2.8)$$

$N = 0, 45, 90, 135 \ldots\ldots 315$ and $0 \leq (\phi - N) \leq 45$, k is a weighting factor the

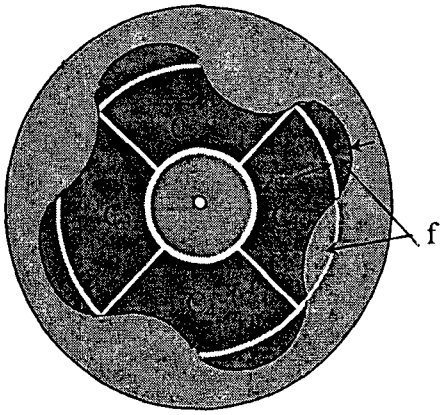

Figure 2.6: The New Shape of The Higher Potential Plate.

choice of which is based on simulations. Selection of the best weighting factor is done using Microsoft Visual C++ software. Sample of the program is shown in Appendix: A-I. Output results, in the range from 0 to 90 degrees, for different values of the weighting factor along with the errors associated with each weighting factor are shown in table 2.3. Again the same results for the complete 360 degrees are shown in Appendix: A-II, and figure 2.7. The modifications due to introduction of the design factor of equation (2.8) are in cyclic fashion over the range of 360° also it is found practically that it reduces the dependency on the tangent formula. This can be seen clearly in the graphical form of the simulation results of Figure 2.8, in which the value for the weighting factor is chosen to be k = 0.0009. This value for k gives a design factor of $0 \leq f < 0.46$ which is practically accepted, since f is the per-unit increase or decrease of radii difference r.

Ideal Output	$k = 0.0002$		$k = 0.0005$		$k = 0.0008$		$k = 0.0009$		$k = 0.001$	
	Output	Error	Output	Error	Output	Error	Output	Error	Output	Error
0.0	0.000	0.000	0.000	0.000	0.000	0.000	0.000	0.000	0.000	0.000
1.0	1.273	0.273	1.272	0.272	1.271	0.271	1.271	0.271	1.271	0.271
2.0	2.544	0.544	2.540	0.540	2.533	0.533	2.530	0.530	2.526	0.526
3.0	3.812	0.812	3.799	0.799	3.775	0.775	3.765	0.765	3.754	0.754
4.0	5.074	1.074	5.046	1.046	4.993	0.993	4.970	0.970	4.944	0.944
5.0	6.330	1.330	6.277	1.277	6.179	1.179	6.136	1.136	6.089	1.089
6.0	7.578	1.578	7.492	1.492	7.331	1.331	7.261	1.261	7.183	1.183
7.0	8.817	1.817	8.688	1.688	8.447	1.447	8.342	1.342	8.225	1.225
8.0	10.046	2.046	9.864	1.864	9.526	1.526	9.378	1.378	9.213	1.213
9.0	11.264	2.264	11.020	2.020	10.568	1.568	10.370	1.370	10.149	1.149
10.0	12.469	2.469	12.157	2.157	11.574	1.574	11.319	1.319	11.034	1.034
11.0	13.662	2.662	13.273	2.273	12.547	1.547	12.230	1.230	11.874	0.874
12.0	14.842	2.842	14.371	2.371	13.490	1.490	13.105	1.105	12.672	0.672
13.0	16.008	3.008	15.450	2.450	14.407	1.407	13.950	0.950	13.436	0.436
14.0	17.159	3.159	16.513	2.513	15.302	1.302	14.770	0.770	14.172	0.172
15.0	18.296	3.296	17.560	2.560	16.179	1.179	15.571	0.571	14.887	-0.113
16.0	19.417	3.417	18.594	2.594	17.044	1.044	16.360	0.360	15.589	-0.411
17.0	20.524	3.524	19.615	2.615	17.900	0.900	17.142	0.142	16.287	-0.713
18.0	21.615	3.615	20.625	2.625	18.754	0.754	17.925	-0.075	16.989	-1.011
19.0	22.690	3.690	21.626	2.626	19.610	0.610	18.714	-0.286	17.702	-1.298
20.0	23.749	3.749	22.620	2.620	20.472	0.472	19.517	-0.483	18.435	-1.565
21.0	24.793	3.793	23.607	2.607	21.346	0.346	20.337	-0.663	19.194	-1.806
22.0	25.822	3.822	24.589	2.589	22.234	0.234	21.181	-0.819	19.987	-2.013
23.0	26.834	3.834	25.566	2.566	23.140	0.140	22.053	-0.947	20.819	-2.181
24.0	27.830	3.830	26.541	2.541	24.067	0.067	22.957	-1.043	21.696	-2.304
25.0	28.811	3.811	27.512	2.512	25.017	0.017	23.896	-1.104	22.620	-2.380
26.0	29.776	3.776	28.481	2.481	25.991	-0.009	24.871	-1.129	23.595	-2.405
27.0	30.724	3.724	29.448	2.448	26.990	-0.010	25.883	-1.117	24.621	-2.379
28.0	31.657	3.657	30.412	2.412	28.013	0.013	26.932	-1.068	25.699	-2.301
29.0	32.574	3.574	31.373	2.373	29.059	0.059	28.016	-0.984	26.826	-2.174
30.0	33.475	3.475	32.330	2.330	30.125	0.125	29.132	-0.868	27.998	-2.002
31.0	34.360	3.360	33.283	2.283	31.209	0.209	30.276	-0.724	29.211	-1.789
32.0	35.229	3.229	34.229	2.229	32.307	0.307	31.443	-0.557	30.458	-1.542
33.0	36.082	3.082	35.168	2.168	33.414	0.414	32.627	-0.373	31.730	-1.270
34.0	36.919	2.919	36.097	2.097	34.525	0.525	33.820	-0.180	33.019	-0.981
35.0	37.739	2.739	37.015	2.015	35.633	0.633	35.015	0.015	34.314	-0.686
36.0	38.542	2.542	37.919	1.919	36.732	0.732	36.203	0.203	35.603	-0.397
37.0	39.329	2.329	38.807	1.807	37.816	0.816	37.375	0.375	36.877	-0.123
38.0	40.099	2.099	39.676	1.676	38.876	0.876	38.521	0.521	38.121	0.121
39.0	40.852	1.852	40.524	1.524	39.906	0.906	39.633	0.633	39.325	0.325
40.0	41.588	1.588	41.348	1.348	40.897	0.897	40.698	0.698	40.475	0.475
41.0	42.306	1.306	42.145	1.145	41.842	0.842	41.709	0.709	41.560	0.560
42.0	43.007	1.007	42.911	0.911	42.733	0.733	42.655	0.655	42.568	0.568
43.0	43.690	0.690	43.645	0.645	43.562	0.562	43.526	0.526	43.486	0.486
44.0	44.354	0.354	44.342	0.342	44.321	0.321	44.311	0.311	44.301	0.301
45.0	45.000	-0.000	45.000	-0.000	45.000	-0.000	45.000	-0.000	45.000	-0.000
46.0	45.646	-0.354	45.658	-0.342	45.679	-0.321	45.689	-0.311	45.699	-0.301
47.0	46.310	-0.690	46.355	-0.645	46.438	-0.562	46.474	-0.526	46.514	-0.486
48.0	46.993	-1.007	47.089	-0.911	47.267	-0.733	47.345	-0.655	47.432	-0.568
49.0	47.694	-1.306	47.855	-1.145	48.158	-0.842	48.291	-0.709	48.440	-0.560

50.0	48.412	-1.588	48.652	-1.348	49.103	-0.897	49.302	-0.698	49.525	-0.475
51.0	49.148	-1.852	49.476	-1.524	50.094	-0.906	50.367	-0.633	50.675	-0.325
52.0	49.901	-2.099	50.324	-1.676	51.124	-0.876	51.479	-0.521	51.879	-0.121
53.0	50.671	-2.329	51.193	-1.807	52.184	-0.816	52.625	-0.375	53.123	0.123
54.0	51.458	-2.542	52.081	-1.919	53.268	-0.732	53.797	-0.203	54.397	0.397
55.0	52.261	-2.739	52.985	-2.015	54.367	-0.633	54.985	-0.015	55.686	0.686
56.0	53.081	-2.919	53.903	-2.097	55.475	-0.525	56.180	0.180	56.981	0.981
57.0	53.918	-3.082	54.832	-2.168	56.586	-0.414	57.373	0.373	58.270	1.270
58.0	54.771	-3.229	55.771	-2.229	57.693	-0.307	58.557	0.557	59.542	1.542
59.0	55.640	-3.360	56.717	-2.283	58.791	-0.209	59.724	0.724	60.789	1.789
60.0	56.525	-3.475	57.670	-2.330	59.875	-0.125	60.868	0.868	62.002	2.002
61.0	57.426	-3.574	58.627	-2.373	60.941	-0.059	61.984	0.984	63.174	2.174
62.0	58.343	-3.657	59.588	-2.412	61.987	-0.013	63.068	1.068	64.301	2.301
63.0	59.276	-3.724	60.552	-2.448	63.010	0.010	64.117	1.117	65.379	2.379
64.0	60.224	-3.776	61.519	-2.481	64.009	0.009	65.129	1.129	66.405	2.405
65.0	61.189	-3.811	62.488	-2.512	64.983	-0.017	66.104	1.104	67.380	2.380
66.0	62.170	-3.830	63.459	-2.541	65.933	-0.067	67.043	1.043	68.304	2.304
67.0	63.166	-3.834	64.434	-2.566	66.860	-0.140	67.947	0.947	69.181	2.181
68.0	64.178	-3.822	65.411	-2.589	67.766	-0.234	68.819	0.819	70.013	2.013
69.0	65.207	-3.793	66.393	-2.607	68.654	-0.346	69.663	0.663	70.806	1.806
70.0	66.251	-3.749	67.380	-2.620	69.528	-0.472	70.483	0.483	71.565	1.565
71.0	67.310	-3.690	68.374	-2.626	70.390	-0.610	71.286	0.286	72.298	1.298
72.0	68.385	-3.615	69.375	-2.625	71.246	-0.754	72.075	0.075	73.011	1.011
73.0	69.476	-3.524	70.385	-2.615	72.100	-0.900	72.858	-0.142	73.713	0.713
74.0	70.583	-3.417	71.406	-2.594	72.956	-1.044	73.640	-0.360	74.411	0.411
75.0	71.704	-3.296	72.440	-2.560	73.821	-1.179	74.429	-0.571	75.113	0.113
76.0	72.841	-3.159	73.487	-2.513	74.698	-1.302	75.230	-0.770	75.828	-0.172
77.0	73.992	-3.008	74.550	-2.450	75.593	-1.407	76.050	-0.950	76.564	-0.436
78.0	75.158	-2.842	75.629	-2.371	76.510	-1.490	76.895	-1.105	77.328	-0.672
79.0	76.338	-2.662	76.727	-2.273	77.453	-1.547	77.770	-1.230	78.126	-0.874
80.0	77.531	-2.469	77.843	-2.157	78.426	-1.574	78.681	-1.319	78.966	-1.034
81.0	78.736	-2.264	78.980	-2.020	79.432	-1.568	79.630	-1.370	79.851	-1.149
82.0	79.954	-2.046	80.136	-1.864	80.474	-1.526	80.622	-1.378	80.787	-1.213
83.0	81.183	-1.817	81.312	-1.688	81.553	-1.447	81.658	-1.342	81.775	-1.225
84.0	82.422	-1.578	82.508	-1.492	82.669	-1.331	82.739	-1.261	82.817	-1.183
85.0	83.670	-1.330	83.723	-1.277	83.821	-1.179	83.864	-1.136	83.911	-1.089
86.0	84.926	-1.074	84.954	-1.046	85.007	-0.993	85.030	-0.970	85.056	-0.944
87.0	86.188	-0.812	86.201	-0.799	86.225	-0.775	86.235	-0.765	86.246	-0.754
88.0	87.456	-0.544	87.460	-0.540	87.467	-0.533	87.470	-0.530	87.474	-0.526
89.0	88.727	-0.273	88.728	-0.272	88.729	-0.271	88.729	-0.271	88.729	-0.271
90.0	90.000	0.000	90.000	0.000	90.000	0.000	90.000	0.000	90.000	0.000

Table (2.3): Output Results for Different Values of the Weighting Factor k.

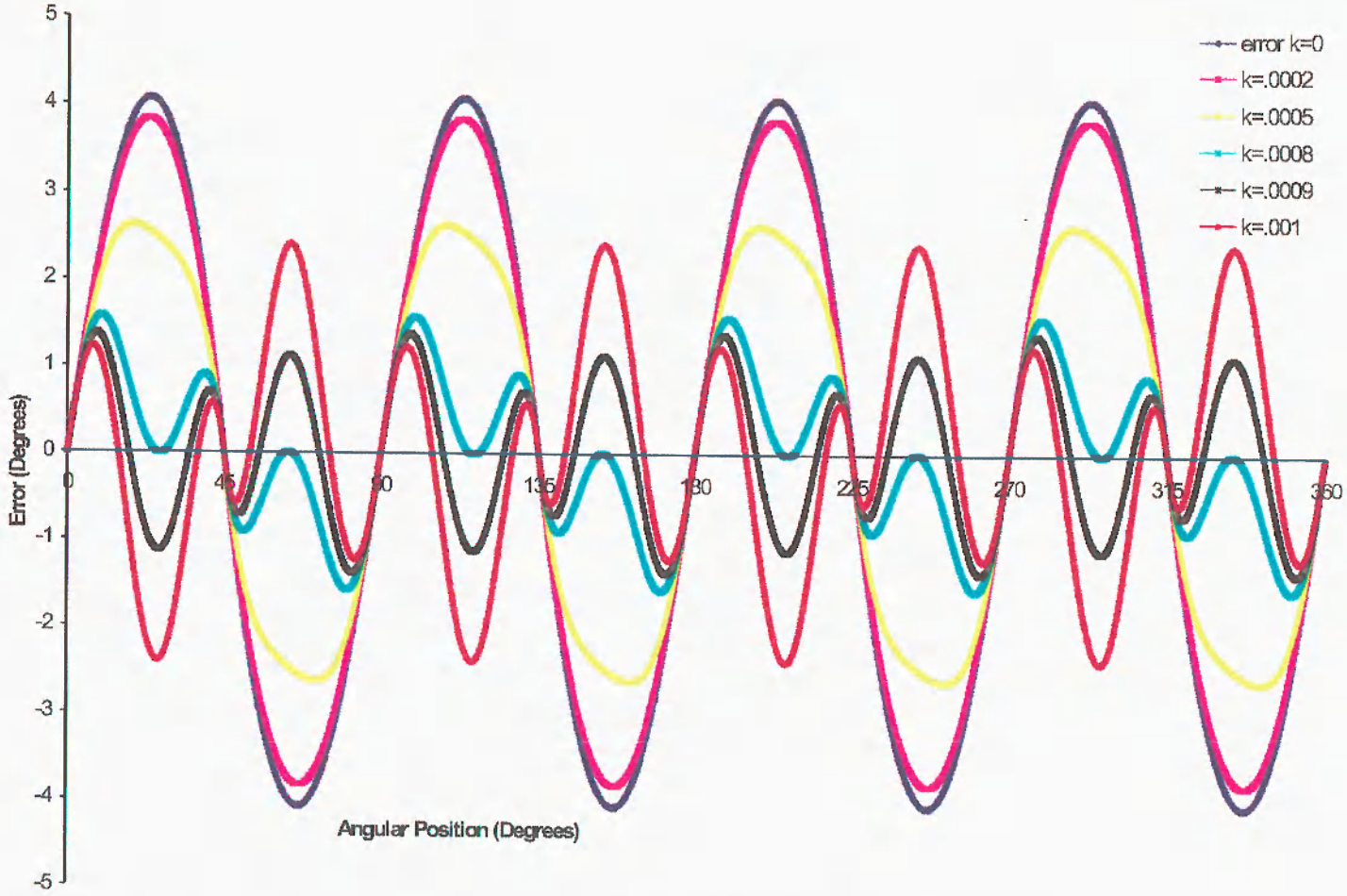

Figure 2.7: Errors in the Output Results for Different Values of Weighting Factor k

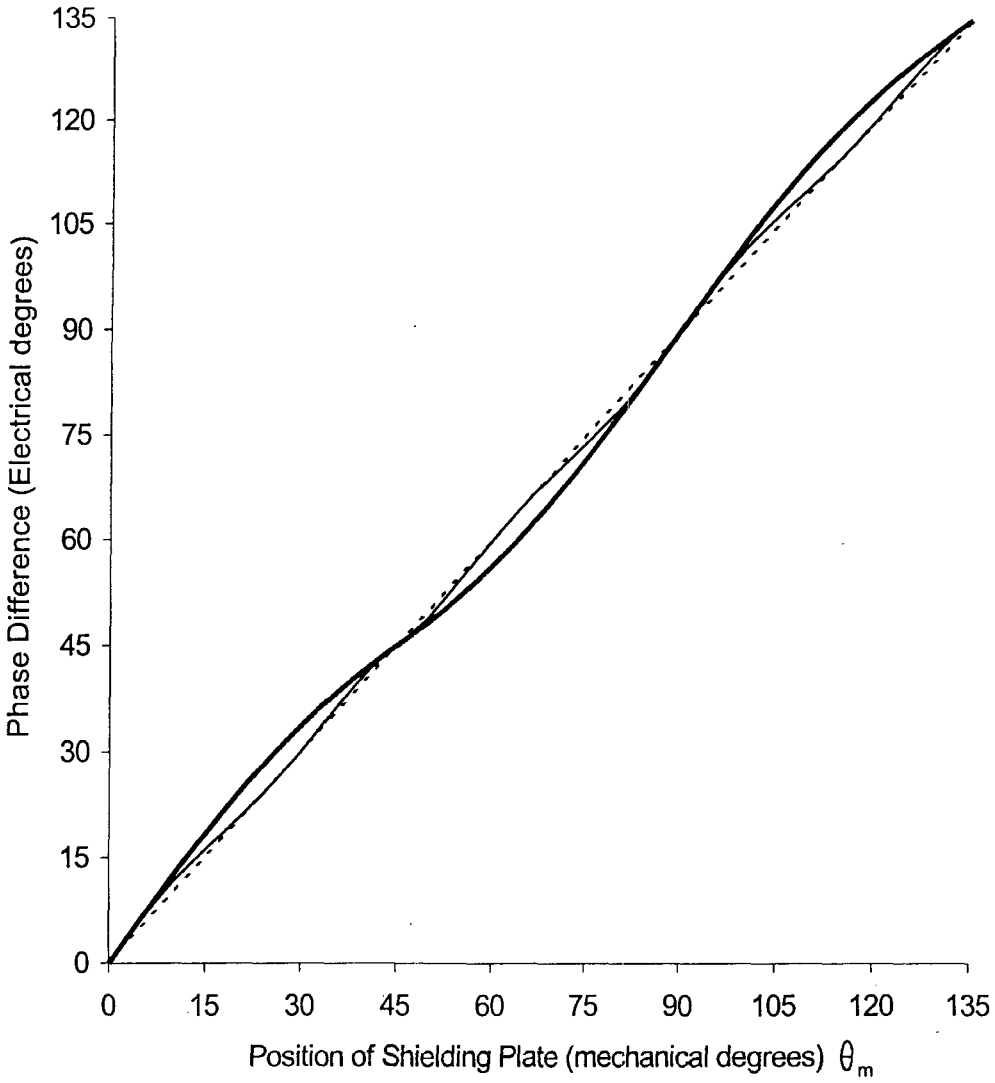

Figure 2.8: Effect of Shaping the Higher Potential Plate

——— *Curve without shaping the H.P.P*

——— *Curve after shaping the H.P.P*

---- *The required line*

2.4 EXPERIMENTAL SETUP AND RESULTS

Figure 2.9 shows the detailed signal processing circuit diagram of the experimental set-up with which the angular displacement sensor compares the phase of the electrical output with the phase of the reference input signal of the electronic circuit and generates counts that are proportional to the phase difference between the two signals. Both the output of the current-to-voltage converter and the reference electrical signal are taken through zero crossing detectors to differentiators and then to half wave rectifiers to get single ramp pulse per cycle. These pulses are taken to the stop and start of the counter, respectively, and they are at the rate of single ramp pulse per cycle. At the starting both the signals coincide with each other. Moving the shielding plate, the position of the ramp sampled from the output of the current-to-voltage converter to stop the counter changes. The counter input is fed through 7.2 MHz, $10V_{pp}$ square-wave generator, thereby the frequency counter performs the measurements of the phase difference. Although the circuit has a single analog input signal of 10kHz, $20V_{pp}$ sinusoidal-wave, its output is in digital form, hence it is a digital angular-position sensor. The input versus the output transfer characteristic curve of the sensor is shown in Figure 2.10(a). As shown here the curve is linear over the full circle range (360 Degrees) and has a conversion gain of 20 counts/ degree. For comparison and to give clearer image the percentage linearity errors before and after shaping of the electrodes are plotted in Figure 2.10(b). Being a proto-type model, very small error exists in the mensined Figure, the curve shows that this error is predominantly random in nature, which will definitely be

improved with improvement in fabrication techniques. The non-linearity is too much reduced using a single designed factor as seen in Figure 2.8. Depending on the application and the accuracy required a second design factor can be introduced in the same manner, but that will be on the expense of the new shape obtained.

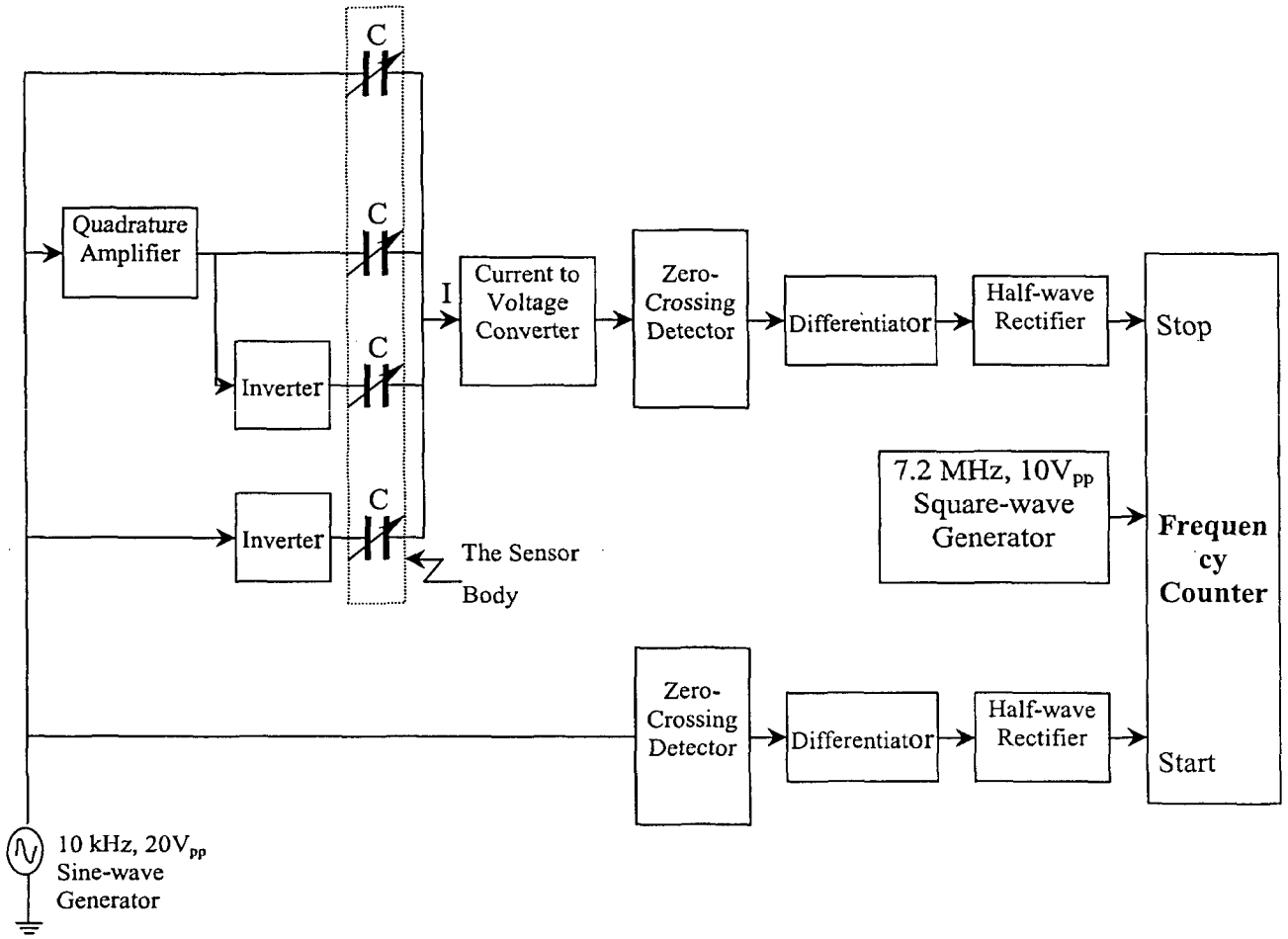

Figure 2.9: The block diagram circuit of the capacitive angular displacement sensor

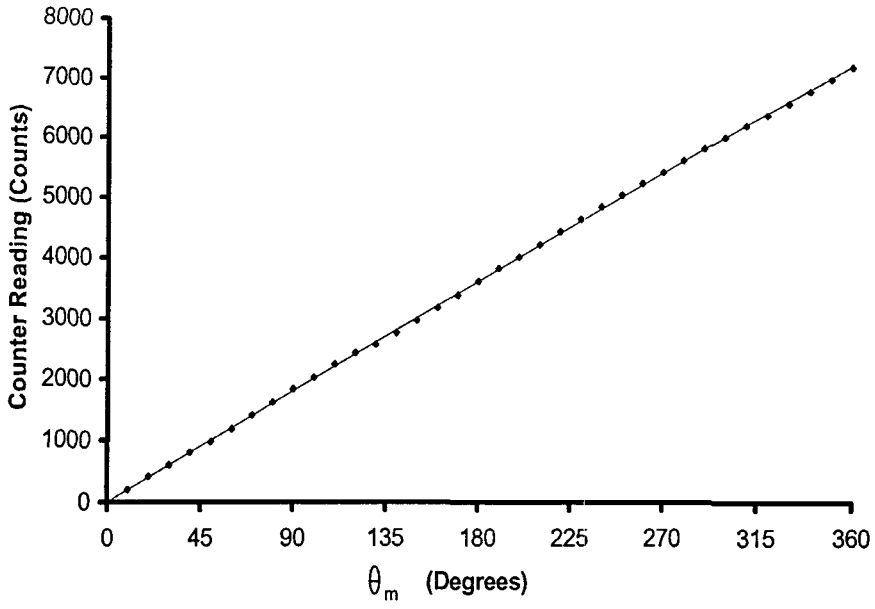

Figure 2.10(a): Angular-Position versus the Counter Readings After Shaping the Electrodes

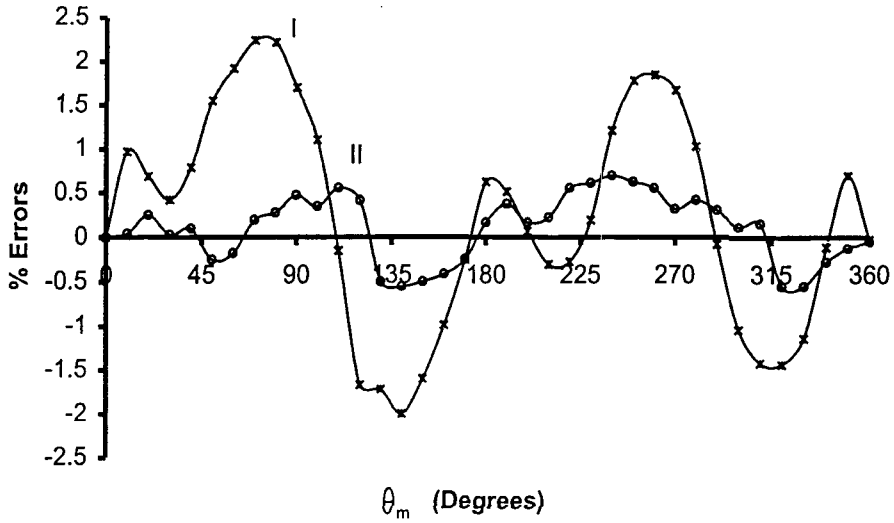

Figure 2.10(b): The Measurement Errors:

I. Before Shaping the Electrodes
II. After shaping the Electrodes.

CHAPTER THREE

Rotation-Speed Measuring System Using A Novel Capacitive Transducer

CHAPTER III

ROTATION-SPEED MEASUREMING SYSTEM USING A NOVEL CAPACITIVE TRANSDUCER

3.1 INTRODUCTION

Capacitors are increasingly being used as sensing elements, because of their negligible energy consumption, low cost, small size and simple structure. As a result, they become more popular and many methods [4,6,47] have been developed which deals with the conversion of capacitance value into other simply measurable quantities such as voltage and frequency.

A continuous variation of capacitance is frequently required for the measurement purposes and usually variable air capacitors are used to provide such type of variation. Capacitance variation generally provides a contactless method. The usual values of the variable capacitor are in the range of1 to 500 pF, and the operating frequency is normally greater than 10 kHz and below 1.0 MHz. This method can be applied to any quantity we are able to convert it into displacement, such as force, pressure, torque, velocity, etc [47].

The capacitive speed transducer designed by Rehman and Murti [18] consists of a set of fixed plates between which a grounded plate having tooth and segments passes so that active area changes from maximum to minimum. When placed in active bridge,

modulated output is obtained which is amplified and demodulated to extract the signal proportional to speed of rotation. However, it had a problem with grounding the shaft of the motor, which is not convenient in most of the cases, plate has to move inside the plates too. In this design, conducting plate rotates outside one of the capacitor and it should not be grounded. When conducting segment comes near the capacitor, total capacitance increases while in the presence of non-conducting part the capacitance remains nearly constant. It is a simple, robust and cheap method and can be developed in the form of a small probe. It can be applied to the measurement of rotation-speed of small motors. Errors due to axial and radial motion of plates can easily be adjusted. It has distinct advantages over other capacitive rotation-speed transducers i.e. grounding of rotating plate is not necessary and the plate moving outside the capacitor instead of inside the capacitor avoids wear and tear.

The design and realization of this novel high-performance capacitive rotation-speed transducer is described in this chapter. The transducer mainly consists of two equal capacitors out of which one is used as reference while the capacitance of the other changes with the increase of stray capacitance due to the presence of tooth of rotating conducting plate, which rotates with the member whose rotation-speed we want to measure. In this way capacitance varies periodically. When these capacitors are connected in an active bridge network, the periodic change in capacitance modulates the output

of the bridge. The low frequency of the periodic signal depends upon the speed of rotation. After amplification and demodulation of the output signal, a frequency proportional to speed of rotation is extracted. Accuracy and precision will depend upon the number of slots in the conducting moving plate. Experimental results comply with the simulated results appreciably.

3.2 PRINCIPLE OF OPERATION

The common transformer ratio bridge of Figure 3.1(a) has in principle its equivalent circuit in Figure 3.1(b), forms one of the basis for this work. In this figure when the third terminal, which is the shield, is connected to earth shielding capacitors C_{s1}, C_{s2} appear parallel to the equal arms of the transformer while C_{s3} is parallel to the detector with no effect on the measured current, and that the detector current is given by:

$$I_D = 2\pi f_1 V_m (C_{1x} - C_{1r}) \cos(2\pi f_1 t) \qquad \ldots (3.1)$$

where $V_m \sin(2\pi f_1 t)$ is the voltage on each of the equal transformer arms with frequency f_1, C_{1r} reference capacitor and C_{1x} is varying capacitor. If we use phase sensitive detector with 90° phase shift between the detector current and the reference signal V_{ref}, the resulting output signal will be proportional to the difference in capacitance (C_{1x} - C_{1r}). In our configuration, instead of the equal arms transformer we have used a simple electronic inverter and we keep the capacitances C_{1x} and

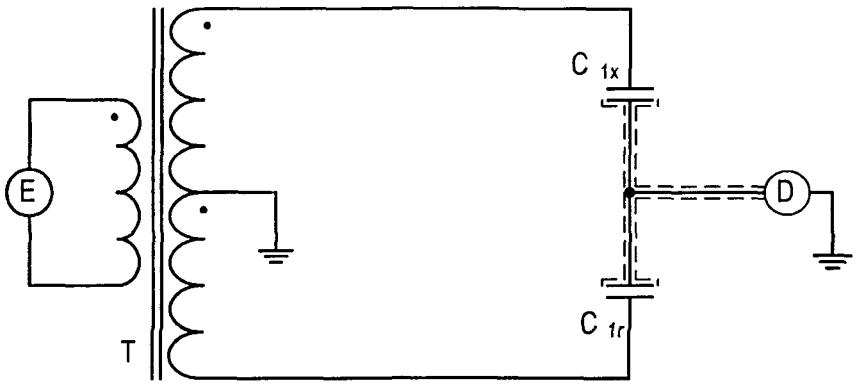

Figure 3.1(a): Transformer Ratio bridge Circuit Configuration and

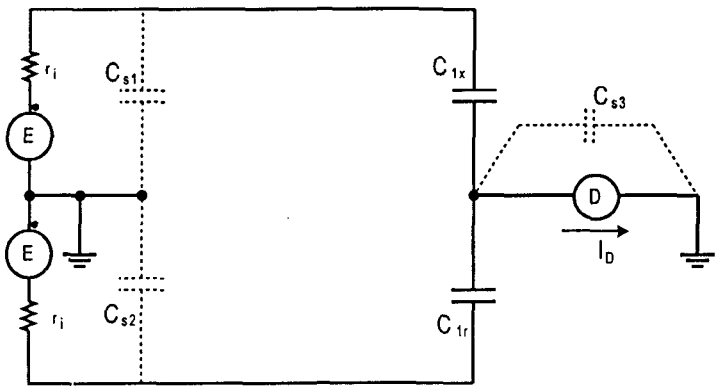

(b)The Equivalent Circuit of the Transformer Bridge

C_{1r} equal at steady state (ie I_D is zero). A floating plate (i.e. not grounded) is allowed to move over the electrodes of C_{1x} thereby affecting the balancing current due to the existence of new parasitic capacitors C_{p1} and C_{p2}, which are developed between the moving plate and the plates of C_{1x}. The rate of change is proportional to the speed of the moving plate.

3.2.1 The Sensor Description and Theoretical Aspects

Precise capacitors are usually completely enclosed by a conducting screen in order to make inter-electrode capacitance more definite. If the screen is connected to one of the electrodes to form two plates capacitor, the dielectric field between the screen and the other electrode contributes to the capacitance. This field affected by external leads to the capacitor with the result that the capacitor is uncertain. If the screen is not connected to either of the electrodes, the unit is said to be a three-terminal capacitor. When such a capacitor is used in suitable circuit, only the inter-electrode capacitance is effective and it is value is quite definite.The three-terminal capacitor principle is used to construct two fixed capacitors C_r is used as reference and C_x is left to be varying with the effect of the third plate moving overthe plates of C_x.

Capacitor C_r and C_x, as shown in Figure 3.2(a), are prepared on an insulating plate and they are of equal values. Each of the fixed electrodes has a maximum thickness T_m and effective area of *LxW*, and hence developing capacitances C_r and C_x, each is,

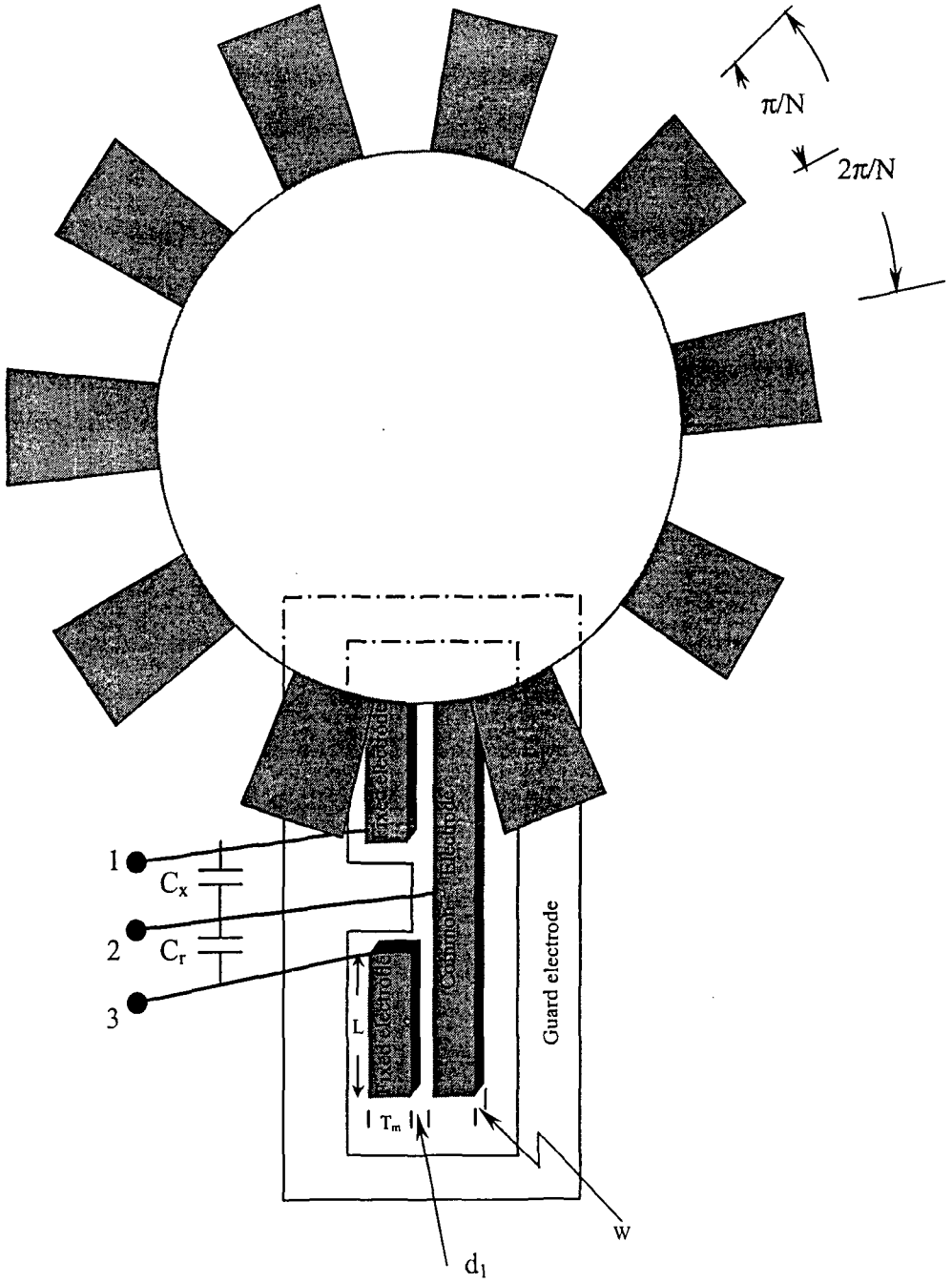

Figure 3.2(a): Physical Structure of The Sensor.

approximately, given by:

$$C_x = C_r = \frac{\varepsilon_o LW}{d_1} \qquad \ldots(3.2)$$

where ε_o is the permittivity of free space and d_1 is the distance between the two fixed electrodes.

When other plate is allowed to move over the fixed electrodes of C_x, acting on their thickness, again inter-plate capacitors C_{1p}, C_{2p} will be developed between the moving and the fixed electrodes see Figure 3.2(b). The equation of both the capacitors can, approximately, be given by: -

$$C_{1p} = C_{2p} = \frac{\varepsilon_o LT(t)}{d_2} \qquad \ldots(3.3)$$

where d_2 is the distance between the moving plate and the fixed electrodes, L is the length of the electrode and $T(t)$ is the active electrode thickness. The later is a function of time since it depends on the availability of the upper plate, which is moving. These generated capacitors are maximum and equal when the conducting segments are moving centrally over the fixed ones. Therefore, their maximum capacitance C_m is:

$$C_{1p} = C_{2p} = C_m = \frac{\varepsilon_o LT_m(t)}{d_2} \qquad \ldots(3.4)$$

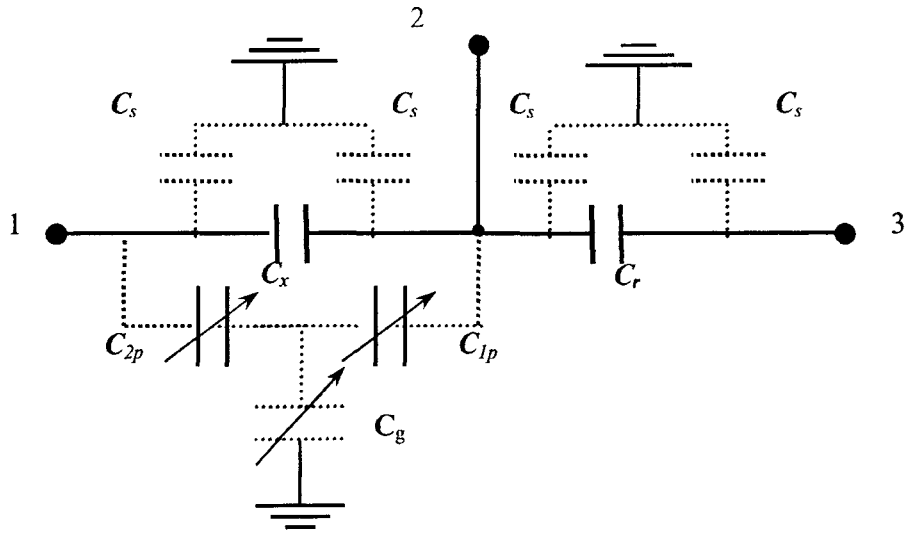

Figure 3.2(b): Electrical Circuit Equivalent of the Designed Sensor.

The series combination of the time dependent inter-plate capacitors C_{1p}, C_{2p} develops a capacitor ΔC_x across C_x, whose equation can be written as: -

$$\Delta C_x = \frac{C_{1p} C_{2p}}{C_{1p} + C_{2p}} \qquad \ldots(3.5)$$

The existence of ΔC_x gives rise to an unbalance current I at test point 1 of the circuit diagram of Figure 3.5, due to charge difference ΔQ that is given by:

$$\Delta Q = \Delta C_x V_m \sin(\omega t) \qquad \ldots (3.6)$$

$$I = d\Delta Q/dt = d(\Delta C_x V_m \sin(\omega t))/dt \qquad \ldots (3.7)$$

$$= \Delta C_x V_m \sin(\omega t + 90) + V_m \sin(\omega t).d(\Delta C_x)/dt \qquad \ldots (3.8)$$

where V_m is the maximum amplitude of the input sinusoidal voltage and ω is its the angular frequency. If ω is taken to be much higher than the angular frequency of the moving plate, this current will be the sum of two modulated functions. In both the functions the sine is the carrier signal and ΔC_x is responsible for the modulating signal. Capacitances to shield whose individual values are represented by C_s do not appear in the expressions because either they appear across supply or detector.

3.2.2 *Effects of the Gap between the guard and the surrounded Electrode*

Equation (3.2) is only in theory valid with infinitesimal small gaps between the guard and the surrounded electrode. In practice infinitesimal small gaps between adjacent electrodes are not realistic and there will be always a gap between the guard and the surrounded electrode. In general, the effective dimensions of electrodes lies in the center of these gaps. For thin electrodes on insulating material, the relative effect of these gaps on thecapacitance, as described by Heerens el at [3], in their analytical calculations, is given by the following equation:

$$\delta = \exp^{(-\pi s/d_1)} \qquad \ldots(3.9)$$

where s is the gap width between the guard and the surrounded electrode and δ is the relative change in the capacitance due to the gap width. This means that for a better than 100 PPM accuracy the gap width have to be smaller than one third of the electrode distance d_1. For thick electrodes with deep gaps between adjacent electrodes, the depth h of the gap s must be at least three times larger than the gap. In this case the relative effect is given by:

$$\delta = \exp^{(-\pi h/s)} \qquad \ldots(3.10)$$

3.3 SIMULATION STUDIES

The simulation studies were done based on the equations (3.3) though (3.8) and the rotation-speed, which is related to them through the time. The software employed in this simulation is Microsoft Visual C++ version 6.0. If the moving plate has N numbers of slot-pairs on the periphery of the conducting plate and it is rotating at a rotation-speed of n revolutions/ second, then the time durations can be calculated as:

Time taken for one revolution (sec.) = $1/n$

Time taken to cover one tooth (sec.) = $1/nN$

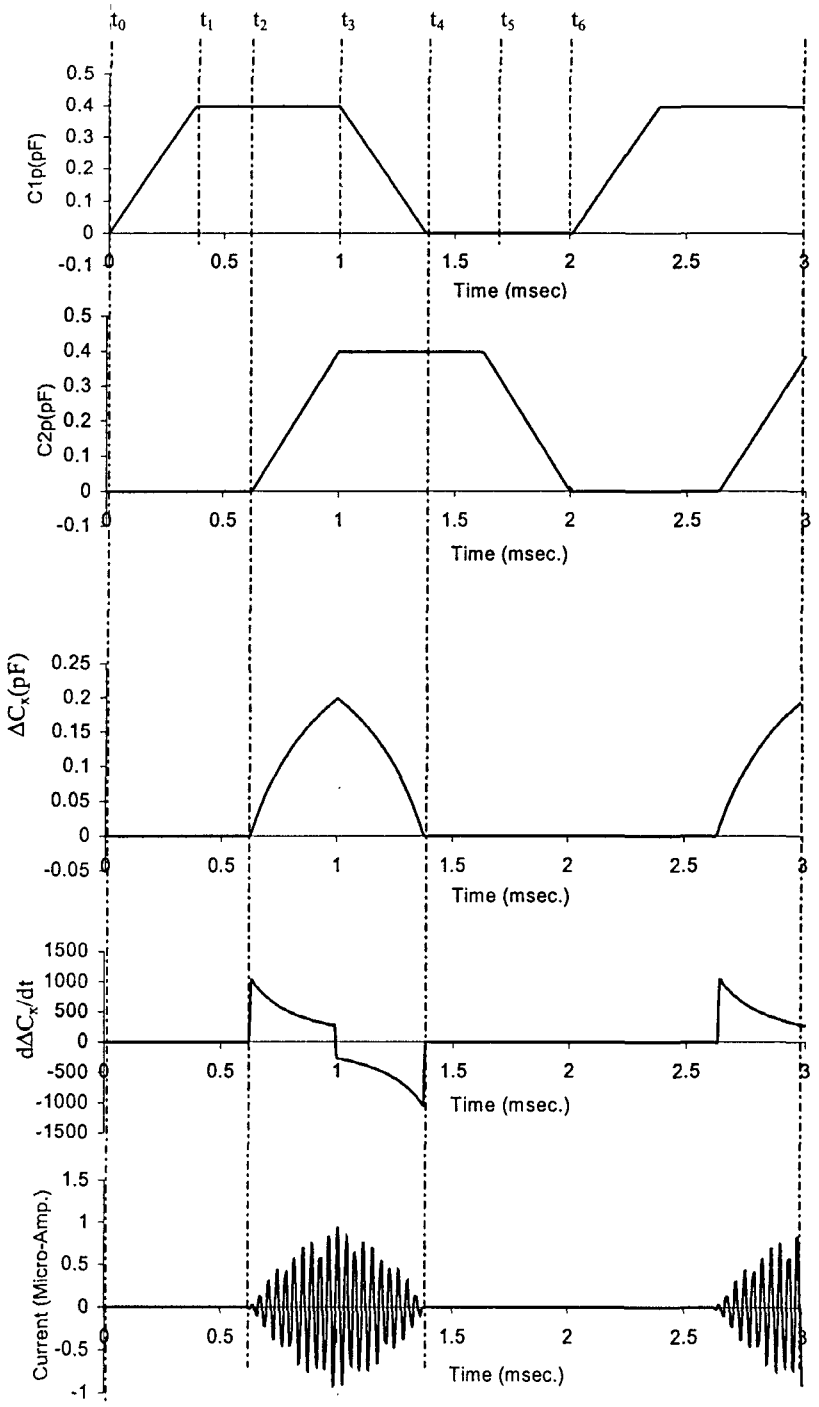

Figure 3.3: The Simulated Waveforms For Different Capacitance and Unbalance Modulated Output Current.

Since one tooth is designed to occupy the two plates each having maximum thickness T_m and the distance d_1 between them, then the time t_j taken by the moving plate to pass any angular distance (say Y) can be given by:

$$t_j\,(\text{sec.}) = \frac{Y}{nN(2T_m + d_1)} \qquad \ldots (3.11)$$

The waveforms of Figure 3.3 show the timing sequence t_1 to t_6 when the moving plate rotates to cross an angular distance of $2T_m + d_1$ (i.e. one tooth thickness). From the same figure, the effective timing is only in the duration between t_2 to t_4, since elsewhere at least one of the capacitors C_{1p} or C_{2p} is zero and the sensor uses the periodic capacitance changes to measure the rotation-speed.

Again Figure 3.3 shows the simulated waveforms for C_{1p}, C_{2p}, ΔC_x, $d\Delta C_x/dt$ and the unbalance modulated output current I for a moving plate with rotation-speed n = 100 revolutions/second, and T_m, d_1, d_2, L are 3, 2, 2, 15mm respectively. The results of this simulation show that it is possible to know the speed of rotation by demodulating and then measuring the frequency of the modulating signal so obtained. At the same time simulations were carried over for examining the characteristics of the output-modulated signal for three geometrical dimensions, (i.e. maximum thickness T_m, distance between the fixed plates d_1 and the distance of the fixed plates to the moving plate d_2). Tabulated results of the simulation are shown in tables (3.1), (3.2) and (3.3). Mathcad PLUS Version 6.0 Software Package is used for construction of the 3-D

T_m (mm)	Distance between the fixed electrodes d_1 (mm)								
	1	4	8	12	16	20	24	28	32
3	0.932	0.935	0.926	0.92	0.914	0.908	0.902	0.894	0.888
6	1.874	1.87	1.864	1.858	1.852	1.846	1.84	1.934	1.828
12	3.75	3.745	3.74	3.734	3.728	3.722	3.716	3.71	3.704
18	5.625	5.621	5.615	5.61	5.604	5.6	5.594	5.588	5.582
24	7.5	7.497	7.491	7.485	7.48	7.473	7.467	7.461	7.455
30	9.38	9.372	9.365	9.36	9.354	9.349	9.343	9.337	9.33
36	11.25	11.248	11.242	11.236	11.23	11.224	11.218	11.212	11.21
42	13.13	13.123	13.117	13.11	13.105	13.1	13.096	13.09	13.08
48	15.03	15	14.994	14.988	14.982	14.976	14.97	14.964	14.96

Table (3.1): The Maximum Output Current (μA) For a Distance d_2 = 1 mm and Different Values of T_m and d_1.

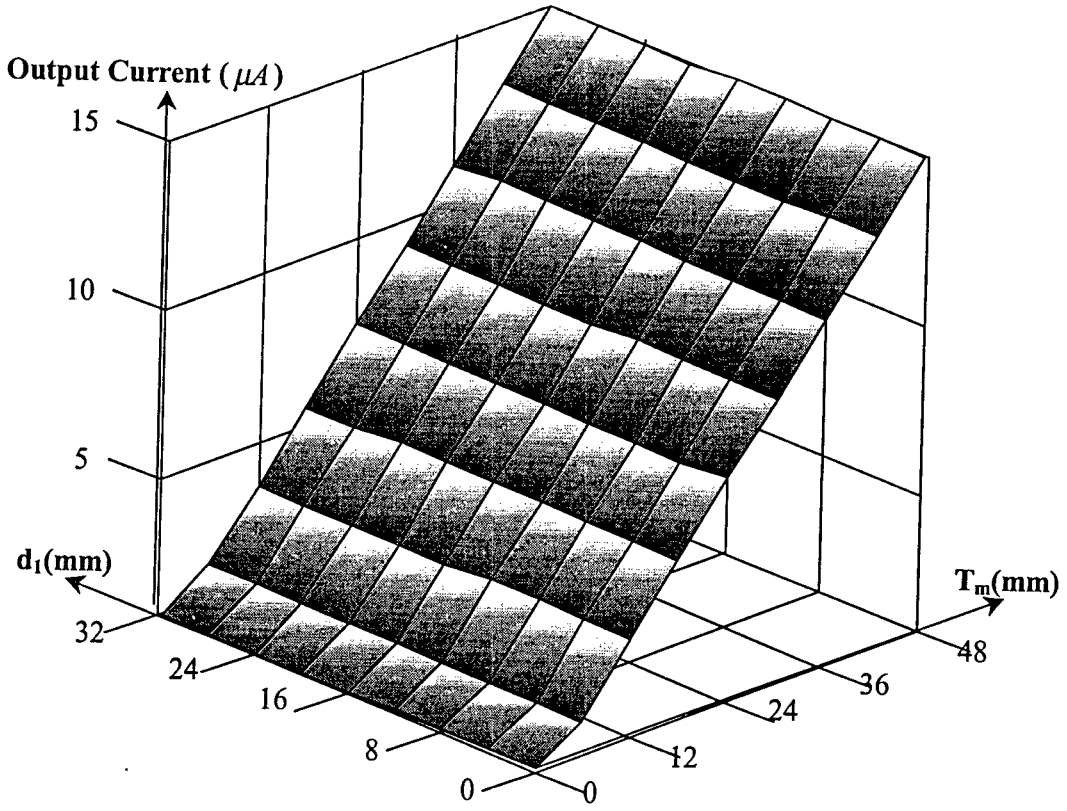

Figure 3.4(a): 3-D Surface Plot of the Maximum Output Current (μA) For a Distance d_2 = 1 mm and Different Values of T_m and d_1.

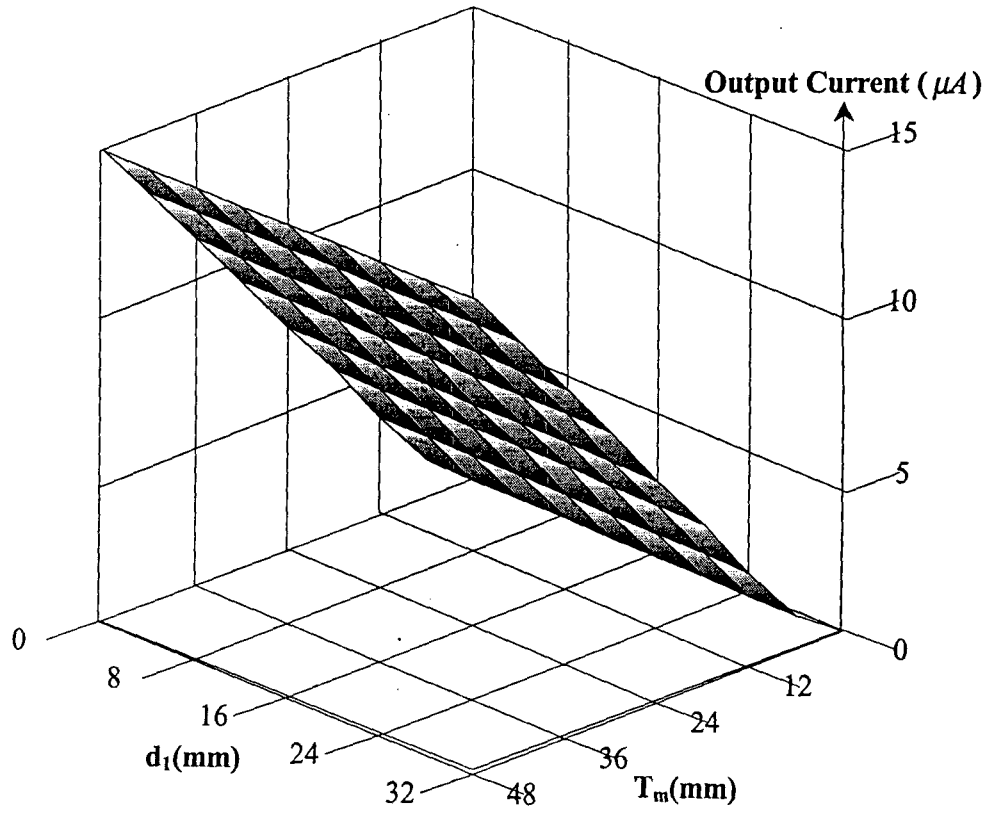

Figure 3.4(b): 3-Dimetional Surface Plot (Rotated 180°) of the Maximum Output Current (μA) For Different Values of T_m & d_1.

T_m (mm)	Distance between the fixed electrodes d_1 (mm)								
	1	4	8	12	16	20	24	28	32
3	0.856	0.6	0.429	0.333	0.273	0.231	0.2	0.177	0.157
6	0.923	0.75	0.6	0.5	0.43	0.375	0.333	0.3	0.273
12	0.961	0.857	0.75	0.667	0.6	0.545	0.5	0.461	0.429
18	0.973	0.9	0.82	0.75	0.693	0.643	0.6	0.563	0.529
24	0.98	0.923	0.857	0.80	0.75	0.705	0.667	0.631	0.6
30	0.983	0.937	0.882	0.833	0.79	0.75	0.715	0.681	0.653
36	0.987	0.947	0.9	0.857	0.819	0.784	0.75	0.721	0.692
42	0.989	0.955	0.913	0.875	0.841	0.807	0.777	0.75	0.725
48	0.989	0.96	0.923	0.889	0.857	0.827	0.8	0.775	0.75

Table (3.2): The Pulse Duration (ms) For a Distance d_2 = 1 mm and Different Values of T_m and d_1.

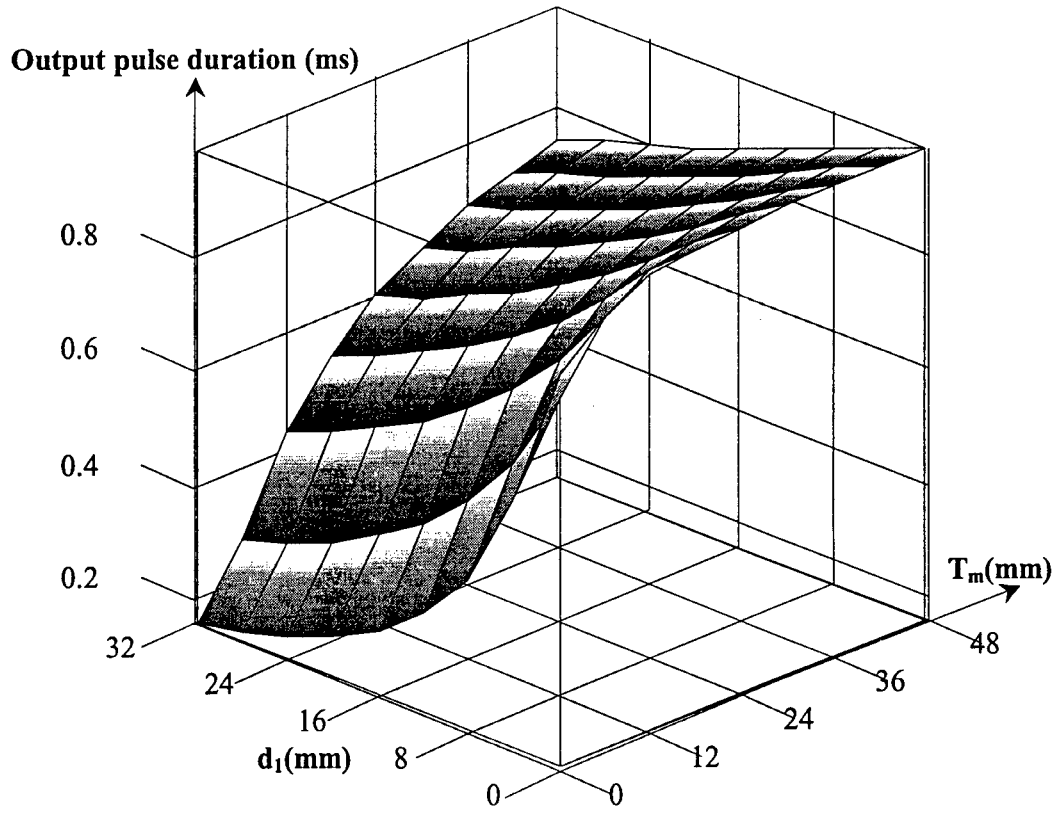

Figure 3.5(a): 3-D Surface Plot of the Pulse Dration (ms) For d_2 = 1 mm and Different Values of T_m & d_1.

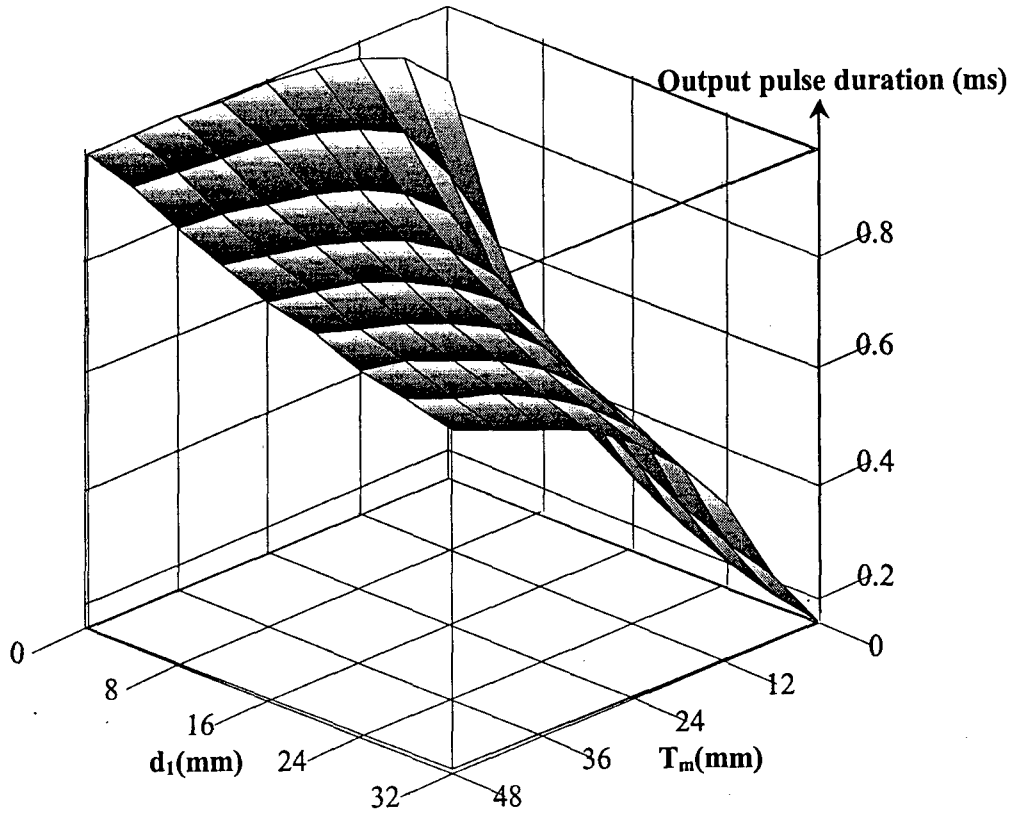

Figure 3.5(b): 3-D Surface Plot (Rotated 180°) of the Pulse Duration (ms) for d_2 = 1 mm and Different Values of T_m and d_1.

T_m (mm)	Distance between the fixed electrodes and the moving d_2 (mm)									Pulse duration (msec)
	1	4	8	12	16	20	24	28	32	
3	0.935	0.227	0.114	0.076	0.057	0.045	0.038	0.032	0.029	0.75
6	1.873	0.462	0.231	0.154	0.115	0.092	0.077	0.066	0.059	0.857
12	3.75	0.93	0.465	0.31	0.232	0.186	0.165	0.1	0.117	0.923
18	5.6	1.4	0.7	0.467	0.35	0.28	0.233	0.166	0.176	0.947
24	7.5	1.884	0.942	0.628	0.47	0.377	0.314	0.233	0.234	0.961
30	9.38	2.34	1.17	0.779	0.584	0.467	0.39	0.3	0.293	0.967
36	11.24	2.8	1.4	0.935	0.7	0.56	0.468	0.367	0.35	0.973
42	13.11	3.275	1.64	1.09	0.82	0.655	0.546	0.434	0.41	0.978
48	14.99	3.744	1.87	1.25	0.936	0.75	0.624	0.535	0.464	0.98

Table (3.3): The Maximum Output Current (μA) For a Distance d_1= 2 mm and Different Values of T_m and d_2.

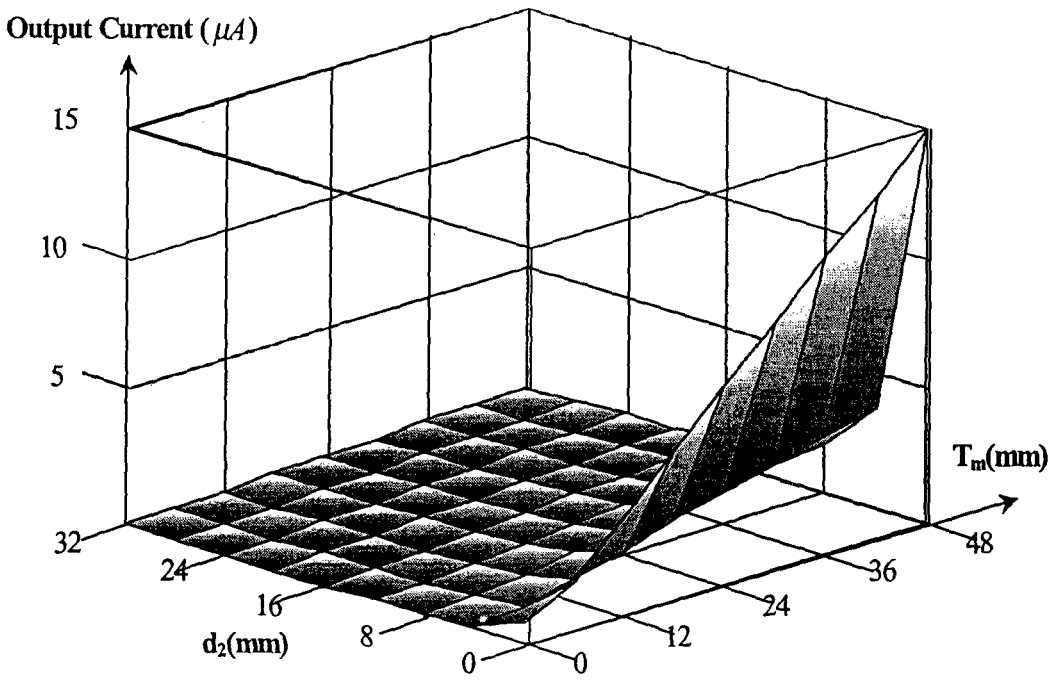

Figure 3.6 (a): 3-D Surface Plot of the Maximum Output Current (μA) For a Distance d_1 = 2mm and Different Values of T_m and d_2.

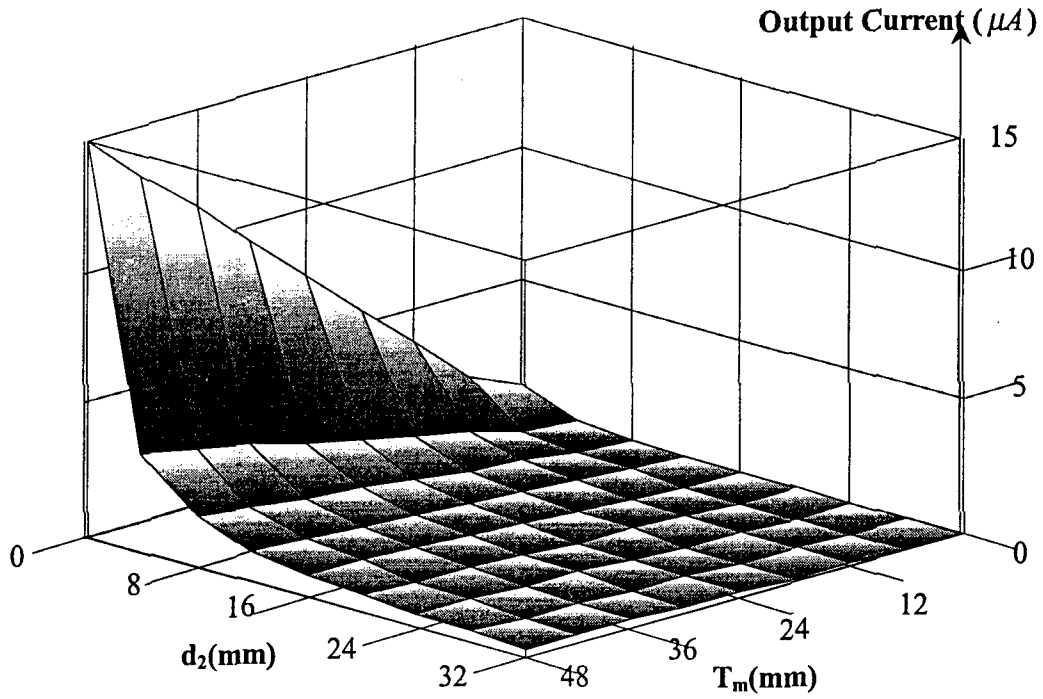

Figure 3.6 (b): 3-D Surface lot (Rotated 180°) of the Maximum Output Current (μA) For a Distance d_1= 2 mm and Different Values of T_m and d_2.

3.4 EXPERIMENTAL SETUP AND RESULTS

The complete experimental signal processing circuit is shown in Figure 3.7. In the current-to-voltage converter, due to the virtual ground at the amplifier input, the current through R_2 is zeroand the unbalance current I flows through R_f. thus the amplifier output voltage $V = -IR_f$. It is common to parallel R_f with a capacitor C_f to reduce the high frequency noise and possibility of oscillations. It must be pointed that the bias current of the inverting input sets the lower limit on the current sensed with this (I-to-V) circuit. This converter and the remaining amplifiers in the circuit have been implemented with the Operational Amplifier LF-356 with it is well known salient features such as low power consumption, high input impedance, the bias current in the order of nano amperes etc. The electrodes of both the reference and varying capacitors were made of brass with dimensions (15x3x3mm) of length, width and thickness, respectively. The simple copper clad plate was used for the moving plate teeth, each with dimensions (15x8mm). They were arranged on a circular plate as in Figure 3.2(a). The reference and varying capacitors were arranged in an active bridge circuit, which is balanced when the conducting part of the rotating plate is not brought near it. The modulated output waves were processed through a demodulator; amplifiers and comparator giving the final circuit output as a square waves whose frequency represents the speed of rotation.

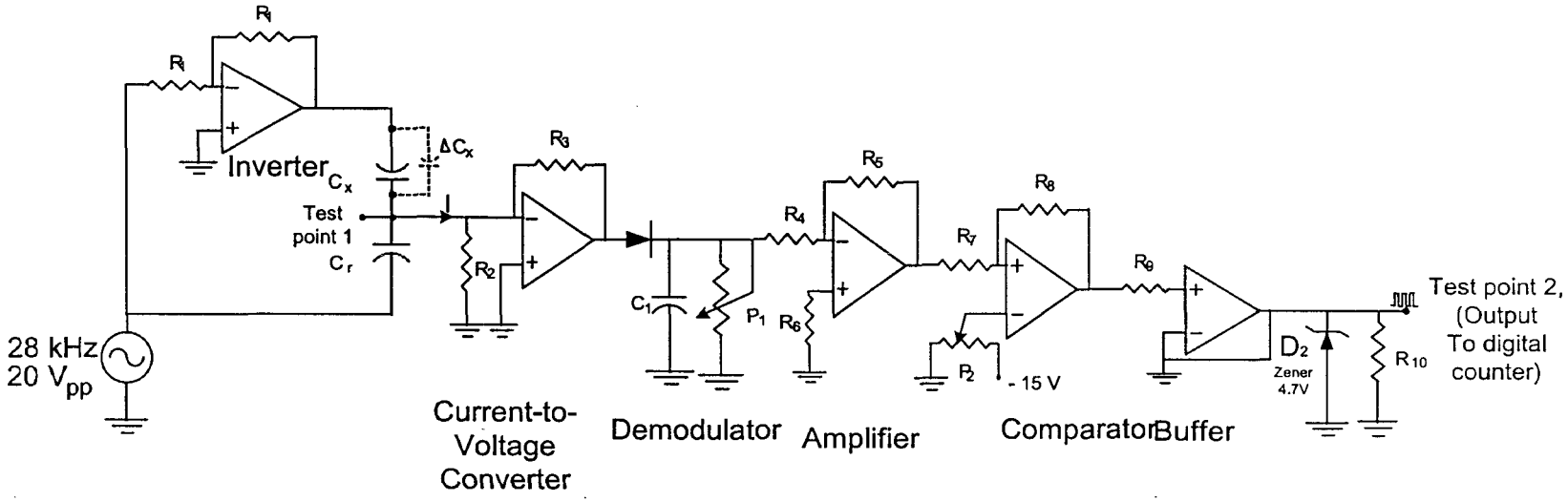

R1 =R2 =22KOhm;
R4 =R6 =R7 =3.3KOhm;
R5 =R8 =R9 =R10 =10KOhm

Figure 3.7:

The Complete Experimental Signal Processing Circuit.

A two-channel digital real-time oscilloscope Tektronix type, Model TDS 360 was used to display the experimental waveforms for the test points 1 and 2 of Figure 3.7, which are shown in Figure 3.8. At test point 1, the output is an amplitude-modulated signal while that of test point 2 is a rectangular signal. These final rectangular output waves of the circuit can be given to a counter to read the frequency that is directly proportional to the rotation speed of the moving member.

All the connecting cables used in the electronic circuit were shielded as this is recommended when dealing with low-level signals. Also the capacitors were guarded in order to ensure that the field changes would not influence the values of the capacitances. In addition, to limit the influence of the guard electrode on the capacitors, Heerens guard rules [1], [3] for the capacitive sensor were applied.

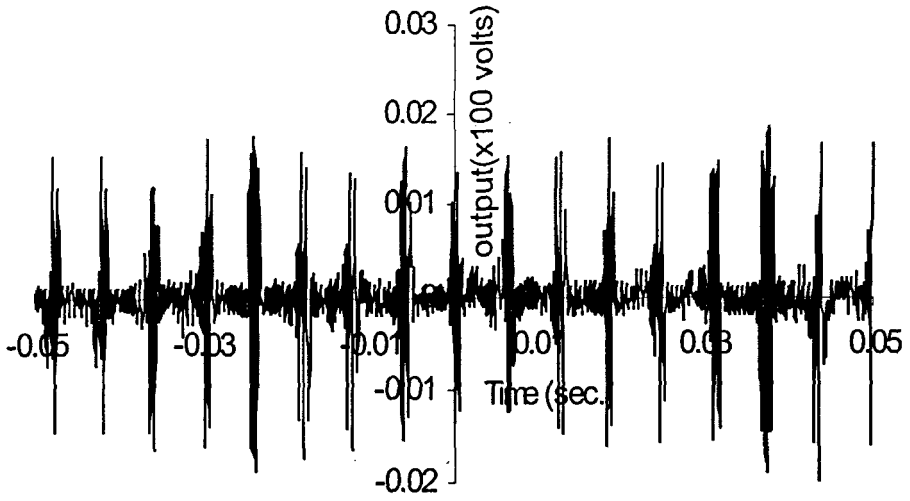

(a) Output at Test point 1.

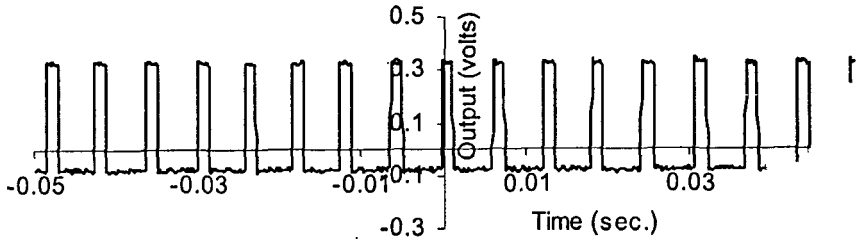

(b) Output at Test point 2.

Figure 3.8: The Experimental Output Waveforms at the Test Points of Figure 3.7.

CHAPTER FOUR

Digital Capacitive Absolute Encoder For Translatory Motion

CHAPTER IV

DIGITAL CAPACITIVE ABSOLUTE ENCODER FOR TRANSLATORY MOTION

4.1 INTRODUCTION

In measurement practice we deal with physical quantities and it's very important that their values should be efficiently and accurately represented. Basically there are two ways for representing the numerical values of these quantities, analog and digital. The devices used for such purposes, in instrumentation, are called analog or digital transducers.

Unfortunately, nature has not provided any phenomena that have direct digital output. But the increasing presence and use of digital systems for measurement, control and data handling leads naturally to a need for transducers which provides a digital output. A digital output from a transducer enables direct acquisition of a digital system and simplifies processing for a digital readout or for control purposes [48]. Also due to the ease and versatility provided by digital signal processing circuits and digital computers now days, digital transducers that gives output signals directly in digital form are preferable over the analog ones [49]. Digital transducers themselves are further divided into two basic forms i.e. absolute and hybrid digital type. As there are only a few such digital transducers, in many cases the

output of analog transducer may be converted to into digital signals using analog-to-digital converter. Similarly, transducers whose output signals are sinusoidal and the frequency of which is related to measurand are considered to be hybrid digital type when working in combination with digital frequency measuring system. With the increasing applications of digital computers, absolute digital transducersthat are compatible with the digital nature of the computer are coming into reality now days to replace both analog and hybrid types. One of the absolute digital transducers is the digital encoder for linear and angular displacements. These convert motion directly into digital output signals. Brush or contact type and optical type encoders both are used in practice.

In this chapter we presents a new digital encoder that is based on the capacitive transduction. Among the advantages of the capacitive sensing principle is its simplicity, high response speed, insensitiveness to dirt and mostly they are compact. Additionally the resolution of this capacitive-encoder can easily be adjusted, according to its application, by adjusting the effective areas of the capacitor plates. It provides direct digital output signal from linear or rotary displacement. Thus overcomes the disadvantages of the practically existing encoders. It can be used in variety of applications in automatic control of machine tools like door monitoring machines, CNC machines & robots, mixing machines, automatic screwdrivers, ultrasonic welding machines, spinning and weaving machines and in the measurement of level, pressure, etc. The prototype developed has five bits output with a resolution of 1 mm when designed for translatory motion.

Liquid-level measurements are widely employed to monitor as well as measure quantitatively the liquid content in vessels, reservoirs and tanks, and variety of other similar cases in industrial processes. One of the most common types of level sensors having wide applications is the capacitive sensor. The device essentially consists of a concentric type electric probe inserted into the tank, and the liquid acts as the dielectric. The main advantage is that the system is not applicable for conducting liquids. Other method utilizes a float or displacer as primary element. The principle is based upon buoyancy effect and any change in the apparent mass density affects the accuracy. The float is mechanically coupled to a displacement sensor such as potentiometer or linear variable differential transformer, which are characterized by proportional analog output. The designed capacitive encoder uses the same principle, but once the system is light in weight and smooth, only very light float is needed. This makes the system indication independent of slight variations in the liquid density. Also brush type encoders are available having friction, wear and tear disadvantages, while optical type suffer mainly from dusty environment. The transducer designed, fabricated and successfully tested in this chapter, may be the best simple, rugged, accurate digital level measuring device.

4.2 THEORY AND OPERATING PRINCIPLES

In this section we present the structure, features and theoretical background along with the treatment of the factors that may affect the sensor output.

4.2.1 Physical Structures of the Developed Encoder

The block diagram given in Figure 4.1(a) shows the details of the encoder that consists of one stationary rectangular copper clad plate, which accommodates five rows. Each row is divided into a small rectangles arranged as conducting and non-conducting forms to represent the bits of the digital code used. The smallest rectangle in the stationary plate has an area of 1x10mm. The conducting rectangles of each row are connected together as well as to the signal processing circuit while the remaining all are grounded to serve as guard electrode. A higher potential plate (HPP) having the length l of 1mm and width covering the width of the whole stationary plate is allowed to move over it parallel to its surface keeping very small gap. When this plate comes over each conducting part of each row in the stationary plate, a capacitance of few Pico-Farads is developed. The equation of this capacitor can be, approximately, given by:

$$C_i = \varepsilon_o wl/d \qquad \ldots(4.1)$$

where ε_o is the permittivity of free space, d is the distance between the two plates; l is the length of the higher-potential plate, w width of each row in the lower-potential plate.

The charge Q developed on the capacitor plates and the current I through it, when supplied with sinusoidal input, can be given by the following equations:

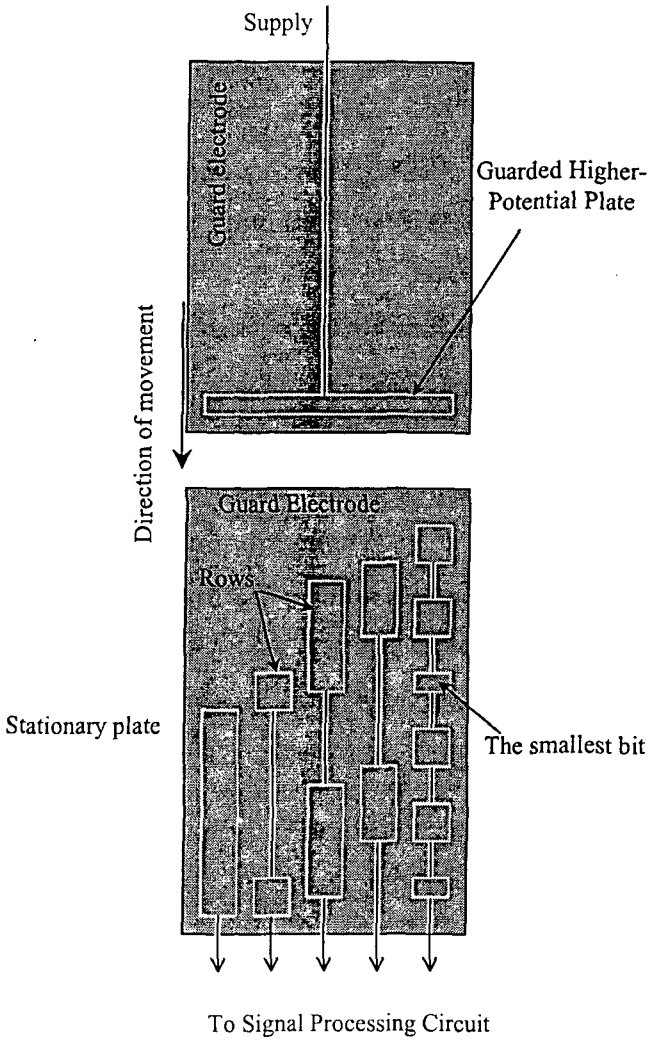

Figure 4.1(a):

Complete Details of Lower-Potential Plate Made on Copper Glade Plate. White Lines Represent Insulator and Black are Conductors.

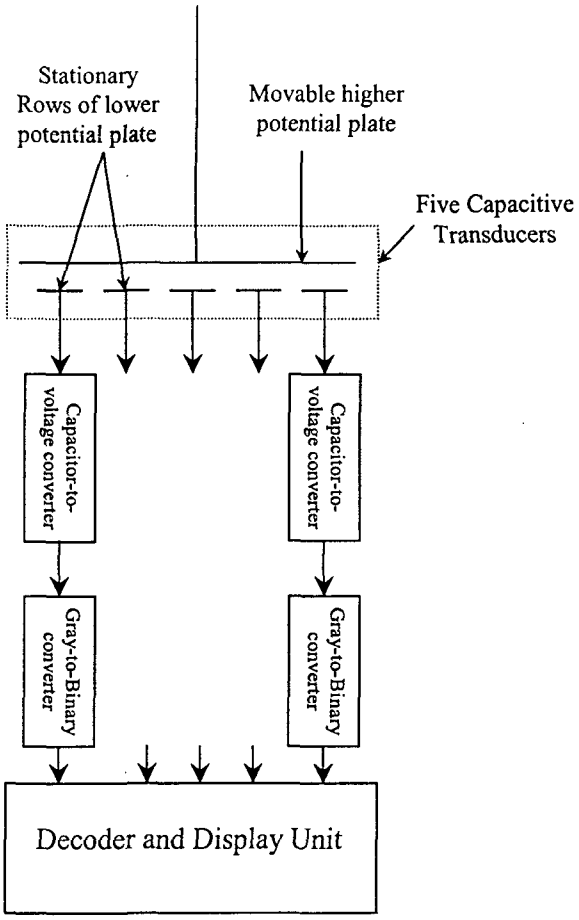

Figure 4.1(b): Parallel Plate Capacitors Formed by Movement of Higher-Potential Plate.

$$Q = C_i V_m \sin(\omega t) \qquad \ldots (4.2)$$

$$I = dQ/dt = d(C_i V_m \sin(\omega t))/dt \qquad \ldots (4.3)$$

$$= C_i V_m \sin(\omega t + 90) + V_m \sin(\omega t).d(C_i)/dt \qquad \ldots (4.3)$$

where V_m is the maximum amplitude of the input sinusoidal voltage and ω is its the angular frequency. The voltage across this capacitance is processed through an electronic circuit, which displays the digits, that corresponds to the position of the moving plate, as it will be discussed in section 4.4.

4.2.2 Features of The New Encoder

Our encoder uses the gray code instead of natural binary code. In the later the motion from one position to the next may require a change in more than one digit. If due to any misalignment during the change, all the digits do not change simultaneously as required an error can occur in indication. While in the gray code during such change, only one digit needs to be changed at a time. The encoder gives digital readout, which is an indication for the position of the higher potential. This system overcomes the disadvantages of the brush type, such as wear of brushes and friction between brushes and the disk and that it's less affected by dirt and dust in comparison to optical type.

Generally, these encoders are cheaper in cost and can be made to have many degrees of accuracy and precision provided that the copper clad plate is made large enough to accommodate the required number of rows for the required number of digits. The resolution of encoder depends upon the number of digits comprising the binary number. And because of their reliability, encoders have been used almost in every sphere of automation.

4.2.3 Sensitivity to the Geometrical Dimensions and Tilt of the Electrode

The capacitance of this transducer, C_i, is of the well-known parallel plate type having its sensitivity follows linearly the change in the effective area of electrodes and the permittivity of the medium separating them, while its non-linear to changes in the electrode's distance. We examine C_i for the effect of tilting the moving electrode through a small angle a that shown in Figure 4.2(a).

The separation on the right border of the electrode will increase by distance δ and the left border decreases the same distance, given by: -

$$\delta = (l \sin\alpha)/2 \text{, For small angles, } \sin\alpha = \alpha \text{ and}$$

$$\delta \cong l\alpha/2 \qquad \ldots(4.5)$$

Assuming the electric field Ψ to be of a two-dimensional polar coordinate (r, φ), Ψ can be written as:-

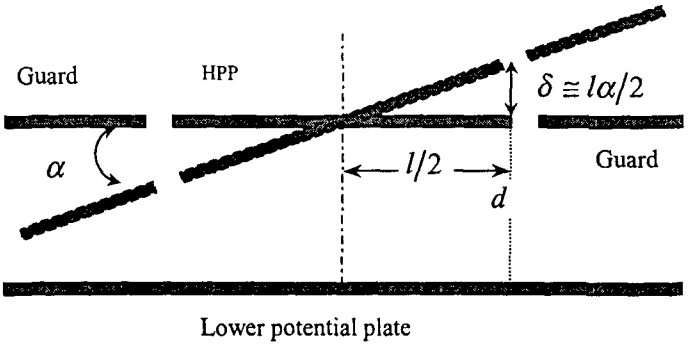

Figure 4.2(a):Moving Electrode Tilted Through an Angle α.

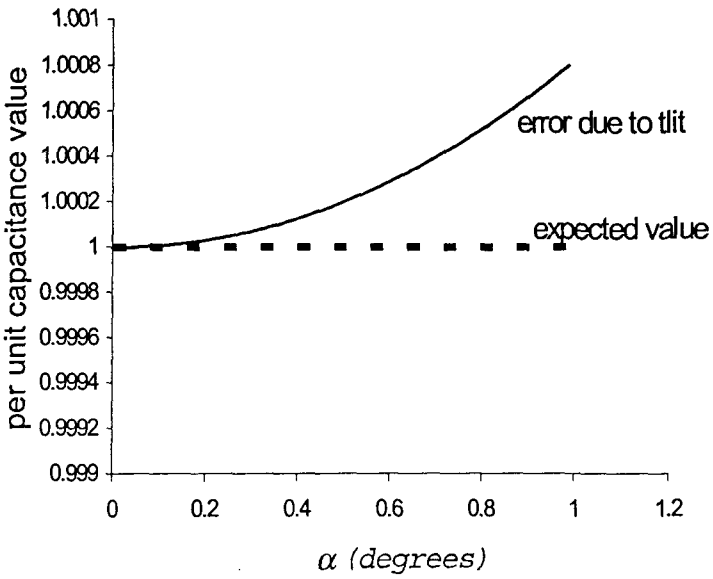

Figure 4.2(b): Per Unit Error Due to the Tilt Angle α.

$$\psi = \begin{pmatrix} -V\sin\alpha/\alpha r \\ V\cos\alpha/\alpha r \end{pmatrix} \qquad \ldots(4.6)$$

Taking integration of Ψ over these new borders, assuming $\varphi = 0$, will give the charge on the stationary electrode to be:

$$Q = \varepsilon_o \int_{d-\delta}^{d+\delta} (V/\alpha r)dr \qquad \ldots(4.7)$$

Solving this results in the following:

$$Q = \frac{\varepsilon_o V}{\alpha} \ln\left(\frac{2d + l\alpha}{2d - l\alpha}\right) \qquad \ldots(4.8)$$

Using Sympson's approximation formula [50]:

$$Q = \frac{\varepsilon_o l V}{d}\left(1 + \frac{l^2\alpha^2}{12d^2 - 3l^2\alpha^2}\right)$$

Or
$$C_i = \frac{\varepsilon_o l}{d}\left(1 + \frac{l^2\alpha^2}{12d^2 - 3l^2\alpha^2}\right) \qquad \ldots(4.9)$$

In this case a tilt angle up to 1° will cause an error of less than 0.08% in the capacitance value. That is due to the fact that we choose l very small compared to d. the change in capacitance for varying tilt angle is shown in Figure 4.2(b).

4.2.4 Elimination of Parasitic Capacitances and Resistors

The measurement of the capacitance C_i between the two parallel plates often has to deal with parasitic capacitances and resistors. All these appear in the equivalent circuit of Figure 4.3. During measurement the parasitic capacitances C_{p1} & C_{p2} appear in parallel with the voltage source V and the low impedance current detector D, respectively. Thus having virtually no effect on the current flowing through C_i. The effect of C_{p3} can be eliminated by offset nulling the detector before the measurement starts. The parasitic resistors R_{pp} & R_{ps} introduce both high and low cutoff frequencies. Therefore, if the operating frequency is chosen such that it lies between the cutoff frequencies, the parasitic resistors will not affect the measurement procedure Joost *el at* [47].

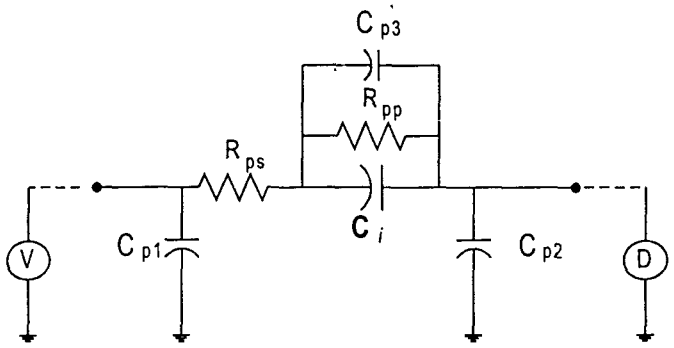

Figure 4.3: Sensor Capacitance C_i With Possible Parasitic Capacitors and Resistors.

4.3 DESCRIBTION OF THE SIGNAL PROCESSING CIRCUIT

The output of each row is processed through an electronic circuit, which consists of two units namely; Capacitor to voltage converter and coding-decoding & display unit.

4.3.1 Capacitor-to-Voltage Converter

The capacitor-to-voltage converter itself contains three blocks charge amplifier, precision half-wave rectifier and low-pass filter.

(a) Charge Amplifier:

In the charge amplifier circuit, C_i is the capacitance of the capacitive transducer (single row of the encoder) and C_f is connected in the feedback path of the amplifier. The potential difference across the plates of the transducer is amplified using operational amplifier having considerably high input resistance and low input capacitance in comparison to those of the transducer. Also, the connecting cables are shielded as this is recommended in the general-purpose low-level signal, otherwise they may affect the measurement [51]. For a sinusoidal input voltage $V_i(j\omega)$, with these assumption, the input-output voltage relationship will be:

$$V_{o1}(j\omega)/V_i(j\omega) = -j\omega R_f C_i/[1+j\omega R_f C_f] \qquad \ldots(4.10)$$

If the feedback capacitor C_f and the resistor R_f are chosen such that $\omega R_f C_f >> 1$, then:

$$V_{o1}(j\omega)/V_i(j\omega) \cong -C_i/C_f \qquad \ldots(4.11)$$

(b) Precision Half-wave Rectifier:

In the circuit of the fast, precision half-wave rectifier V_{o1} is a sinusoidal input voltage as it is derived in equation (4.11) above. In order to rectify milli-volts we place the rectifying element in the feedback pass of the operational amplifier. Hence its threshold voltage $(\cong 0.6V)$ is divided by the open loop gain of the amplifier $(\cong 10^5)$. Now it approaches ideal rectifying component by conducting for a voltage of $(\cong 6\mu V)$. When V_{o1} goes negative, D_1 is forward bias (ON), D_2 is reverse bias (OFF) hence the output of the inverting amplifier is:

$$V_o = -(R_2/R_1)V_{o1} \qquad \ldots(4.12)$$

If V_{o1} goes positive, D_1 is OFF and D_2 ON. Because of the feedback through D_2, a virtual ground exists at the inverting input and V_o is equal to zero. In this way the circuit performs half-wave rectification. Its principal limitation is the slew rate of the operational amplifier. In order for the conduction to switch very rapidly from $-V_{ss}$ to $+V_{ss}$ (or vise versa) the switching time of the amplifier must be a small fraction of period of the input sinusoidal voltage.

(c) Low-pass Filter:

Cascading this with the low-pass filter as shown in Figure 4.4, if V_{o1} is an amplitude-modulated carrier, the RC filter removes the carrier and the output is proportional to the average value of the low frequency signal. In other words, this configuration represents an average voltage detector. This followed by a comparator circuit for controlling the final output to + 5 volts through so as to be suitable for digital applications.

4.3.2 Coding-Decoding And Display Unit

Each group of 4-adjacent rows of the encoder, starting from the least significant bit (LSB), forms a group of 4-gray code taken to the inputs of the exclusive OR-gates which convert them into their binary code equivalent. These binaries are fed to the decoder that converts them into their appropriate decimal number. Figure 4.5 shows this arrangement, in which the most significant bit (MSB) remains unchanged during conversion or decoding process. The decoder is a combinational logic circuit that recognizes the presence of specific binary number. It converts the binary number into the format required to activate the appropriate segments in a seven-segment decimal display. The whole circuit interprets these incoming binaries produced by the movement of the higher potential plate and produces an output that derives a seven-segment common-anode LED display [52].

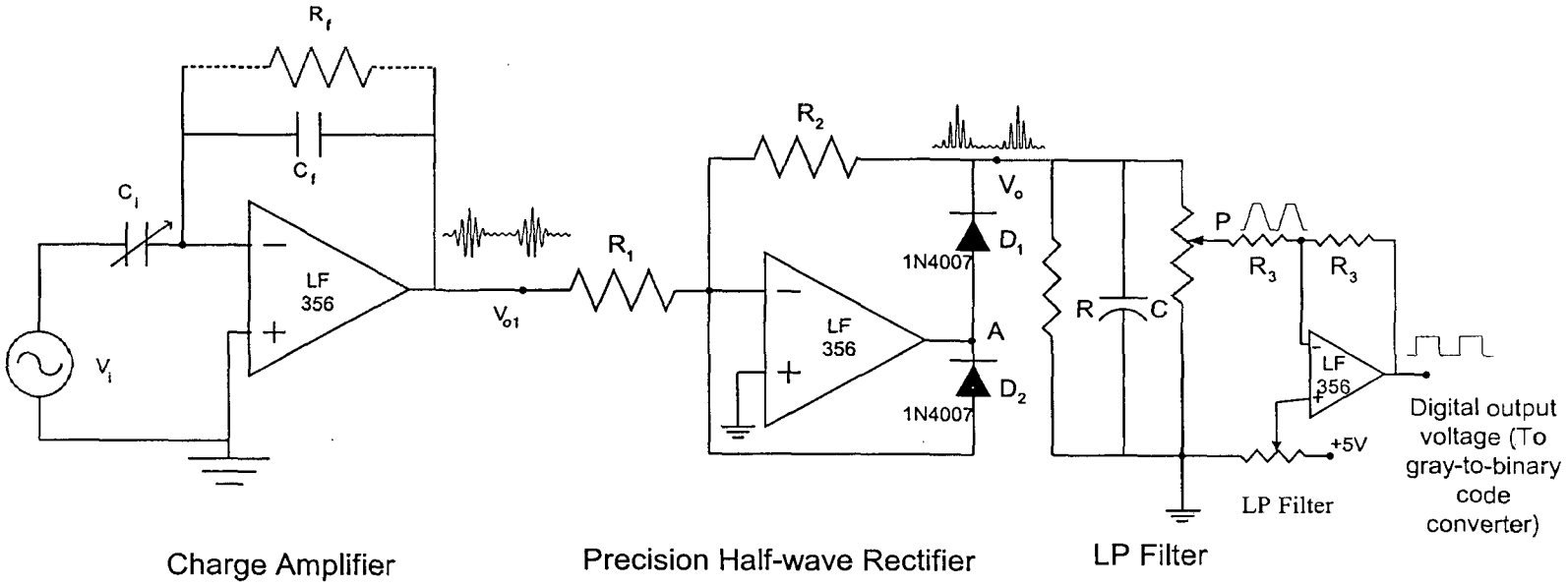

Figure 4.4: Capacitance-to-voltage Converter

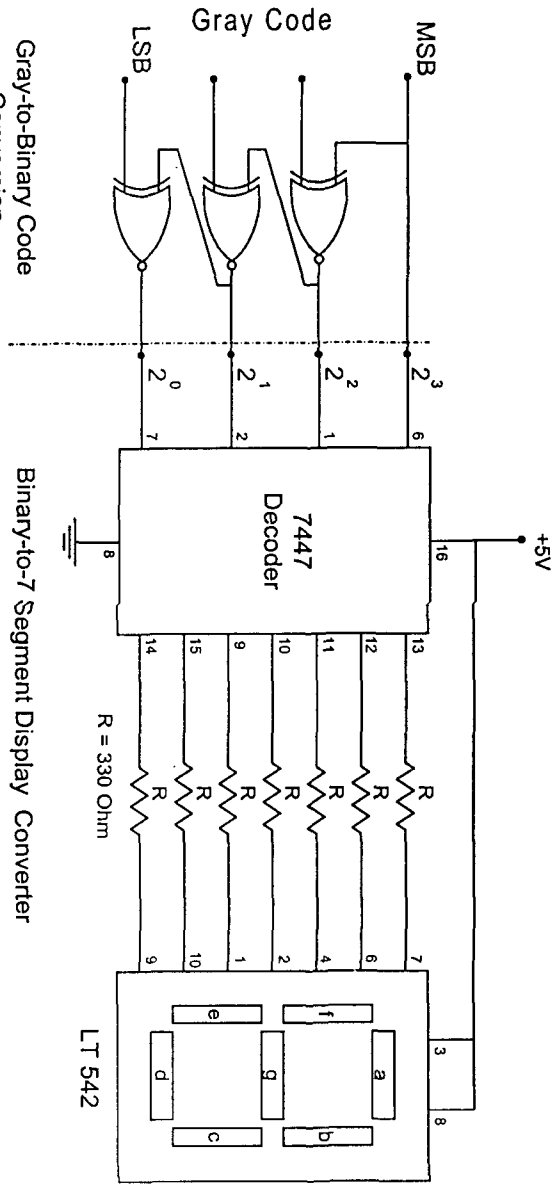

Figure 4.5: Coding-Decoding And Display Unit

4.4 EXPERIMENTAL RESULTS

Prior the implementation, a simulation studies were carried out based on the above equations and the position of the higher-potential plate, which is related to the capacitance developed in each row of the stationary plate. Considering the capacitor to be placed in a signal processing circuit and supplied with a sinusoidal voltage of 20 volts (peak-to-peak) and frequency of 1 kHz. The simulated normalized capacitance values along with the output waveforms of the modulated, rectified and digital output voltages for two rows of the encoder are shown in Figure 4.6. This simulation was done using Microsoft Visual C++ package. The results of this simulation shows that it is possible to get pure digital output by rectifying and demodulating the output signal so obtained from the encoder capacitance and that is displaying the position digitally. The experimental work is then carried with a signal processing circuit, which consists of capacitance to voltage converter and coding-decoding and display unit.

As an application, the encoder was tested for measuring a liquid-level. The output results are tabulated in table (4.1), which are consistent with the predicted theory and the digital output signal obtained is free from errors.

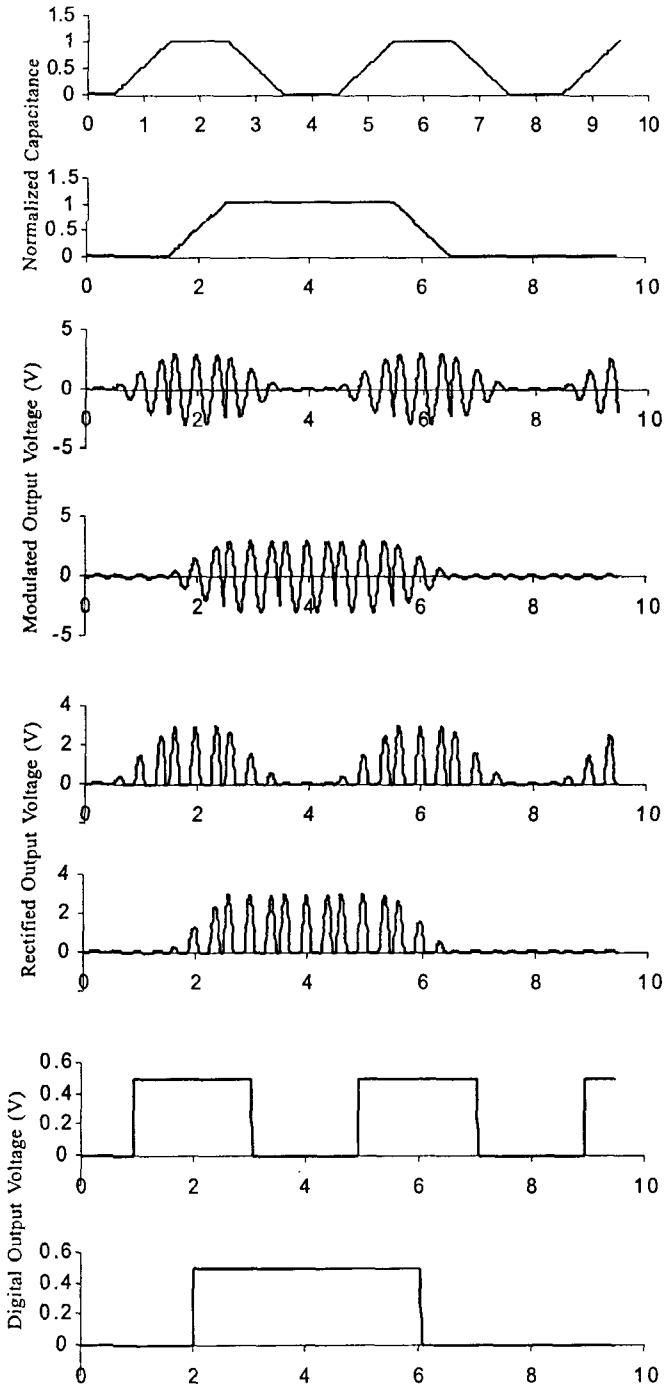

Figure 4.6:

Simulated Output Results for Two Rows of the Encoder.

Level (mm),	Gray output	Binary output	Displayed output
0	00000	00000	0
1	00001	00001	1
2	00011	00010	2
3	00010	00011	3
4	00110	00100	4
5	00111	00101	5
6	00101	00110	6
7	00100	00111	7
8	01100	01000	8
9	01101	01001	9
10	10000	01010	10
11	10001	01011	11
12	10011	01100	12
13	10010	01101	13
14	10110	01110	14
15	10111	01111	15
16	10101	10000	16
17	10100	10001	17
18	11100	10010	18
19	11101	10011	19

Table (4.1):
Experimental Results for Liquid Level Measurements

CHAPTER FIVE

A Novel Method For Liquid Viscosity Measurement Using Piezoceramic (PZT) Transducer

CHAPTER V

A NOVEL METHOD FOR LIQUID VISCOSITY MEASUREMENT USING PIEZOCERAMIC (PZT) TRANSDUCER

5.1 INTRODUCTION

The determination of the viscosity is one of the important parameters to characterize the dynamic physical properties of fluid materials. It must be monitored during industrial production of fluid-type materials in order to ensure consistent quality and automatic control. If a fluid is flowing over a surface, the molecules next to the surface (the ones clinging to the walls) have zero speed. As we get farther away from the surface the speed of molecules increases. This difference in speed is due to the friction of molecules being pushed past each other. The amount of clinging-ness between the molecules is called viscosity and it is proportional to the friction. An other definition is that; If a shear stress is applied to any portion of confined fluid, the fluid will move and a velocity gradient will be set within it. If the shear stress per unit area at any point is divided by the velocity gradient, the ratio obtained is defined as the viscosity of the fluid medium. Therefore, the viscosity is a measure of the internal fluid friction, which tends to oppose any dynamic change in the fluid motion [53]. Thus, viscosity determines the amount of friction, which in turn determines the amount of energy absorbed by the flow. Viscosity is resistance of a fluid to a

change in shape, or movement of neighboring portions relative to one another and viscosity denotes opposition to flow. Continuous viscometers generally measure either the resistance of flow or drag or torque produced by movement of an element through the fluid.

There are many ways developed in the past to measure viscosity; capillary tubes are used by the great French physician, Jean Louis Poiseuille (1799 - 1869) while he is interested in the forces that affected the blood flow in small blood vessels caused him to perform meticulous tests on the flow resistance of liquids. Attaching a torque wrench to a paddle and twisting it in a fluid is an other method. Using a spring to push a rod into a fluid, and seeing how fast a fluid pours through a hole is a third method. These three methods are suitable for comparison type of viscosity measurement. One of the oldest and easiest ways is to see how fast a sphere of known size and mass falls through a fluid and measuring its terminal speed. The faster the sphere falls, the lower the viscosity. This makes sense; if the fluid has a high viscosity it strongly resists flow, so the sphere falls slowly. If the fluid has a low viscosity, it offers less resistance to flow, so the ball falls faster. The measurement involves determining the velocity of the falling sphere, which is accomplished by dropping the sphere through a measured distance of fluid and measuring how long it takes to traverse the distance. Thus, knowing the distance and time, Stokes came up with a formula (known as Stroke's great law of viscosity) that can predict the rate at which a sphere falls through a viscous gas or liquid. The

formula for determining the viscosity is given as:

$$viscosity = \eta = \frac{2(\Delta\rho)ga^2}{9v} \qquad \ldots(5.1)$$

$\Delta\rho$ = Difference in density between the sphere and the liquid.

g = Acceleration of gravity.

a = Radius of sphere.

v = Velocity = (distance sphere falls)/(time of it takes to fall).

The measurement should be repeated many times to arrive at a good average value. This allows an assessment of the uncertainty in the measurement. Using spheres of different radii and densities and measuring the viscosities of at least two liquids gives an idea of this unusual physical property and the power of the equation to predict the behavior [54].

Each of the above methods has its own principle of operation and unique features for measurement [55]. But they are all either made under steady state or low frequency. It is not always possible to take periodic samples for viscometer, on the account of high pressure, high temperature, etc. In these situations acoustics can play an important role in determining the dynamic viscosity of the liquid materials, since this viscosity is related to the acoustical properties of the material under test. Among the advantages of acoustic waves, which we believe make their use preferred over the previous methods, is that: at low intensities, they are not dangerous to human over a wide frequency range; transparency has no bearing on acoustic measurements. In addition acoustic dev-

ices can provide continuous viscosity monitoring and hence automatic process control.

This chapter presents a new method in the implementation of a piezoceramic Lead Zirconate Titanate (PZT) disk-type transducer for the measurement of liquid viscosity in kHz frequency range, which is much higher than that of vibrating piezoelectric transducer (400 - 700Hz), which has been reported for viscosity measurements [56]. The natural resonance frequency of the unloaded PZT transducer (75KHz) and the higher harmonics (190,305, and 420KHz) are used in the experiment with a water-glycerin mixture as a sample. When the PZT transducer is immersed inside the liquid sample and becomes in complete contact with it, the properties of the liquid reflected on the resonance resistance of the transducer. This resistance was determined by measuring the electrical input impedance of the transducer at resonance. The experimental results, for viscosity measurement in the frequency ranges from fundamental resonance of the disk to the 7^{th} harmonic, shows straightforward relationship between the resonance resistance and the square root of the viscosity density product. Knowing the liquid density, this method is very useful in monitoring the viscosity during production of materials such as plastic, polymers, and petrochemicals in order to ensure consistent quality.

Water-glycerin mixture, with different glycerin/water contents is used as an experimental liquid sample. Here, the measurements are made for the reaction of the liquid on the

source (i.e changes of voltage and current at the source) when the liquid medium is at resonance together with the disk located in side it. Internal friction, density, viscosity, and thermal conduction are all responsible for these changes. If some of these factors are carefully controlled, direct measurements of voltage and current changes at the source will give indications for the remaining factors. The disk used is made of Lead Zirconate Titanate (PZT) ceramic which has good thermal stability, with it's surfaces are micromachined such that they can be treated as smooth enough that friction effects due to the surface roughness can be neglected. Therefore, we can treat the viscosity and density as the main factors causing the changes in the voltage and current of the transducer.

5.2 PRINCIPLES AND METHODS

5.2.1 Fundamentals of Viscosity Measurement

Viscosity is the property of the flowing fluids and it quantifies the resistance to flow set-up within the fluid. It is entirely due to the friction between the moving particles of the fluid. Viscosity is responsible for most of the dissipation of energy in transportation of liquids and gases through pipelines. The effectiveness of lubricating oils depends, among other factors, on the viscosity of the oils. On-line measurement of the viscosity of oils is a common need in industry as well as for studying the fluid flow.

Fluid flow is said to be viscous if the flow is taking place in such a way that adjacent layers of the fluid moves slowly in one direction only. And if the adjacent layers are moving with different velocities, the constant interchange of molecules and momentum creates resistance to the relative motion of the layer. Hence viscosity can be understood as that property which determines the magnitude of the resistance of the fluid to a shearing force that creates the particles motion.

The acoustic impedance is a fundamental physical property of any material (solid, liquid, or gas). It determines the amount of acoustic energy reflected at the boundary between any two mediums having difference in their acoustic impedance. If acoustic transducer is in perfect contact with other material, the acoustic impedance of the material can be determined by measuring the electrical input parameters (i.e. voltage, current and so the electrical impedance) of the transducer. The electrical impedance of the transducer is related to the acoustic impedance through the electromechanical coupling factor of the transducer [57]. In section 5.2.3 we present electrical method for the measurement procedure to predict the fluid viscosity using piezoceramic transducer.

5.2.2 Temperature Dependence of Viscosity

Continuous viscometers generally calibrated over a range of viscosities. This empirical calibration allows use on both Newtonian fluids, in which the ratio of shear stress to the rate of shear strain is constant and non-Newtonian fluids in which viscosity is not a constant parameter.

Viscosity is highly dependent on temperature and it decreases with increasing temperature. Over a large temperature range the relation often found to be approximated by:

$$\eta = Ae^{BT} \qquad \ldots(5.2)$$

where η is the viscosity, T is the temperature , A and B are constants which exhibit a large variation between different fluids and for the same temperature they increase with increasing viscosity [58]. Therefore, the fluid under viscosity measurement should be kept at known and constant temperature throughout the measurement.

5.2.3 Circuit Considerations of Piezoelectric Transducer

To obtain optimum performance from a piezoelectric transducer device, the circuit to which it is connected must have certain characteristics that are dictated by the design of the device. In discussing this subject, it is convenient to divide piezoelectric devices into two broad categories as resonant and non-resonant devices.

In the case of non-resonant piezoelectric devices, which are electrically driven, the electrical impedance of the device may, for most practical purposes, be considered to be purely capacitive. For all frequencies well bellow the first mechanical resonance of the device, the electromechanical relationships are such that the displacement of the piezoelectric element from its normal position, at any instant, is proportional to electric charge applied at that instant. The electrical impedance of piezoelectric device is in reality more complicated than the simple capacitor representation generally employed in discussing the non-resonant devices. A more proper representation would be a capacitor representing the static capacitance of the piezoelectric element, shunted by the impedance representing the mechanical vibrating system. In most non-resonant devices, the latter impedance may be approximated by a capacitor. Therefore, we have a capacitor in parallel with capacitor and hence the single capacitor representation.

In devices designed for operation at resonance, the impedance representing the mechanical system may become, at resonance, a resistance of relatively low value and this is shunted by the same static capacitance. This shunt static capacitor generally is undesirable especially if the device is designed to operate in the resonance mode. In electrically driven devices, it shunts the driving amplifier or other signal source requiring that the source be capable of supplying extra current. In the case of mechanically driven device, the static capacitance

acts as a load on the active part of the transducer, reducing the electrical output. In the non-resonant device, not much can be done about the shunt capacitance, except choose a piezoelectric material having maximum activity. In the case of resonant devices, neutralization of the static capacitance may be through a shunt or series inductor chosen to resonate with the static capacitance at the operating frequency [39]. Thereby the impedance of the transducer at resonance becomes pure resistance of low value.

In it's over all electrical properties, the two-terminal piezoceramic (PZT) disk-type transducer represents the resonance properties of its internal elasto-inertial system. The electrical equivalent network of figure 5.1(a) represents the response of the disk to the external circuit voltage and current, at any one of its resonance frequencies. The series elements L, C represents the resonance circuit components, R_r the radiation load on the transducer surface, and R_i the internal dissipation load resistance of the transducer, while the capacitance C_o represents the purely dielectric property of the piezceramic disk [59]. Considering the electrical equivalent circuit of Figure 5.1(a), the equation of the electrical admittance Y_T can be written as:

$$\begin{aligned} Y_T &= j\omega C_o + [R + j(\omega L - 1/\omega C)]^{-1} \\ &= G + jB \end{aligned} \qquad \ldots(5.3).$$

where the resistance $R = R_i + R_r$, G is the conductance given by:

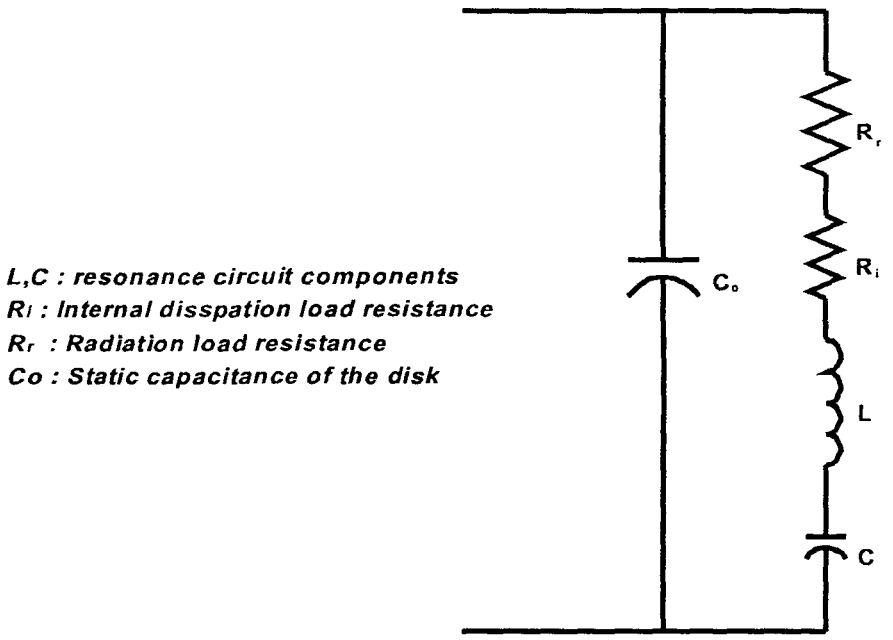

Figure 5.1(a):
Electrical Equivalent Circuit of the piezoceramic Disk

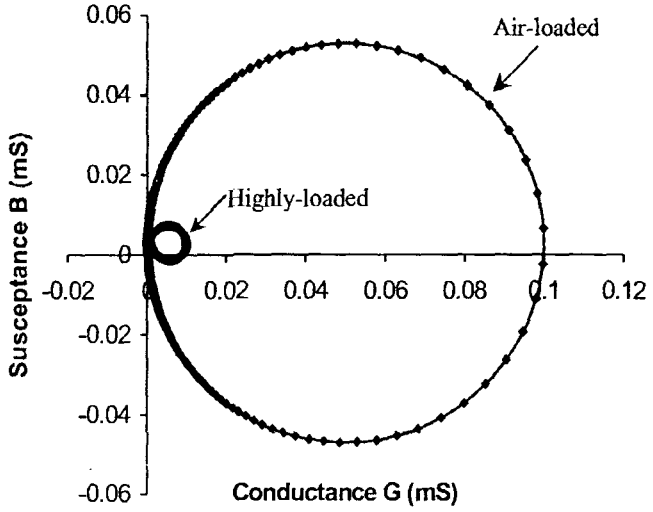

Figure 5.1(b):
Simulated Admittance Locus of the Equivalent Circuit

$$G = R/\left[R^2 + (\omega L - 1/\omega C)^2\right] \qquad \ldots(5.4)$$

and the susceptance

$$B = \omega C_o - \frac{(\omega L - 1/\omega C)}{\left[R^2 + (\omega L - 1/\omega C)^2\right]} \qquad \ldots(5.5)$$

For resonance condition equation (5.5), which is the imaginary part is equated to zero, giving the following quadratic equation:

$$\omega^4 + \left(\frac{R^2}{L^2} - \frac{2}{LC} - \frac{1}{LC_o}\right)\omega^2 + \frac{1}{L^2CC_o} + \frac{1}{L^2C} = 0 \qquad \ldots(5.6)$$

Solving this equation for ω results in four roots, those are the fundamental resonance frequency, 3rd, 5th, and 7th harmonics.

The admittance locus of the equivalent circuit is shown in Figure 5.1(b). The locus is a circle of diameter 1/R, which corresponds to the conductance at resonance, with its center displaced from the real axis in the positive direction by fixed a mount equal to $j\omega C_o$. The frequency increases clockwise around the circle and the diameter decreases with increasing load on the disk surface. The resonance frequency is at the point of intersection between the circle and the horizontal line parallel to X-axis and passing through the center. For different loading, a simple measurement of the deriving voltage and current at resonance determines the value of the electrical resonance resistance R, which in turn gives a measure for the properties of the material in contact with the disk transducer surface.

5.2.4 Viscosity and Radiation Load Resistance

The method developed is based upon measuring the acoustic load impedance of the test liquid, which is in complete contact with one surface of the transducer. The PZT disk transducer is located in side the liquid to produce the shear wave, when excited, in which the particles motion is parallel to the surface of the disk. For an ideal transducer, the lumped electrical resonance components and the radiation load R_r are related to the mechanical parameters (mass of the transducer and its stiffness) through the following equations:

$$L = M/k^2 \qquad \ldots(5.7)$$

$$C = k^2/K \qquad \ldots(5.8)$$

$$R_r = Z_L/k^2 \qquad \ldots(5.9)$$

Where, M, K, Z_L, and k are the mechanical mass, stiffness, complex impedance and the electromechanical coupling factor of the transducer, respectively.

In special case where the radiation area is much larger than the wavelength of the emitted sound in the fluid media, the complex impedance of the transducer and the fluid are equal and may be written in the usual form of the complex impedance's [60]:

$$Z_L = R_L + jX_L = j\omega\rho_L\bar{\eta}_L = j\omega\rho_L(\eta_1 - j\eta_2) \qquad \ldots(5.10)$$

ρ_L is the density of the liquid and $\bar{\eta}_L$ its complex viscosity given by: $\bar{\eta}_L = (\eta_1 - j\eta_2)$. For simple Newtonian liquid the real and imaginary parts of the above equation are equal, and that its complex impedance is given as:

$$Z_L = (1+j)\sqrt{(\omega\rho_L\eta_L/2)} \qquad \ldots(5.11)$$

At resonance this acoustic or mechanical radiation impedance appears as purely mechanical resistance R_m and that is given by:

$$R_m = \sqrt{(\omega\rho_L\eta_L/2)} \qquad \ldots(5.12)$$

As in equation (5.9), the electromechanical coupling factor k relates the mechanical resistance R_m to the electrical radiation load resistance R_r of the PZT transducer through the following equation:

$$R_r = R_m/k^2 = K_1\sqrt{\eta_L} \qquad \ldots(5.13)$$

where the constant $K_1 = \sqrt{\omega\rho_L/2}/k^2$.

When the liquid density is accurately known or can be determined, the viscosity will be obtained by measuring the acoustic load impedance of the liquid under test.

5.3 EXPERIMENTAL SETUP AND MEASUREMENT PROCEDURE

The block diagram of the experimental setup ant the disk while immersed in the test liquid are shown in Figure 5.2(a) and 5.2(b). The piezoceramic disk is of 3 Cm diameter and 2 mm thick. Sparkler Piezoceramic -India, has manufactured it as SP-4 high power ferroelectrically hard material, the manufacturer specifies its working temperature as 90°C. A very thin layer of a standard epoxy adhesive manufactured by Vantico performance polymer Pvt. limited-India coats one surface of the disk. This layer provides very good electrical insulation and rigid enough for supporting the disk. This disk is suspended by means of thin lead wires in the center of a sample cell containing 200ml of the test liquid. The circuit was excited by a sinusoidal wave of 20 $V_{(peak\text{-}peak)}$ from function generator (HM 8130) having the capability of varying the frequency smoothly from 1.0Hz to 1.0MHz. A small sampling resistor (to sample the current through the disk) of 10 Ohms value is connected in series with the PZT disk for sensing its current.

To determine the exact resonance frequency, the input frequency was varied till the minimum voltage across the series combination of the disk and the sampling resistance is reached. For loaded disk, this voltage and the sampled current are not in phase due to the existence of the static capacitance C_o and the connecting lead capacitance. Neutralizing this effect can be done by connecting an inductor either in series or in parallel with the disk and resonate them at the same resonance

frequency of the disk. In parallel resonance the small resistance of the inductor will remain in parallel and it shares the current with the disk. For that the sampling resistor will not give the exact disk current. Therefore, we go for the series tuning where only the very high (in the order of M.Ohms) shunt resistor of C_o will appear across the disk with negligible effect on the disk current.

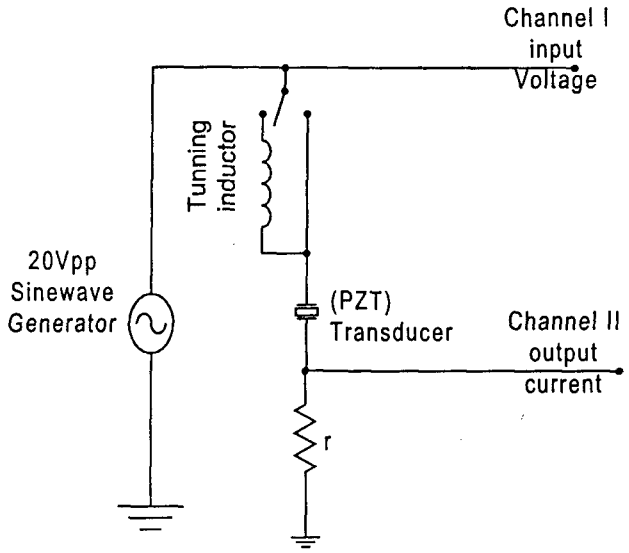

Figure 5.2(a): Block Diagram of the Experimental Setup.

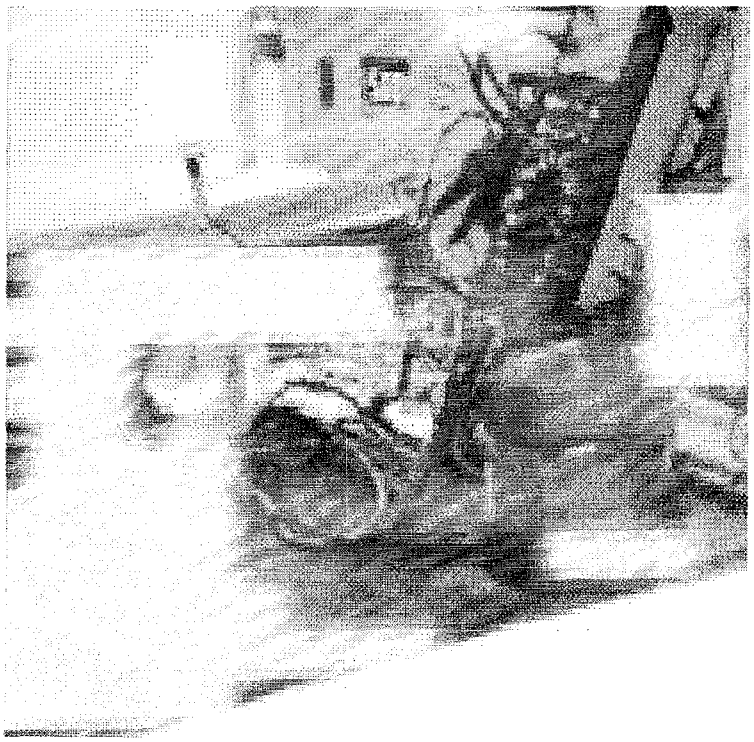

Figure 5.2(b): Photograph of the Practical Circuit

5.4 EXPERIMENTAL RESULTS

Determination of the fundamental and the higher harmonics resonance frequencies were done through the measurements on Hewlett Packard Precision LCR Meter, 20 Hz - 1MHz (Model 4284A). Figure 5.3 shows the practical results of the frequency versus the logarithmic impedance for the PZT disk transducer when it is air-loaded. The graph shows the curve decreasing to minimum impedance followed by an increase to a maximum in four different portions on the curve. The corresponding frequencies for each pair of maximum-minimum are the resonance and anti-resonance respectively. The performance of the disk will have a maximum response at a point, which lies between these points. The first portion repesents the fundamental resonance frequency in which the increase take place sharply that make the disk more sensitive to measurements at this frequency than the higher harmonics.

The experimental results for various viscosities for water-glycerin mixture are shown in Figure 5.4. The results show a linear relationship between the electrical resonance resistance, normalized to the resonance resistance of water, and the square root of the viscosity of the liquid under test. The density as its defintion is weight per unit volume of the material, it was determined by weighting a known volume of the liquid mixture. A newly developed ultrasonic densitometers may be used in the future such as those discussed by Adamowski el. in [61] and Hauptmann el. in [62], indeed these are developed for liquid density measurement specially they empl-

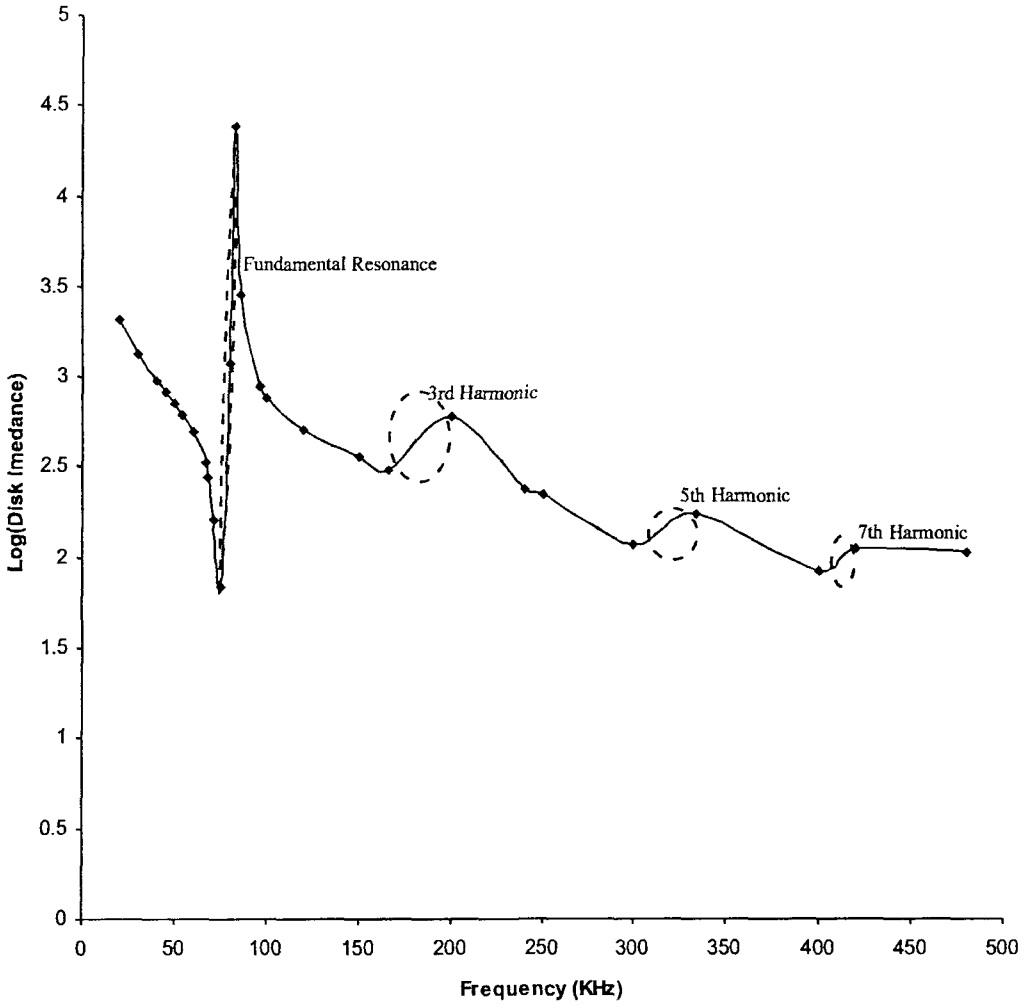

Figure 5.3:
Practical Results for the Fundamental Resonance Frequency of the Disk and its Harmonics

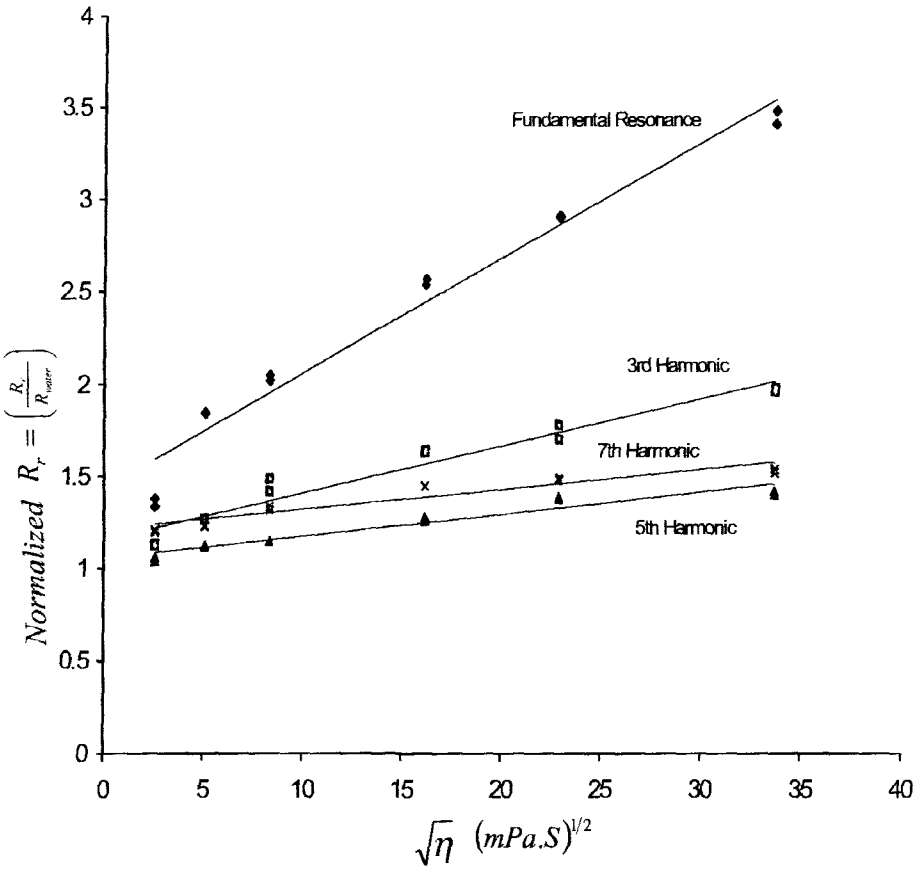

Figure 5.4:

Square-Root of Viscosity Versus The Normalized Resonance Resistance

oys the same principle of ultrasonic.

Viscosity of liquids is highly dependent on temperature and it decrease considerably with increasing temperature [63]. The change in viscosity as a result of the change temperature for three different samples is given in figure 5.5(a). While Figure 5.5(b) shows the electrical resonance resistance at the fundamental resonance as measured for the above three samples. The result in all the three different curves shows the lower the temperature the higher is the radiation load resistance, which agreed well with the literature. From this we conclude that the liquid under test must be kept at a known and constant temperature throughout the measurement or compensation for temperature changes should be provided.

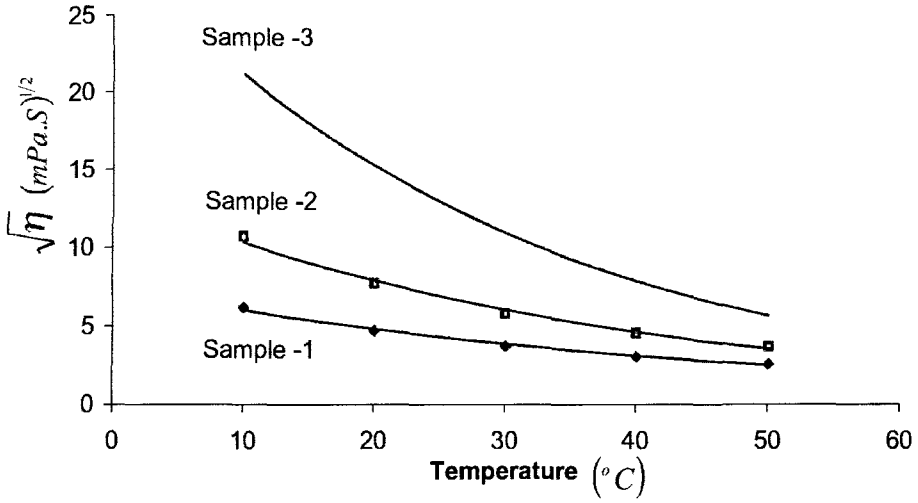

Figure 5.5(a):
The Square Root of Viscosity and the Temperature Relationship.

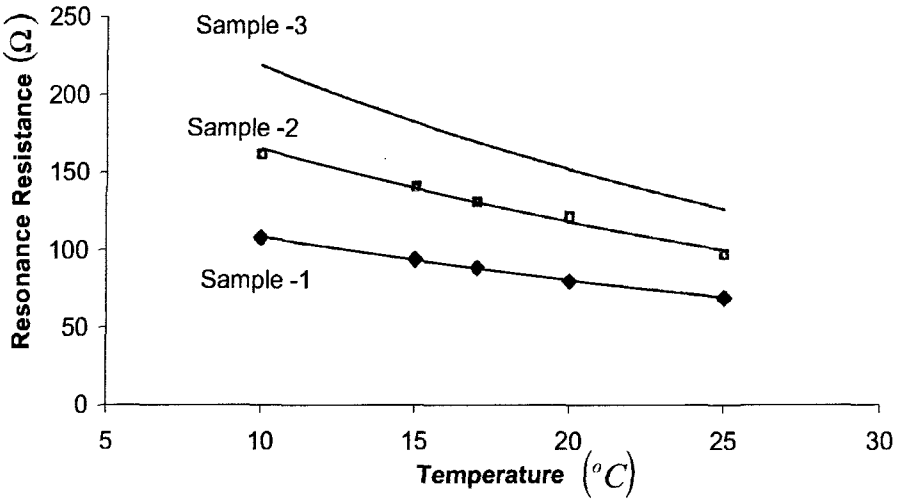

Figure 5.5(b):
Resistance of the Disk At Fundamental Resonance Versus Temperature.

CHAPTER SIX

Low Vacuum Measurements Using Ultrasonic Technique

CHAPTER VI

LOW VACUUM MESUREMENTS USING ULTRASONIC TECHNIQUE

6.1 INTRODUCTION

Ultrasonic measurement techniques are used extensively in laboratories and industries, finding endless applications from level measurements to nondestructive testing and robot navigation [64]. In this chapter we are investigating the use of ultrasonic technique for the measurement of low vacuum pressure using suitable ultrasonic transducers without any other primary sensor.

Measurement of pressure is of considerable importance in all stages of scientific and engineering measurements. Most of these pressures range from a little below atmosphere to hundreds of atmospheres. Pressure is not an independent variable as it is derived from force and area (Pressure is a force per unit area) and it is not "ideal" as it depends on other factors like fluid density, temperature, flow velocity, etc. Therefore, pressure-measuring systems probably vary over a greater range of complexity than any other type of measuring systems. In many cases, pressure is expressed in terms of atmospheric, which is the height of the barometric column at 0°C at sea level, being equal to 76 cm of mercury (density 13.59 g/cm^3). Pressure may or may not be referred to the atmospheric datum.

We know, of course, positive magnitude of absolute pressure exists at all times. It is impossible to reach the absolute zero value. Atmospheric pressure, however, serves as a reference. In general, pressures below atmospheric called low pressures or vacuum and that above the atmospheric refer to as gauge pressure. Therefore, pressure measurement consists of three scales; that of gauge pressure scale, absolute pressure scale and vacuum scale. On gauge pressure scale, the zero point is at atmospheric pressure. While on the absolute scale the zero point is at the absolute zero pressure point, the vacuum scale has its zero at atmospheric and its maximum at absolute zero pressure point. In this study we are concerned with the measurement of very low vacuum pressure or what is known as vacuum. Generally there are two basic methods for measuring low vacuum pressure. The first one is the direct measurement resulting from a displacement caused by the action of force due to a column of liquid of known density. And the second is the indirect methods wherein pressure is determined through the measurement of certain other pressure-controlled properties, such as volume, thermal conductivity, etc, [65].

The various types of manometers are examples of the devices used for direct measurement and that their use is generally limited to the low vacuum pressure values. Manometers are self-balancing deflection devices and they are surprisingly accurate; they are often used as standards. Occasionally they are used as visual indicators of air pressure in industrial locations, but rarely for control applications, unless they

are coupled to laser, capacitive, ultrasonic or other means of level measurement device. The ordinary U-tube manometer is one of the most elementary measuring devices imaginable. It is simple, inexpensive, and relatively free from errors. Therefore, in the setup for measuring a low vacuum pressure in this work, the U-tube manometer has been chosen as a calibration device due to its mentioned above advantages.

As ultrasonic wave get attenuated while it is traveling through any medium from one place to another, the attenuation depends upon the physical properties of the medium. This chapter deals with the study of the effect of varying the pressure of the medium upon the output of ultrasonic transducer. A continuous ultrasonic wave of 40 KHz has been produced by the transmitter and passed through the medium and received on the ultrasonic transducers working as receiver. The medium pressure was decreased below atmospheric pressure up to 40 K Pascal and the receiver output is recorded. The measurement was carried with a sensitivity of 0.124mV/Pascal. This study forms a base for low vacuum pressure measurement using ultrasonic transducers.

6.2 PRINCIPLE OF OPERATION

6.2.1 General

Ultrasonic waves need a medium to travel from one point to the other and every medium has its own properties such as elasticity, pressure, density, temperature, viscosity, etc. The me-

dium properties have a direct effect on the waves passing through it and it may be possible to make use of some of these effects for measuring physical quantities. The easiest obtainable information from ultrasonic waves, in time domain, is through measuring the waveform attenuation (pulse attenuation measurement) as it passes the medium, or through the analysis of the propagation velocity of the wave (pulse velocity measurement). In many applications the time elapsed between the transmitted pulse and its echo (transit time) is taken as basis for ultrasound velocity measurement. The transmitted ultrasound pulse propagates through the medium and received by the receiving transducer. If the path length between the transducers is known then the transit time is a measure of the velocity of sound through the given material. The velocity of sound in gaseous medium is proportional to the ratio of the medium pressure and its density. As this ratio is constant for gases obeying Boyle's law [66]; the pulse velocity measurement cannot be suitable for studying the effect of pressure variation. The attenuation measurement can be obtained by measuring the difference in peak levels of the transmitted signal and the received signal. It requires one pulse generator, transmitter-receiver pair and dual channel oscilloscope.

6.2.2 Effects of Temperature and Pressure on the Velocity of Ultrasound waves

The velocity of sound wave depends on the type of wave, the density and the elastic constant of the material in which it

is traveling. The equation that relates the velocity v of a longitudinal sound wave in air or other fluid having density ρ, was given by Newton as [67]:

$$v=\sqrt{\mu/\rho} \qquad \ldots(6.1)$$

where μ, is the modulus of elasticity for the fluid. Later, Laplace pointed out that compression and rarefaction in a sound wave of even moderate frequency were taking place too rapidly for temperature equalizations. Then he proved that $\mu = \gamma p$; hence equation (6.1) becomes:

$$v=\sqrt{\gamma P/\rho} \qquad \ldots(6.2)$$

where P is the pressure, γ is the ratio of specific heat determined by Röntgen to be 1.405 for air and remain constant for temperature range from -80°C to at least 150°C [68, 69].

The velocity of sound in air is not independent of its temperature. In case the air in which the sound wave traveling is enclosed and kept at constant volume, any increase in temperature results in an increase in the pressure with no consequent change in density. Therefore, the velocity is increased. Nevertheless, when the sound is traveling in the atmosphere and the density of the air being decreased by a rise in temperature, while the barometric pressure is kept constant; the velocity is increased due to temperature rise, just as in the case of the enclosed air. Therefore, both density and pressure are related to the temperature through the gas laws. Thus the

new equation for the sound velocity at any temperature t°C will be given by:

$$v_t = v_0\sqrt{[1+\beta t]} \qquad \ldots(6.3)$$

where v_o is the sound velocity at 0°C and β =0.00578/°C, is the temperature coefficient of expansion of the gas. A calculations using equation (6.3), shows that for air medium the sound velocity increase approximately 0.6 m/sec. per degree centigrade rise in temperature [70].

For gases obeying Boyle's law if there exist a given volume (m/ρ_1) of gas with known pressure P_1, when expanded or compressed to a new volume (m/ρ_2) the resultant pressure P_2 is given by:

$$P_2 m/\rho_2 = P_1 m/\rho_1 \qquad \ldots(6.4)$$

where m is the mass, ρ_1, ρ_2 are the densities at pressures P_1 and P_2, respectively.

Thus the ratio of pressure P to density ρ remains constant. Consequently the velocity of ultrasound wave in gases is not affected by variations of pressure.

Again the gas density ρ_g depends on the gas pressure P_g according to:

$$\rho_g = P_g / RT \qquad \ldots(6.5)$$

where R = 289J/KgKelvan is the universal gas constant divided by the average molecular weight of air and T is the temperature. For constant temperature the gas density is directly proportional to the gas pressure P_g.

6.2.3 Arrangements Of Ultrasonic Transmitter and Receiver

An ultrasonic transmitter is a device designed to generate ultrasonic energy. The transmitter which are most frequently used are either piezoelectric or magnitostrictive devices. Piezoelectric transducers may be used for generation of low intensity ultrasonic waves through out the ultrasonic range of frequencies. Magnitostrictive are useful for generating high intensity ultrasonic energy at frequencies of approximately 50 KHz. The design of the transmitter depends upon the application for which it is to be used.

The device that detects ultrasonic signals is called ultrasonic receiver. As the ear is a passive device responding to sounds and making the information available for recording in the brain, ultrasonic receiver receives the ultrasonic signal and transforming it faithfully into another form of energy (usually electrical) where it can be processed and analyzed as desired.

The electrical equivalent series resonance circuit of the ultrasonic transducer was shown in the previous chapter Figure 5.1(a). At resonance, L_1 and C_1 will drop out leaving C_o in parallel with the resistor R_1. When this device is working in

transmitting mode, the maximum power transfer is obtained by matching the transducer impedance with the impedance of the source. If the transducer is having higher impedance than that of the source, the current through the circuit is limited. If the source impedance is higher than the impedance of the transducer, higher voltage is dropped across the source impedance. In both the cases the electrical power transferred to the transducer element is lower than the maximum and so the mechanical power transmitted.

Figure 6.1 shows the electrical equivalent series resonance circuit of the transducer for transmitting and receiving modes of operation. The mechanical power transmitted by the transmitter is assumed to be proportional to the electrical voltage applied to its terminals. This mechanical power propagates through the medium and part of it will be received by the piezoelectric element of the receiver. Again the output voltage produced at the receiver terminals is according to the amount of the mechanical power exerted on its piezoelectric element.

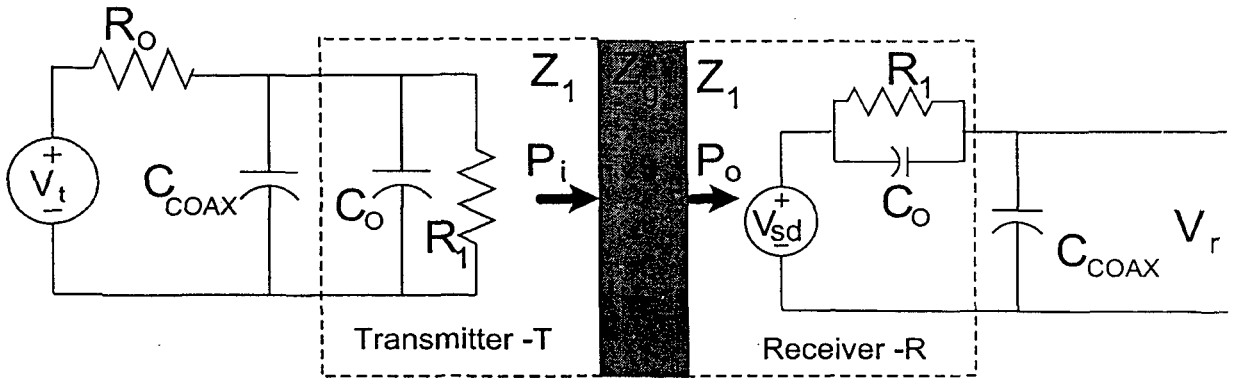

Figure 6.1: Piezoelectric Transducer Equivalent Circuit for Transmitting-mode and Receiving-mode

6.2.3 Role of Acoustic Impedance in the Measurement

In many aspects, ultrasonic is like electricity. Forces acting across an area at a given point in the wave are analogous to electrical voltage and the velocity potential at that point is analogous to current. Just as the ratio of the voltage to current is electrical impedance, the ratio of force to velocity is the acoustic impedance [60]. Again as the condition for maximum power transfer is when electrical impedance of the load is equal to the electrical impedance of the source, the maximum ultrasonic power is transferred from acoustic source when it's acoustic impedance is matched with the acoustic impedance of the medium in which the wave is traveling. If the two media do not have the same impedance, the maximum power transfer may be achieved by matching the acoustic impedance of the transducer and the propagation medium. In this case impedance matching layer should be used.

The proper choice of the operating parameters is quite delicate in the case of ultrasonic sensors for air applications. In fact, in this case, the attenuation of ultrasonic waves is much greater than that in the liquid at the same frequency, therefore; only relative low frequencies are adequate. The lower limit for the frequency should be higher than the acoustic frequencies of the mechanical parts around the meter (in order to discriminate this acoustic noise from the signal).

Among many other factors such as geometric spreading, conduction and shear viscosity losses, molecular relaxation, boundaries, refraction, etc. the overall attenuation of ultrasonic waves in air is a function of the distance and is affected by secondary factors like temperature, humidity and atmospheric pressure. This study was done under constant temperature and very low humidity such that its effect can be neglected. As ultrasonic waves travel from a medium of low to that of high acoustic impedance, only a fraction of energy is transferred to the latter. This acoustic impedance Z_g of the gaseous medium is the medium density ρ_g multiplied by the sound velocity v in that medium and it's written as:

$$Z_g = \rho_g v \qquad \ldots(6.6)$$

On substituting equation (6.5) we get:

$$Z_g = \rho_g v = P_g v/RT \qquad \ldots(6.7)$$

Since the ultrasound velocity of gas is independent of pressure and it is a function of temperature only [71], for constant temperature the acoustic impedance Z_g of the gas is directly proportional to its pressure P_g.

The general form of the ultrasonic energy transmitted from one medium to the other is governed by the transmission co-efficient α_t that is given as:

$$\alpha_t = 4Z_1 Z_g / (Z_1 + Z_g)^2 \qquad \ldots (6.8)$$

For $Z_1 >> Z_g$ $\qquad \alpha_t \cong 4Z_g / (Z_1)$

where, Z_1 is the acoustic impedance of the medium from which the ultrasonic is transmitted (or originated), Z_g is the acoustic impedance of the medium in which the ultrasonic is transmitted, which is air in this case. Substituting equation (6.7) in (6.8) we get:

$$\alpha_t = 4Z_1 P_g v / RT (Z_1 + P_g v / RT)^2 \qquad \ldots (6.9)$$

$$\cong 4P_g v / RTZ_1$$

The transmission losses increase as the acoustic impedance decreases due to decrement of the gas pressure. As a consequence the amount of ultrasonic energy transmitted through gaseous medium and thus the voltage at the output of the receiving transducer is a function of its pressure P_g.

6.3 EXPERIMENTAL SETUP AND RESULTS

Transducers most frequently used are piezoelectric types due to their high sensitivity and small size. The transmitter and receiver used in this application are piezoelectric transducers type (T- 40- 1680) and (R- 40- 1680) respectively, which are designed to work properly in air medium. Generally in this aspect we treat the output voltage of the receiver and correlate it with the low vacuum pressure of the medium.

The major objective of this chapter is to illustrate that the ultrasonic transducers can be used for vacuum measurement. The proposed measurement technique was experimentally examined over pressure range from atmospheric pressure to 40 K Pascal. The experimental setup for the measurement is shown in Figure 6.2. The reservoir works as a medium, which has two taps; one was connected to a piston for changing the pressure of the medium. The other tap was connected to a U-tube manometer, which measure the pressure variation. Inside this reservoir is pair of ultrasonic transducers (Transmitter-T and Receiver-R) was fixed distance apart. The peizoelectric transmitter type was driven using a continuous sinusoidal wave of constant amplitude and 40KHz frequency. The receiver receives this signal after it propagates through the medium of variable pressure. This signal was amplified and displayed on a dual channel oscilloscope. Figure 6.3 shows the experimental results of varying the pressure and the corresponding voltages at the receiver output. In the range of measurement, this relation was found to have a pattern containing two components; one is directly proportional to the pressure of the medium while the other is approximately constant, which corresponds to the loss due to geometric spreading, molecular relaxation, boundaries, etc. The two lines in the graph are for two different input voltages to the transmitter (namely $10V_{pp}$ and $20V_{pp}$) that is agreed with the theory. Higher the applied voltage to the transmitter more is the transferred energy, results in higher voltage at the receiver output terminals. The experimental results are found to be more

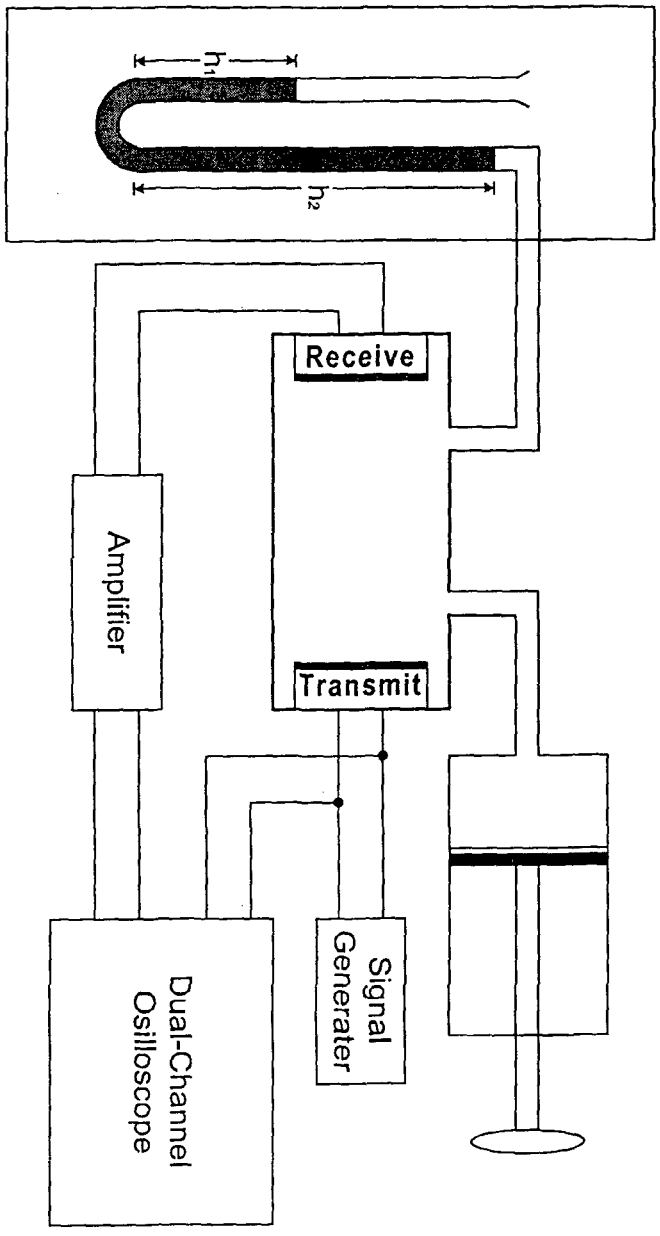

Figure 6.2 Experimental Setup For Vacuum Measurement

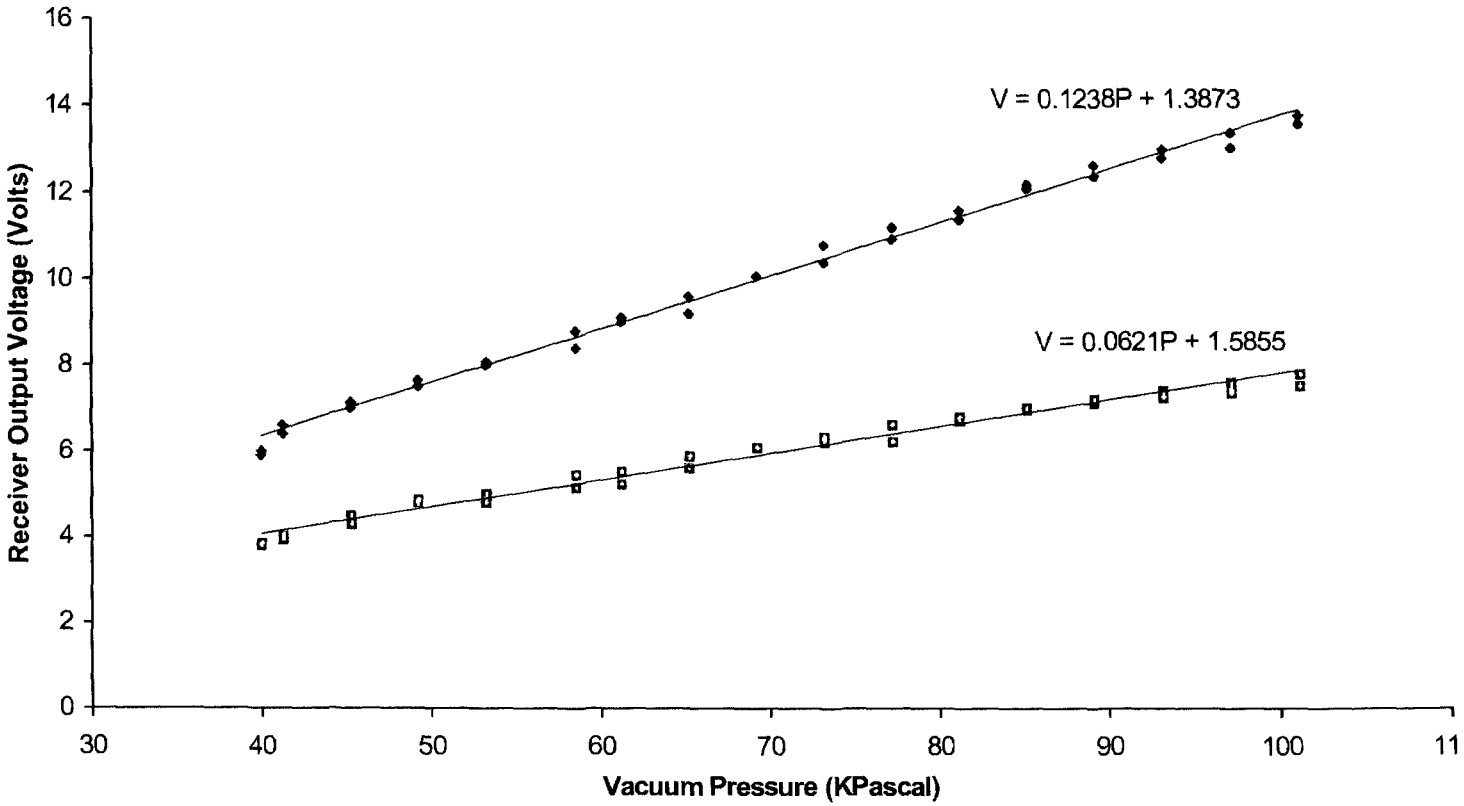

Figure 6.3 Vacuum Pressure versus Receiver Output Voltage

sensitive to the higher applied voltage as the slope of the curve is doubled for twice the applied voltage. The measurements were carried at a temperature of 26°C.

6.4 POSSIBLE SOURCES OF ERRORS

A - Temperature effects: Both the density and the pressure of the medium in which the sound wave is traveling are temperature dependent. Therefore, any change in temperature will result in a change in the sound velocity as shown in equation (6.3). During measurement the temperature should be kept constant.

B - Directivity of the transducers: The ideal beam pattern of ultrasonic transducer is to project the energy out ward from the transducer in a straight and narrow beam. The radiation can be thought of as traveling out ward in a form of cone whose apex is at the center of the crystal. When an ultrasonic power is confined in a narrow beam, the power density increases and therefore the maximum output is achieved. However, small highly focused transducers have to be carefully aligned, otherwise the transmitted beam can be out of the receiving transducer cone and could not be detected.

Provided that the pressure is precisely determined throughout the measurement range and the uncertainty in the values of gravity, density of the manometer liquid and the reference pressure is acceptable.

CHAPTER SEVEN

Conclusions And Future Scope

CHAPTER VII

CONCLUSIONS AND THE FUTURE SCOPE

7.1 CONCLUSIONS

In this thesis a number of important and novel transducers have been designed, fabricated and tested. To have exhaustive knowledge of the variations of different parameters on the performance of the devices, systems are simulated using computer programming in Visual C++ and then analyzed. It has been found that simulated results are very close to practical results and provide data to get optimum performance of the device.

Very important part of the thesis is related to the development of a sensitive digital capacitive angular-position sensor. The initial studies shows that the shape of the higher potential plates should be modified in order to get linear outputs. The shape of each of these higher potential plates has been selected prior the final implementation. The selection criterion is to get the output as linear as possible depending on the choice of a design factor. The equation for the design factor has been selected that includes a weighting factor, the value of which is to be chosen also. This was done after intensive simulation using Microsoft Visual C++ 6.0 software. This digital angular-position sensor is capable of covering precisely the complete circle range from 0 to 360°

with an error of less than ±0.5% of the full-scale deflection and resolution of 3 arc minutes. It can, for inst-ance, be used in industrial robots; throttle flap position or steering in vehicles. The system is implemented with simple electrodes and inexpensive electronic components. When this circuitry is accurately fabricated it can be used to replace expensive angular-position systems.

Next application regarding a new design of capacitive rotation-speed transducer is presented. The rotation speed is deduced from the modulated output due to presence of the periodic changes of stray capacitances caused by the rotating tooth of a disc. The simulation studies were carried over prior the practical implementation. This design has some distinct advantages over those, which were reported in this field. It doesn't require grounding of the rotating plate, which becomes a problem in most of the reported cases. The rotating plate, responsible for producing the modulated output, rotates outside the fixed electrodes of the capacitor instead of inside the capacitor plates. It can be developed in the form of a small probe, which can be held in hand or fixed on a stationary part of the system. The effects of varying the geometrical dimensions, thickness of the fixed electrodes and the distance between them, have been studied based on simulations done for the sensor model. That small distance between the electrodes, which ensures small size, and comparatively large thickness are recommended for high output currents and long output pulse duration. The results of this study can be

used to optimize the structure of the sensor electrodes according to its application with respect to size, simplicity, and accuracy.

Another important application developed under this thesis is complete encoder system including digital display readout is represented. Detailed electronics of the signal processing circuit is given in which fast transition from one state to the next is of great importance to avoid erroneous readings. Placing a rectifying diode in the feedback path of operational amplifier ensures the fast transition by conducting on application of few microvolts and that the operational amplifier having fast rise time is used. The encoder has been examined for the tilting of the moving higher potential electrode and it was found that a tilt angle of up to one degree introduces an error of less than 0.08%. Also the encoder was applied for liquid level. If it is compared with other types of encoders, it overcomes the disadvantages of the brush type, such as wear of brushes and friction between brushes and the disk. At the same time it voids optical type, which suffers mainly from dusty environment and that any misalignment in the optics position will create serious errors in the readings.

Some important development work was regarding the applications of ultrasonic techniques in the field of viscosity and pressure measurement. First application was related to the measurement of dynamic viscosity of liquids. The measurement is based on the determination of piezoceramic (PZT) disk resi-

stance while it is completely immersed in the liquid and driven at it is fundamental resonance frequency or any of its higher harmonics. The resonance frequency and the higher harmonics of the PZT disk were determined experimentally. With the results that the fundamental is more clear and sharp than the other frequencies, it's found to be more sensitive in the viscosity measurements. The sensor can be inexpensive enough to competitive with other types of viscometers available in the field. In the studies, it was found that this measurement is highly affected by temperature variations. Therefore, this measurement either it should be made at constant temperature or a proper means of compensation must be provided according to the environment and the liquid type.

Second application of ultrasonic technique, which was successfully implemented, related to the measurement of low vacuum pressure. In this case the acoustic impedance of the medium played an important role in the transfer of energy between the transmitter and receiver. Irrespective of the amount of this energy at atmospheric pressure, it is continuously decreasing with the decease in the pressure of the medium separating the ultrasonic transducers. The method is relatively simple, direct and inexpensive. The relationship between the pressure of the medium and the output voltage of the receiver can be represented by a straight line and it is easy to calibrate a device for direct low vacuum pressure measurements. The results of this study suggest the ultrasonic technique could be utilized for low vacuum pressure measurements where its prop-

posed to measure from outside i.e. in a CRT tube etc. The range that was covered in this application is from atmospheric pressure down to 40K Pascal with a sensitivity of 0.124mV/ Pascal.

7.2 DISCUSSIONS AND FUTURE SCOPE

Both the angular-position sensor and the rotation-speed sensor are now ready for production in the form of portable devices. The digital encoder can be further extended for measurement of rotary motion.

During measurements of viscosity we noticed that there were very small deviations in the resonance frequencies and that were due to the variations of radiation resistance which involved in the equation of the resonance frequency. Momozawa S. *et al.* investigated these deviations and they reported that these deviations themselves are base for the viscosity measurement, but they could not be used for measurement of high viscosity because they are very much small and they are only of the order of 2 to 3% of the resonance frequency. The measurement using such small variations will probably results in low accuracy. The second notice is that the viscosity of liquids varies considerably with temperature; it decreases with increasing temperature. The measurements in this work were done at constant temperature. Future scope is to incorporate a temperature compensation circuit so that errors due to

temperature variation may be decreased. Ultrasonic pressure measurement technique may be tried for very low vacuums where other methods either fail or have low sensitivity.

REFERENCES

REFERENCES

[1] Ferry, N. Toth, Dorus Bertels, Gerard C. M. Meijer *1996* "A low-cost, Stable reference capacitor for capacitive sensor systems." *IEEE Trans. Instrum. & meas. Vol. 45, No. 2, pp 526 - 530.*

[2] Hauge, B. and Foord, T. 1971 *'Alternating current bridge methods'* 6th edition, pp 194 - 201, Sir Isaac Pitman Publishing LTD, (London).

[3] Willem C. Heerens 1986 " Applications of Capacitance Techniques in Sensor Design" *J. Phys. E: Sci. Instrum. Vol. 19, pp. 897 - 906.*

[4] Joost, C. Lötters, Wouter Olthuis, Peter H. Veltink and Piet Bergveld. 1999 " A Sensitive Differential Capacitance to Voltage Converter for Sensor Applications" *IEEE Trans. Instrum. & meas. Vol. 48, No. 1, pp 89 - 95.*

[5] Frank M. L., Van der Goes and Gerard C. M. Meijer 1996 "A Novel Low-Cost Capacitive-Sensor Interface" *IEEE Trans. Instrum. Meas., Vol. 45, No.25, pp. 536 - 540.*

[6] Ferry N Toth and Gerard C. M. Meijer, 1992 " A Low-cost, Smart Capacitive Position Sensor" *IEEE Trans. Instrum. Meas., Vol. 41, No. 6, pp. 1041-1044.*

[7] M. Rehman and V. G. K. Murti 1981 " New Capacitive Micromanometer" *Rev. Sci. Instrum. (USA), Vol. 52, No.6, pp. 883 - 887.*

[8] Willem C. Heerens 1982 " Multi-Capacitor Sensors" *J. Phys. E: Sci. Instrum. Vol. 15, pp. 136 -141.*

[9] M. Rehman and V. G. K. Murti 1981 " A sensitive and Linear Pressure Transducer" *J. Phys. E: Sci. Instrum. Vol. 14, pp. 1 -4.*

[10] Nobumi Hagiwara, Masaru Yanase and Takeo Saegusa 1987 "A Self-Balance-Type Capacitance-to-DC-Voltage Converter for Measuring Small Capacitance" *IEEE Trans. Instrum. Meas., Vol. IM-36, No. 2, pp. 385-389.*

[11] Reinoud. F. Wolffenbuttel and Paul P. L. Regetien 1987 "Capacitance-to-Phase Angle Conversion for Detection of Extremely Small Capacities" *IEEE Trans. Instrum. Meas., Vol. IM-36, No. 4, pp. 866-872.*

[12] Alfonso Carlosena, Rafael Cabeza and Luis Serrano 1993 "A New Method for Low-Capacitance Probing" *IEEE Trans. Instrum. Meas., Vol. 42, No. 3, pp. 775 - 778.*

[13] Gregory A. Bertone, Z. H. Meiksin, and Norman L. Carroll 1990 " Noise Analysis for the Triaxial Capacitive Displacement Transducer" *IEEE Trans. Instrum. Meas., Vol. 39, No. 5, pp. 735 - 739.*

[14] Hans U. Meyer "An Integrated Capacitive Position Sensor 1996 " *IEEE Trans. Instrum. Meas., Vol. 45, No. 2, pp. 521 - 525.*

[15] Georg Brasseur, Paul L. Fulmek and Walter Smentana, 2000 "Virtual Rotor Grounding of Capacitive Angular Position Sensor" *IEEE Trans. Instrum. Meas., Vol. 49, No. 5, pp. 1108-1111.*

[16] Georg Brasseur 2001 "Modeling of the Front End of a New Capacitive Finger-Type Angular Position Sensor" *IEEE Trans. Instrum. Meas., Vol. 50, No. 1, pp. 111 - 116.*

[17] Xiujun Li, Gerard C. M. meijer, Gerben W. de Jong and Jo W. Spronck, 1996 "An Accurate Low-cost Capacitive Absolute Angular-Position Sensor With a Full-Circle Range" *IEEE Trans. Instrum. Meas., Vol. 45, No. 2, pp. 516-519.*

[18] M. Rehman and V. G. K. Murti 1980 " A New Capacitive Speed Transducer" *J. Phys. E: Sci. Instrum. Vol. 13, pp. 655 - 657.*

[19] Ferry N Toth, Gerard C. M. Meijer and Matthijs Van der Lee 1997 "A planar Capacitive Precision Gauge For Liquid-Level and leakage Detection" *IEEE Trans. Instrum. Meas., Vol. 46, No. 2, pp. 644 - 646.*

[20] Willem C. Heerens 1984 " The Comparison of Two Layer Thickness Gauges" *J. Phys. E: Sci. Instrum. Vol. 17, pp. 664 - 668.*

[21] Xiujun Li, Gerben W. de Jong and Gerard C. M. meijer, 2000 "The Influence of Electric-Field Bending on the Nonlinearity of Capacitive Sensors" *IEEE Trans. Instrum. Meas., Vol. 49, No. 2, pp. 256-259.*

[22] Cady, W. G. 1964, *'Piezoelectricity'* Dover Book Pub., New York.

[23] Anil Kumar, P. 2001 "Piezoceramics - Carving A Niche." *All India Seminar on Instrumentation Engineering-Practice, Teaching and Research.*

[24] K. A. Klicker, J. V. Biggers, and R. E. Newnham, 1981 "Composite of PZT and Epoxy for Hydrostatic Transducer Applications" *J. Amer. Ceram. Soc., Vol. 64, 5* .

[25] A. Safari, R. E. Newnham, L. E. Cross, and W. A. Schulze, 1982 "Perforated PZT-Polymer Composites for Piezoelectric Transducer Applications" *Ferroelectrics, 41,* 197.

[26] R. E. Newnham, L. J. Bowen, K. A. Klicker, and L. E. Cross, 1980 "Composites Piezoelectric Transducers" *Mater. Eng., 112.*

[27] T. R. Gururaja, W. A. Schulze, L. E. Cross, R. E. Newnham, B. A. Auld, and J. Wang, 1985 "Piezoelectric Composite Materials for Ultrasonic Transducer Applications -I. Resonant Modes of PZT Rods-polymer Composites." *IEEE Trans. Sonic Ultrasonics, SU-32, 481.*

[28] T. R. Gururaja, W. A. Schulze, L. E. Cross, and R. E. Newnham, 1985 "Piezoelectric Composites Materials for Ultrasonic Transducer Applications. II. Evaluation of Ultrasonic Medical Applications." *IEEE Trans. Sonic Ultrasonics, SU-32, 499.*

[29] S. Sa-Gong, A. Safari, X. J. Jang, and R. E. Newnham, 1986 "Poling Flexible Piezoelectric Composites" *Ferroelectric Lett., 5, 131.*

[30] H. Takeuchi, S. Jyomura, E. Yamamoto, and Y. Ito, 1982 "Electromechanical Properties of $(Pb,Ln)(Ti,Mn)O_3$ Ceramics" *J. Acoustic Soc. Amer., 72, 4.*

[31] H. P. Savakus, K. A. Klicker and R. E. Newnham, 1981 "PZT Epoxy Piezoelectric Transducer: A Simplified Fabrication procedure" *Mater. Res. Bull. 16, 677.*

[32] T. R. Shrout, L. J. Bowen, and W. A. Schulze, 1980 "Extruded PZT-Polymer Composites for Electromechanical Transducer Applications" *Mater. Res. Bull. 15, 1371.*

[33] H. Banno, S. Saito, 1983 "Piezoelectric properties of Composites of Synthetic Rubber and $PbTiO_3$ or PZT" *Jpn. J. Appl. Phys. 22 (Suppl. 22-2), 67.*

[34] T. R. Gururaja, W. A. Schulze, T. R. Shrout, A. Safari, L Webster, and L. E. Cross, 1981 "High Frequency Applications of PZT/Polymer Composite Materials" *Ferroelectrics 39, 1245.*

[35] A. A. Shaulov, W. A. Smith, and B. M. Singer, 1984 "Performance of Ultrasonic Transducers Made from Composite Piezoelectric Materials" *Proceedings IEEE Ultrasonics Symposium, 545.*

[36] W. A. Smith. A. A. Shaulov, and B. A. Auld 1985 "Tailoring the Properties of composite piezoelectric Materials for Medical Ultrasonic Transducers" *Proceedings IEEE Ultrasonics Symposium, 642.*

[37] H. Honda. Y. Yamashita, and K. Uchida, 1982 "Array Transducer Using New Modified $PbTiO_3$ Ceramics" *Proceedings IEEE Ultrasonics Symposium, 845.*

[38] H. Takeuchi, S. Jyomura Y. Ishikawa, and L. E. Yamamoto 1982 "A 7.5 MHz Linear Array Ultrasonic Probe Using Modified $PbTiO_3$ Ceramics" *Proceedings IEEE Ultrasonics Symposium, 849.*

[39] Transducer Products Division "*Piezoelectric Ceramic Data Book for Designers" Morgan Matroc Inc. limited UK.*

[40] R. L. Goldberg, S. W. Smith 1994 "Multilayer Piezoelectric Ceramics for Two-Dimensional Array Transducer." *IEEE Trans. Ultrason. Ferroelec. Freq. Contr., Vol. 41. No. 5. pp 761-771.*

[41] G. R. Lockwood, D. H. Turnbull, and F. S. Foster, 1994 "Fabrication of High Frequency Spherically Shaped Ceramic Transducers" *IEEE Trans. Ultrason. Ferroelec. Freq. Contr., Vol. 41. No. 2. PP 231-235.*

[42] S. Saitoh, T. Kobayashi, K. Harada, S. Shimanuki, and Y. Yamashita, 1998 "A 20MHz Single-Element Ultrasonic Probe Using $0.91Pb(Zn_{1/3}Nb_{2/3})O_3$-$0.09PbTiO_3$ Single Crystal" *IEEE Trans. Ultrason. Ferroelec. Freq. Contr., Vol. 45. No.4. PP 1071-1076.*

[43] H. Kanbara, H. Kobayashi and K. Nakamura, 2000 "Analysis of Piezoelectric Thin Film Resonators with Acoustic Quarter-Wave Multilayers" *Jpn. J. Appl. Phys. Vol.39, PP. 3049-3053.*

[44] M. Lukacs, M. Sayer, and S. Foster, 2000 "Single Element High Frequency (>50 MHz) PZT Sol Gel Composite Ultrasound Transducers" *IEEE Trans. Ultrason. Ferroelec. Freq. Contr., Vol. 47. No.1. PP 148-159.*

[45] T. Ritter, X. Geng, K. K. Shung, P. D. Lopath, S. Park, and T. R. Shrout, 2000 "Single Crystal PZT/PT-Polymer Composite for Ultrasound Transducer Applications" *IEEE Trans. Ultrason. Ferroelec. Freq. Contr., Vol. 47. No.4. PP 792-800,1996.*

[46] Reinoud F. Wolffenbuttel & Jens A. Foerster, 1990 "Non-contact Capacitive Torque Sensor For Use on Rotating Axle" *IEEE Trans. Instrum. Meas., Vol. 39, No. 6, pp. 1008-1013.*

[47] R. Palla's-Areny & J. G Webster, 1991 *'Sensors and Signal Conditioning'* John Willey & sons, Inc., New York.

[48]G. A. Woolvet 1982 "Digital Transducers" *Instrument Science & Technology, Vol 15, pp 1271 - 1280.*

[49] Murty, D.V.S., 1999 *'Transducers and instrumentation'* Prentice-Hall of India.

[50] Thomas, G. B and Finney, R. L 1984 *'Calculus and Analytic Geometry'* 6th edition, pp 398-400. Narosa Publishing House, New Delhi.

[51] Millman, J. and Grabel, A., 1987 *'Microelectronics'* 2nd edition. McGraw-Hill Book Co.- Singapore.

[52] Petrozella, F. D., 1996 '*Industrial Electronics*' Glencoe McGraw-Hill Book Co.- Singapore.

[55] Reid, C. R., Praunitz, J. M. and Sherwood, T. K. 3rd edition. 1977. *The Properties of Gases and Liquids*. McGraw-Hill, USA.

[54] http://www.hanssummers.com/

[55] Momozawa, S., and Imano, K. 2001. "Viscosity Measurements in Liquid Using Transversal Effects of Piezoceramic Disk-Type PZT Transducer in the Frequency Range of 70-430 KHz" Japanese Journal of Applied Physics 40: 3654-3657.

[56] Vladimir and Nosov, R. vol.2 —. Soviet Progress in Applied Ultrasonic. - Ultrasonic in the chemical industry.

[57] Shirley, D. J. 1977. "Method for Measuring in *situ* Acoustic Impedance of Marine Sediments" J. Acoust. Soc. Am. 62: 1028-1032.

[58] http://www.spacegrant.hawaii.edu/

[59] Hippel, R. V. 1954. '*Dielectric Materials and Applications*' Technology Press, New York.

[60] Ensminger, D. 1973 '*Ultrasonics the low-and high-intensity applications*' Mircel Dekker, Inc. New York.

[61] Adamowski, J. C., Buiochi, F. and Sigelmann, R. A. 1998. "Ultrasonic Density Sensor for Liquids" IEEE Trans. on Ultrason. Ferroelectr. Freq. Control; 45: 85-92.

[62] Hauptmann, P. Hoppe, N. and Püttmer, A. 2002. Application of Ultrasonic Sensors in the Process Industry. IOP on Meas. Sci. Technol. Vol.13, PP 73 - 83.

[63] Robert H. Perry, Don W. Green and James O. Maloney 1984 *'Perry's Chemical Engineering Handbook'* 6th edition, McGraw-Hill, Singapore.

[64] G. Bucci and C. Landi 1997 "Numerical method for transit time measurement in ultrasonic sensor applications," *IEEE Trans. Instum. Meas., Vol. 46.*

[65] G. B. Thomas, N. B. Lewis, and D. M. Roy *1987 'Mechanical Measurements'* Narosa publishing house.

[66] J. W. Dally, W. F. Riley, and K. G. McConnell 1993 *'Instrumentation for Engineering Measurements'* 2nd edition, John Willy & Sons, Inc. (Canada).

[67] Colby, M.Y. 1958. *Velocity of sound, Vibrating air columns & Doppler effect*, "Sound Waves & Acoustics," Henry Hot & Company, Inc., pp.127-133.

[68] David Webster 1994 "A Pulsed Ultrasonic Distance Measurement System Based on Phase Digitizing," *IEEE Trans. Inst. and Meas. Vol.43, No.4*: pp578-582.

[69] Canali, C DeCicco, G. Morten, B. Prudenziali, M and Taroni, A. 1982, "A Temperature Compensated Ultrasonic Sensor Operating in Air for Distance and Proximity Measurements," *IEEE Trans. Indust. Electro. Vol.-29, No.4: pp.336-341.*

[70] R. Goldman 1992 *'Ultrasonic Technology'* Reinhold Publishing Company, New York.

[71] P. B. Nagy and D. L. Johnson 1996 "Improved material characterization by pressure-dependent ultrasonic attenuation in air-filled permeable solids" *American Institute of Physics, Appl. Phys. Lett. Vol. 68, No. 26.*

APPENDIXES

```
//************** FROM 45 TO 135 DEGREES ***********//
     if (x>45)
     c1=(135-x),c2=0,c3=(x-45),c4=90;
     do
{
     f=k*(x-45)*(90-x),f1=k1*(x-45)*(90-x),f2=k2*(x-45)*(90-
x);
     f3=k3*(x-45)*(90-x),f4=k4*(x-45)*(90-x),f5=k5*(x-
45)*(90-x);
     //vr=v*sin(0.001*w*t);
     //vo=50*v*r*w*c*((c1-c3)*cos(.001*w*t)+(c4-
c2)*sin(0.001*w*t));
     z=atan((2*x-180)*(1-f*f)/90),z1=atan((2*x-180)*(1-
f1*f1)/90),z2=atan((2*x-180)*(1-f2*f2)/90);
     z3=atan((2*x-180)*(1-f3*f3)/90),z4=atan((2*x-180)*(1-
f4*f4)/90),z5=atan((2*x-180)*(1-f5*f5)/90);
     if(x>90) f=k*(x-90)*(135-x),z=atan((2*x-180)*(1-f*f)/
90),f1=k1*(x-90)*(135-x),z1=atan((2*x-180)*(1-f1*f1)/
90),f2=k2*(x-90)*(135-x),z2=atan((2*x-180)*(1-f2*f2)/
90),f3=k3*(x-90)*(135-x),z3=atan((2*x-180)*(1-f3*f3)/
90),f4=k4*(x-90)*(135-x),z4=atan((2*x-180)*(1-f4*f4)/
90),f5=k5*(x-90)*(135-x),z5=atan((2*x-180)*(1-f5*f5)/90);
y=(180*z/pi)+90,y1=(180*z1/pi)+90,y2=(180*z2/pi)+90;
y3=(180*z3/pi)+90, y4=(180*z4/pi)+90,y5=(180*z5/pi)+90;

e=y-x,e1=y1-x,e2=y2-x,e3=y3-x,e4=y4-x,e5=y5-x;
     printf("%1.2f  %1.2f     %1.2f     %1.2f     %1.2f
%1.2f     %1.2f     %1.2f     %1.2f     %1.2f     %1.2f
%1.2f     %1.2f\n",x,y,e,y1,e1,y2,e2,y3,e3,y4,e4,y5,e5);
     fprintf(fp,"%1.2f   %1.2f     %1.2f     %1.2f     %1.2f
%1.2f     %1.2f     %1.2f     %1.2f     %1.2f     %1.2f
%1.2f     %1.2f\n",x,y,e,y1,e1,y2,e2,y3,e3,y4,e4,y5,e5);
     x=x+0.5;
 }
     while (x<=135);
```

```
////************** FROM 135 TO 225 DEGREES***********////
     if (x>135)
          c1=0,c4=(x-135),c3=90,c2=(225-x);
     do
{
     f=k*(x-135)*(180-x),f1=k1*(x-135)*(180-x),f2=k2*(x-
135)*(180-x);
     f3=k3*(x-135)*(180-x),f4=k4*(x-135)*(180-x),f5=k5*(x-
135)*(180-x);

     //vr=v*sin(0.001*w*t);
     //vo=50*v*r*w*c*((c1-c3)*cos(.001*w*t)+(c4-
c2)*sin(0.001*w*t));
          z=atan((2*x-360)*(1-f*f)/90),z1=atan((2*x-360)*(1-
f1*f1)/90),z2=atan((2*x-360)*(1-f2*f2)/90);
     z3=atan((2*x-360)*(1-f3*f3)/90),z4=atan((2*x-360)*(1-
f4*f4)/90),z5=atan((2*x-360)*(1-f5*f5)/90);

     if(x>180) f=k*(x-180)*(225-x), z=atan((2*x-360)*(1-
f*f)/90),f1=k1*(x-180)*(225-x), z1=atan((2*x-360)*(1-f1*f1)/
90),f2=k2*(x-180)*(225-x), z2=atan((2*x-360)*(1-f2*f2)/
90),f3=k3*(x-180)*(225-x), z3=atan((2*x-360)*(1-f3*f3)/
90),f4=k4*(x-180)*(225-x), z4=atan((2*x-360)*(1-f4*f4)/
90),f5=k5*(x-180)*(225-x), z5=atan((2*x-360)*(1-f5*f5)/90);
y=(180*z/pi)+180,y1=(180*z1/pi)+180,y2=(180*z2/pi)+180;
y3=(180*z3/pi)+180,y4=(180*z4/pi)+180,y5=(180*z5/pi)+180;
     e=y-x,e1=y1-x,e2=y2-x,e3=y3-x,e4=y4-x,e5=y5-x;
     printf("%1.2f  %1.2f     %1.2f     %1.2f     %1.2f
%1.2f     %1.2f     %1.2f     %1.2f     %1.2f     %1.2f
%1.2f     %1.2f\n",x,y,e,y1,e1,y2,e2,y3,e3,y4,e4,y5,e5);
     fprintf(fp,"%1.2f   %1.2f     %1.2f     %1.2f     %1.2f
%1.2f     %1.2f     %1.2f     %1.2f     %1.2f     %1.2f
%1.2f     %1.2f\n",x,y,e,y1,e1,y2,e2,y3,e3,y4,e4,y5,e5);
     x=x+0.5;
}
     while (x<=225);
```

```
////************** FROM 225 TO 315 DEGREES   ***********////
     if(x>225)
          c1=(x-225),c2=90,c3=(315-x),c4=0;
     do
{
     f=k*(x-225)*(270-x),f1=k1*(x-225)*(270-x),f2=k2*(x-
225)*(270-x);
     f3=k3*(x-225)*(270-x),f4=k4*(x-225)*(270-x),f5=k5*(x-
225)*(270-x);
     //vr=v*sin(0.001*w*t);
     //vo=50*v*r*w*c*((c1-c3)*cos(.001*w*t)+(c4-
c2)*sin(0.001*w*t));

     z=atan((2*x-540)*(1-f*f)/90),z1=atan((2*x-540)*(1-
f1*f1)/90),z2=atan((2*x-540)*(1-f2*f2)/90);
     z3=atan((2*x-540)*(1-f3*f3)/90),z4=atan((2*x-540)*(1-
f4*f4)/90),z5=atan((2*x-540)*(1-f5*f5)/90);

     if(x>270) f=k*(x-270)*(315-x), z=atan((2*x-540)*(1-
f*f)/90),f1=k1*(x-270)*(315-x), z1=atan((2*x-540)*(1-f1*f1)/
90),f2=k2*(x-270)*(315-x), z2=atan((2*x-540)*(1-f2*f2)/
90),f3=k3*(x-270)*(315-x), z3=atan((2*x-540)*(1-f3*f3)/
90),f4=k4*(x-270)*(315-x), z4=atan((2*x-540)*(1-f4*f4)/
90),f5=k5*(x-270)*(315-x), z5=atan((2*x-540)*(1-f5*f5)/90);
     y=(180*z/pi)+270,y1=(180*z1/pi)+270,y2=(180*z2/pi)+270;
     y3=(180*z3/pi)+270,y4=(180*z4/pi)+270,y5=(180*z5/
pi)+270;
     e=y-x,e1=y1-x,e2=y2-x,e3=y3-x,e4=y4-x,e5=y5-x;
     printf("%1.2f  %1.2f     %1.2f     %1.2f     %1.2f
%1.2f     %1.2f     %1.2f     %1.2f     %1.2f     %1.2f
%1.2f     %1.2f\n",x,y,e,y1,e1,y2,e2,y3,e3,y4,e4,y5,e5);
     fprintf(fp,"%1.2f   %1.2f     %1.2f     %1.2f     %1.2f
%1.2f     %1.2f     %1.2f     %1.2f     %1.2f     %1.2f
%1.2f     %1.2f\n",x,y,e,y1,e1,y2,e2,y3,e3,y4,e4,y5,e5);
```

```
x=x+0.5;
}
     while (x<=315);
////************** FROM 315 TO -45 DEGREES***********////
     if(x>315)
     c1=90,c2=(405-x),c3=0,c4=(x-315);
     do
{
     f=k*(x-315)*(360-x),f1=k1*(x-315)*(360-x),f2=k2*(x-
315)*(360-x);
     f3=k3*(x-315)*(360-x),f4=k4*(x-315)*(360-x),f5=k5*(x-
315)*(360-x);
     //vr=v*sin(0.001*w*t);
     //vo=50*v*r*w*c*((c1-c3)*cos(.001*w*t)+(c4-
c2)*sin(0.001*w*t));
     z=atan((2*x-720)*(1-f*f)/90),z1=atan((2*x-720)*(1-
f1*f1)/90),z2=atan((2*x-720)*(1-f2*f2)/90);
     z3=atan((2*x-720)*(1-f3*f3)/90),z4=atan((2*x-720)*(1-
f4*f4)/90),z5=atan((2*x-720)*(1-f5*f5)/90);
y=(180*z/pi)+360,y1=(180*z1/pi)+360,y2=(180*z2/pi)+360;
y3=(180*z3/pi)+360,y4=(180*z4/pi)+360,y5=(180*z5/pi)+360;
     e=y-x,e1=y1-x,e2=y2-x,e3=y3-x,e4=y4-x,e5=y5-x;
     printf("%1.2f  %1.2f    %1.2f     %1.2f     %1.2f
%1.2f     %1.2f     %1.2f     %1.2f     %1.2f
%1.2f     %1.2f\n",x,y,e,y1,e1,y2,e2,y3,e3,y4,e4,y5,e5);
     fprintf(fp,"%1.2f   %1.2f     %1.2f     %1.2f     %1.2f
%1.2f     %1.2f     %1.2f     %1.2f     %1.2f
%1.2f     %1.2f\n",x,y,e,y1,e1,y2,e2,y3,e3,y4,e4,y5,e5);
     x=x+0.5;
}
     while (x<=360);
     return 0;
     fclose(fp);
}
```

APPEDIX: A-II RESULTS OF VISUAL C++ PROGAMME

Ideal	k=0		k=.0002		k=.0005k		k=.0008		k=.0009		k=.001	
Output	Output	error	Output	error	Output	error	Output	error	Output	error	Output	error
0	0	0	0	0	0	0	0	0	0	0	0	0
0.5	0.64	0.14	0.64	0.14	0.64	0.14	0.64	0.14	0.64	0.14	0.64	0.14
1	1.27	0.27	1.27	0.27	1.27	0.27	1.27	0.27	1.27	0.27	1.27	0.27
1.5	1.91	0.41	1.91	0.41	1.91	0.41	1.9	0.4	1.9	0.4	1.9	0.4
2	2.54	0.54	2.54	0.54	2.54	0.54	2.53	0.53	2.53	0.53	2.53	0.53
2.5	3.18	0.68	3.18	0.68	3.17	0.67	3.16	0.66	3.15	0.65	3.14	0.64
3	3.81	0.81	3.81	0.81	3.8	0.8	3.78	0.78	3.77	0.77	3.75	0.75
3.5	4.45	0.95	4.44	0.94	4.42	0.92	4.39	0.89	4.37	0.87	4.35	0.85
4	5.08	1.08	5.07	1.07	5.05	1.05	4.99	0.99	4.97	0.97	4.94	0.94
4.5	5.71	1.21	5.7	1.2	5.66	1.16	5.59	1.09	5.56	1.06	5.52	1.02
5	6.34	1.34	6.33	1.33	6.28	1.28	6.18	1.18	6.14	1.14	6.09	1.09
5.5	6.97	1.47	6.96	1.46	6.89	1.39	6.76	1.26	6.7	1.2	6.64	1.14
6	7.59	1.59	7.58	1.58	7.49	1.49	7.33	1.33	7.26	1.26	7.18	1.18
6.5	8.22	1.72	8.2	1.7	8.09	1.59	7.89	1.39	7.81	1.31	7.71	1.21
7	8.84	1.84	8.82	1.82	8.69	1.69	8.45	1.45	8.34	1.34	8.23	1.23
7.5	9.46	1.96	9.43	1.93	9.28	1.78	8.99	1.49	8.87	1.37	8.73	1.23
8	10.08	2.08	10.05	2.05	9.86	1.86	9.53	1.53	9.38	1.38	9.21	1.21
8.5	10.7	2.2	10.66	2.16	10.44	1.94	10.05	1.55	9.88	1.38	9.69	1.19
9	11.31	2.31	11.26	2.26	11.02	2.02	10.57	1.57	10.37	1.37	10.15	1.15
9.5	11.92	2.42	11.87	2.37	11.59	2.09	11.08	1.58	10.85	1.35	10.6	1.1
10	12.53	2.53	12.47	2.47	12.16	2.16	11.57	1.57	11.32	1.32	11.03	1.03
10.5	13.13	2.63	13.07	2.57	12.72	2.22	12.06	1.56	11.78	1.28	11.46	0.96
11	13.74	2.74	13.66	2.66	13.27	2.27	12.55	1.55	12.23	1.23	11.87	0.87
11.5	14.34	2.84	14.25	2.75	13.82	2.32	13.02	1.52	12.67	1.17	12.28	0.78
12	14.93	2.93	14.84	2.84	14.37	2.37	13.49	1.49	13.1	1.1	12.67	0.67
12.5	15.52	3.02	15.43	2.93	14.91	2.41	13.95	1.45	13.53	1.03	13.06	0.56
13	16.11	3.11	16.01	3.01	15.45	2.45	14.41	1.41	13.95	0.95	13.44	0.44
13.5	16.7	3.2	16.59	3.09	15.98	2.48	14.86	1.36	14.36	0.86	13.81	0.31
14	17.28	3.28	17.16	3.16	16.51	2.51	15.3	1.3	14.77	0.77	14.17	0.17
14.5	17.86	3.36	17.73	3.23	17.04	2.54	15.74	1.24	15.17	0.67	14.53	0.03
15	18.43	3.43	18.3	3.3	17.56	2.56	16.18	1.18	15.57	0.57	14.89	-0.11
15.5	19.01	3.51	18.86	3.36	18.08	2.58	16.61	1.11	15.97	0.47	15.24	-0.26
16	19.57	3.57	19.42	3.42	18.59	2.59	17.04	1.04	16.36	0.36	15.59	-0.41
16.5	20.14	3.64	19.97	3.47	19.11	2.61	17.47	0.97	16.75	0.25	15.94	-0.56
17	20.7	3.7	20.52	3.52	19.61	2.61	17.9	0.9	17.14	0.14	16.29	-0.71
17.5	21.25	3.75	21.07	3.57	20.12	2.62	18.33	0.83	17.53	0.03	16.64	-0.86
18	21.8	3.8	21.61	3.61	20.63	2.63	18.75	0.75	17.92	-0.08	16.99	-1.01
18.5	22.35	3.85	22.15	3.65	21.13	2.63	19.18	0.68	18.32	-0.18	17.34	-1.16
19	22.89	3.89	22.69	3.69	21.63	2.63	19.61	0.61	18.71	-0.29	17.7	-1.3
19.5	23.43	3.93	23.22	3.72	22.12	2.62	20.04	0.54	19.11	-0.39	18.07	-1.43
20	23.96	3.96	23.75	3.75	22.62	2.62	20.47	0.47	19.52	-0.48	18.43	-1.57
20.5	24.49	3.99	24.27	3.77	23.11	2.61	20.91	0.41	19.92	-0.58	18.81	-1.69
21	25.02	4.02	24.79	3.79	23.61	2.61	21.35	0.35	20.34	-0.66	19.19	-1.81
21.5	25.54	4.04	25.31	3.81	24.1	2.6	21.79	0.29	20.76	-0.74	19.59	-1.91
22	26.05	4.05	25.82	3.82	24.59	2.59	22.23	0.23	21.18	-0.82	19.99	-2.01
22.5	26.57	4.07	26.33	3.83	25.08	2.58	22.68	0.18	21.61	-0.89	20.4	-2.1
23	27.07	4.07	26.83	3.83	25.57	2.57	23.14	0.14	22.05	-0.95	20.82	-2.18
23.5	27.57	4.07	27.33	3.83	26.05	2.55	23.6	0.1	22.5	-1	21.25	-2.25
24	28.07	4.07	27.83	3.83	26.54	2.54	24.07	0.07	22.96	-1.04	21.7	-2.3
24.5	28.57	4.07	28.32	3.82	27.03	2.53	24.54	0.04	23.42	-1.08	22.15	-2.35
25	29.05	4.05	28.81	3.81	27.51	2.51	25.02	0.02	23.9	-1.1	22.62	-2.38
25.5	29.54	4.04	29.3	3.8	28	2.5	25.5	0	24.38	-1.12	23.1	-2.4
26	30.02	4.02	29.78	3.78	28.48	2.48	25.99	-0.01	24.87	-1.13	23.59	-2.41

Ideal	k=0		k=.0002		k=.0005k		k=.0008		k=.0009		k=.001	
Output	Output	error	Output	error	Output	error	Output	error	Output	error	Output	error
26.5	30.49	3.99	30.25	3.75	28.96	2.46	26.49	-0.01	25.37	-1.13	24.1	-2.4
27	30.96	3.96	30.72	3.72	29.45	2.45	26.99	-0.01	25.88	-1.12	24.62	-2.38
27.5	31.43	3.93	31.19	3.69	29.93	2.43	27.5	0	26.4	-1.1	25.15	-2.35
28	31.89	3.89	31.66	3.66	30.41	2.41	28.01	0.01	26.93	-1.07	25.7	-2.3
28.5	32.35	3.85	32.12	3.62	30.89	2.39	28.53	0.03	27.47	-1.03	26.26	-2.24
29	32.8	3.8	32.57	3.57	31.37	2.37	29.06	0.06	28.02	-0.98	26.83	-2.17
29.5	33.25	3.75	33.03	3.53	31.85	2.35	29.59	0.09	28.57	-0.93	27.41	-2.09
30	33.69	3.69	33.48	3.48	32.33	2.33	30.13	0.13	29.13	-0.87	28	-2
30.5	34.13	3.63	33.92	3.42	32.81	2.31	30.67	0.17	29.7	-0.8	28.6	-1.9
31	34.56	3.56	34.36	3.36	33.28	2.28	31.21	0.21	30.28	-0.72	29.21	-1.79
31.5	34.99	3.49	34.8	3.3	33.76	2.26	31.76	0.26	30.86	-0.64	29.83	-1.67
32	35.42	3.42	35.23	3.23	34.23	2.23	32.31	0.31	31.44	-0.56	30.46	-1.54
32.5	35.84	3.34	35.66	3.16	34.7	2.2	32.86	0.36	32.03	-0.47	31.09	-1.41
33	36.25	3.25	36.08	3.08	35.17	2.17	33.41	0.41	32.63	-0.37	31.73	-1.27
33.5	36.67	3.17	36.5	3	35.63	2.13	33.97	0.47	33.22	-0.28	32.37	-1.13
34	37.07	3.07	36.92	2.92	36.1	2.1	34.52	0.52	33.82	-0.18	33.02	-0.98
34.5	37.48	2.98	37.33	2.83	36.56	2.06	35.08	0.58	34.42	-0.08	33.67	-0.83
35	37.87	2.87	37.74	2.74	37.01	2.01	35.63	0.63	35.02	0.02	34.31	-0.69
35.5	38.27	2.77	38.14	2.64	37.47	1.97	36.18	0.68	35.61	0.11	34.96	-0.54
36	38.66	2.66	38.54	2.54	37.92	1.92	36.73	0.73	36.2	0.2	35.6	-0.4
36.5	39.05	2.55	38.94	2.44	38.36	1.86	37.28	0.78	36.79	0.29	36.24	-0.26
37	39.43	2.43	39.33	2.33	38.81	1.81	37.82	0.82	37.38	0.38	36.88	-0.12
37.5	39.81	2.31	39.72	2.22	39.24	1.74	38.35	0.85	37.95	0.45	37.5	0
38	40.18	2.18	40.1	2.1	39.68	1.68	38.88	0.88	38.52	0.52	38.12	0.12
38.5	40.55	2.05	40.48	1.98	40.1	1.6	39.4	0.9	39.08	0.58	38.73	0.23
39	40.91	1.91	40.85	1.85	40.52	1.52	39.91	0.91	39.63	0.63	39.32	0.32
39.5	41.28	1.78	41.22	1.72	40.94	1.44	40.41	0.91	40.17	0.67	39.91	0.41
40	41.63	1.63	41.59	1.59	41.35	1.35	40.9	0.9	40.7	0.7	40.48	0.48
40.5	41.99	1.49	41.95	1.45	41.75	1.25	41.38	0.88	41.21	0.71	41.03	0.53
41	42.34	1.34	42.31	1.31	42.14	1.14	41.84	0.84	41.71	0.71	41.56	0.56
41.5	42.68	1.18	42.66	1.16	42.53	1.03	42.29	0.79	42.19	0.69	42.07	0.57
42	43.03	1.03	43.01	1.01	42.91	0.91	42.73	0.73	42.66	0.66	42.57	0.57
42.5	43.36	0.86	43.35	0.85	43.28	0.78	43.16	0.66	43.1	0.6	43.04	0.54
43	43.7	0.7	43.69	0.69	43.65	0.65	43.56	0.56	43.53	0.53	43.49	0.49
43.5	44.03	0.53	44.02	0.52	44	0.5	43.95	0.45	43.93	0.43	43.91	0.41
44	44.36	0.36	44.35	0.35	44.34	0.34	44.32	0.32	44.31	0.31	44.3	0.3
44.5	44.68	0.18	44.68	0.18	44.68	0.18	44.67	0.17	44.67	0.17	44.67	0.17
45	45	0	45	0	45	0	45	0	45	0	45	0
45.5	45.32	-0.18	45.32	-0.18	45.32	-0.18	45.33	-0.17	45.33	-0.17	45.33	-0.17
46	45.64	-0.36	45.65	-0.35	45.66	-0.34	45.68	-0.32	45.69	-0.31	45.7	-0.3
46.5	45.97	-0.53	45.98	-0.52	46	-0.5	46.05	-0.45	46.07	-0.43	46.09	-0.41
47	46.3	-0.7	46.31	-0.69	46.35	-0.65	46.44	-0.56	46.47	-0.53	46.51	-0.49
47.5	46.64	-0.86	46.65	-0.85	46.72	-0.78	46.84	-0.66	46.9	-0.6	46.96	-0.54
48	46.97	-1.03	46.99	-1.01	47.09	-0.91	47.27	-0.73	47.34	-0.66	47.43	-0.57
48.5	47.32	-1.18	47.34	-1.16	47.47	-1.03	47.71	-0.79	47.81	-0.69	47.93	-0.57
49	47.66	-1.34	47.69	-1.31	47.86	-1.14	48.16	-0.84	48.29	-0.71	48.44	-0.56
49.5	48.01	-1.49	48.05	-1.45	48.25	-1.25	48.62	-0.88	48.79	-0.71	48.97	-0.53
50	48.37	-1.63	48.41	-1.59	48.65	-1.35	49.1	-0.9	49.3	-0.7	49.52	-0.48
50.5	48.72	-1.78	48.78	-1.72	49.06	-1.44	49.59	-0.91	49.83	-0.67	50.09	-0.41
51	49.09	-1.91	49.15	-1.85	49.48	-1.52	50.09	-0.91	50.37	-0.63	50.68	-0.32
51.5	49.45	-2.05	49.52	-1.98	49.9	-1.6	50.6	-0.9	50.92	-0.58	51.27	-0.23
52	49.82	-2.18	49.9	-2.1	50.32	-1.68	51.12	-0.88	51.48	-0.52	51.88	-0.12
52.5	50.19	-2.31	50.28	-2.22	50.76	-1.74	51.65	-0.85	52.05	-0.45	52.5	0

Ideal	k=0		k=.0002		k=.0005k		k=.0008		k=.0009		k=.001	
Output	Output	error	Output	error	Output	error	Output	error	Output	error	Output	error
53	50.57	-2.43	50.67	-2.33	51.19	-1.81	52.18	-0.82	52.62	-0.38	53.12	0.12
53.5	50.95	-2.55	51.06	-2.44	51.64	-1.86	52.72	-0.78	53.21	-0.29	53.76	0.26
54	51.34	-2.66	51.46	-2.54	52.08	-1.92	53.27	-0.73	53.8	-0.2	54.4	0.4
54.5	51.73	-2.77	51.86	-2.64	52.53	-1.97	53.82	-0.68	54.39	-0.11	55.04	0.54
55	52.13	-2.87	52.26	-2.74	52.99	-2.01	54.37	-0.63	54.98	-0.02	55.69	0.69
55.5	52.52	-2.98	52.67	-2.83	53.44	-2.06	54.92	-0.58	55.58	0.08	56.33	0.83
56	52.93	-3.07	53.08	-2.92	53.9	-2.1	55.48	-0.52	56.18	0.18	56.98	0.98
56.5	53.33	-3.17	53.5	-3	54.37	-2.13	56.03	-0.47	56.78	0.28	57.63	1.13
57	53.75	-3.25	53.92	-3.08	54.83	-2.17	56.59	-0.41	57.37	0.37	58.27	1.27
57.5	54.16	-3.34	54.34	-3.16	55.3	-2.2	57.14	-0.36	57.97	0.47	58.91	1.41
58	54.58	-3.42	54.77	-3.23	55.77	-2.23	57.69	-0.31	58.56	0.56	59.54	1.54
58.5	55.01	-3.49	55.2	-3.3	56.24	-2.26	58.24	-0.26	59.14	0.64	60.17	1.67
59	55.44	-3.56	55.64	-3.36	56.72	-2.28	58.79	-0.21	59.72	0.72	60.79	1.79
59.5	55.87	-3.63	56.08	-3.42	57.19	-2.31	59.33	-0.17	60.3	0.8	61.4	1.9
60	56.31	-3.69	56.52	-3.48	57.67	-2.33	59.87	-0.13	60.87	0.87	62	2
60.5	56.75	-3.75	56.97	-3.53	58.15	-2.35	60.41	-0.09	61.43	0.93	62.59	2.09
61	57.2	-3.8	57.43	-3.57	58.63	-2.37	60.94	-0.06	61.98	0.98	63.17	2.17
61.5	57.65	-3.85	57.88	-3.62	59.11	-2.39	61.47	-0.03	62.53	1.03	63.74	2.24
62	58.11	-3.89	58.34	-3.66	59.59	-2.41	61.99	-0.01	63.07	1.07	64.3	2.3
62.5	58.57	-3.93	58.81	-3.69	60.07	-2.43	62.5	0	63.6	1.1	64.85	2.35
63	59.04	-3.96	59.28	-3.72	60.55	-2.45	63.01	0.01	64.12	1.12	65.38	2.38
63.5	59.51	-3.99	59.75	-3.75	61.04	-2.46	63.51	0.01	64.63	1.13	65.9	2.4
64	59.98	-4.02	60.22	-3.78	61.52	-2.48	64.01	0.01	65.13	1.13	66.41	2.41
64.5	60.46	-4.04	60.7	-3.8	62	-2.5	64.5	0	65.62	1.12	66.9	2.4
65	60.95	-4.05	61.19	-3.81	62.49	-2.51	64.98	-0.02	66.1	1.1	67.38	2.38
65.5	61.43	-4.07	61.68	-3.82	62.97	-2.53	65.46	-0.04	66.58	1.08	67.85	2.35
66	61.93	-4.07	62.17	-3.83	63.46	-2.54	65.93	-0.07	67.04	1.04	68.3	2.3
66.5	62.43	-4.07	62.67	-3.83	63.95	-2.55	66.4	-0.1	67.5	1	68.75	2.25
67	62.93	-4.07	63.17	-3.83	64.43	-2.57	66.86	-0.14	67.95	0.95	69.18	2.18
67.5	63.43	-4.07	63.67	-3.83	64.92	-2.58	67.32	-0.18	68.39	0.89	69.6	2.1
68	63.95	-4.05	64.18	-3.82	65.41	-2.59	67.77	-0.23	68.82	0.82	70.01	2.01
68.5	64.46	-4.04	64.69	-3.81	65.9	-2.6	68.21	-0.29	69.24	0.74	70.41	1.91
69	64.98	-4.02	65.21	-3.79	66.39	-2.61	68.65	-0.35	69.66	0.66	70.81	1.81
69.5	65.51	-3.99	65.73	-3.77	66.89	-2.61	69.09	-0.41	70.08	0.58	71.19	1.69
70	66.04	-3.96	66.25	-3.75	67.38	-2.62	69.53	-0.47	70.48	0.48	71.57	1.57
70.5	66.57	-3.93	66.78	-3.72	67.88	-2.62	69.96	-0.54	70.89	0.39	71.93	1.43
71	67.11	-3.89	67.31	-3.69	68.37	-2.63	70.39	-0.61	71.29	0.29	72.3	1.3
71.5	67.65	-3.85	67.85	-3.65	68.87	-2.63	70.82	-0.68	71.68	0.18	72.66	1.16
72	68.2	-3.8	68.39	-3.61	69.37	-2.63	71.25	-0.75	72.08	0.08	73.01	1.01
72.5	68.75	-3.75	68.93	-3.57	69.88	-2.62	71.67	-0.83	72.47	-0.03	73.36	0.86
73	69.3	-3.7	69.48	-3.52	70.39	-2.61	72.1	-0.9	72.86	-0.14	73.71	0.71
73.5	69.86	-3.64	70.03	-3.47	70.89	-2.61	72.53	-0.97	73.25	-0.25	74.06	0.56
74	70.43	-3.57	70.58	-3.42	71.41	-2.59	72.96	-1.04	73.64	-0.36	74.41	0.41
74.5	70.99	-3.51	71.14	-3.36	71.92	-2.58	73.39	-1.11	74.03	-0.47	74.76	0.26
75	71.57	-3.43	71.7	-3.3	72.44	-2.56	73.82	-1.18	74.43	-0.57	75.11	0.11
75.5	72.14	-3.36	72.27	-3.23	72.96	-2.54	74.26	-1.24	74.83	-0.67	75.47	-0.03
76	72.72	-3.28	72.84	-3.16	73.49	-2.51	74.7	-1.3	75.23	-0.77	75.83	-0.17
76.5	73.3	-3.2	73.41	-3.09	74.02	-2.48	75.14	-1.36	75.64	-0.86	76.19	-0.31
77	73.89	-3.11	73.99	-3.01	74.55	-2.45	75.59	-1.41	76.05	-0.95	76.56	-0.44
77.5	74.48	-3.02	74.57	-2.93	75.09	-2.41	76.05	-1.45	76.47	-1.03	76.94	-0.56
78	75.07	-2.93	75.16	-2.84	75.63	-2.37	76.51	-1.49	76.9	-1.1	77.33	-0.67
78.5	75.66	-2.84	75.75	-2.75	76.18	-2.32	76.98	-1.52	77.33	-1.17	77.72	-0.78
79	76.26	-2.74	76.34	-2.66	76.73	-2.27	77.45	-1.55	77.77	-1.23	78.13	-0.87

Ideal	k=0		k=.0002		k=.0005k		k=.0008		k=.0009		k=.001	
Output	Output	error	Output	error	Output	error	Output	error	Output	error	Output	error
53	50.57	-2.43	50.67	-2.33	51.19	-1.81	52.18	-0.82	52.62	-0.38	53.12	0.12
53.5	50.95	-2.55	51.06	-2.44	51.64	-1.86	52.72	-0.78	53.21	-0.29	53.76	0.26
54	51.34	-2.66	51.46	-2.54	52.08	-1.92	53.27	-0.73	53.8	-0.2	54.4	0.4
54.5	51.73	-2.77	51.86	-2.64	52.53	-1.97	53.82	-0.68	54.39	-0.11	55.04	0.54
55	52.13	-2.87	52.26	-2.74	52.99	-2.01	54.37	-0.63	54.98	-0.02	55.69	0.69
55.5	52.52	-2.98	52.67	-2.83	53.44	-2.06	54.92	-0.58	55.58	0.08	56.33	0.83
56	52.93	-3.07	53.08	-2.92	53.9	-2.1	55.48	-0.52	56.18	0.18	56.98	0.98
56.5	53.33	-3.17	53.5	-3	54.37	-2.13	56.03	-0.47	56.78	0.28	57.63	1.13
57	53.75	-3.25	53.92	-3.08	54.83	-2.17	56.59	-0.41	57.37	0.37	58.27	1.27
57.5	54.16	-3.34	54.34	-3.16	55.3	-2.2	57.14	-0.36	57.97	0.47	58.91	1.41
58	54.58	-3.42	54.77	-3.23	55.77	-2.23	57.69	-0.31	58.56	0.56	59.54	1.54
58.5	55.01	-3.49	55.2	-3.3	56.24	-2.26	58.24	-0.26	59.14	0.64	60.17	1.67
59	55.44	-3.56	55.64	-3.36	56.72	-2.28	58.79	-0.21	59.72	0.72	60.79	1.79
59.5	55.87	-3.63	56.08	-3.42	57.19	-2.31	59.33	-0.17	60.3	0.8	61.4	1.9
60	56.31	-3.69	56.52	-3.48	57.67	-2.33	59.87	-0.13	60.87	0.87	62	2
60.5	56.75	-3.75	56.97	-3.53	58.15	-2.35	60.41	-0.09	61.43	0.93	62.59	2.09
61	57.2	-3.8	57.43	-3.57	58.63	-2.37	60.94	-0.06	61.98	0.98	63.17	2.17
61.5	57.65	-3.85	57.88	-3.62	59.11	-2.39	61.47	-0.03	62.53	1.03	63.74	2.24
62	58.11	-3.89	58.34	-3.66	59.59	-2.41	61.99	-0.01	63.07	1.07	64.3	2.3
62.5	58.57	-3.93	58.81	-3.69	60.07	-2.43	62.5	0	63.6	1.1	64.85	2.35
63	59.04	-3.96	59.28	-3.72	60.55	-2.45	63.01	0.01	64.12	1.12	65.38	2.38
63.5	59.51	-3.99	59.75	-3.75	61.04	-2.46	63.51	0.01	64.63	1.13	65.9	2.4
64	59.98	-4.02	60.22	-3.78	61.52	-2.48	64.01	0.01	65.13	1.13	66.41	2.41
64.5	60.46	-4.04	60.7	-3.8	62	-2.5	64.5	0	65.62	1.12	66.9	2.4
65	60.95	-4.05	61.19	-3.81	62.49	-2.51	64.98	-0.02	66.1	1.1	67.38	2.38
65.5	61.43	-4.07	61.68	-3.82	62.97	-2.53	65.46	-0.04	66.58	1.08	67.85	2.35
66	61.93	-4.07	62.17	-3.83	63.46	-2.54	65.93	-0.07	67.04	1.04	68.3	2.3
66.5	62.43	-4.07	62.67	-3.83	63.95	-2.55	66.4	-0.1	67.5	1	68.75	2.25
67	62.93	-4.07	63.17	-3.83	64.43	-2.57	66.86	-0.14	67.95	0.95	69.18	2.18
67.5	63.43	-4.07	63.67	-3.83	64.92	-2.58	67.32	-0.18	68.39	0.89	69.6	2.1
68	63.95	-4.05	64.18	-3.82	65.41	-2.59	67.77	-0.23	68.82	0.82	70.01	2.01
68.5	64.46	-4.04	64.69	-3.81	65.9	-2.6	68.21	-0.29	69.24	0.74	70.41	1.91
69	64.98	-4.02	65.21	-3.79	66.39	-2.61	68.65	-0.35	69.66	0.66	70.81	1.81
69.5	65.51	-3.99	65.73	-3.77	66.89	-2.61	69.09	-0.41	70.08	0.58	71.19	1.69
70	66.04	-3.96	66.25	-3.75	67.38	-2.62	69.53	-0.47	70.48	0.48	71.57	1.57
70.5	66.57	-3.93	66.78	-3.72	67.88	-2.62	69.96	-0.54	70.89	0.39	71.93	1.43
71	67.11	-3.89	67.31	-3.69	68.37	-2.63	70.39	-0.61	71.29	0.29	72.3	1.3
71.5	67.65	-3.85	67.85	-3.65	68.87	-2.63	70.82	-0.68	71.68	0.18	72.66	1.16
72	68.2	-3.8	68.39	-3.61	69.37	-2.63	71.25	-0.75	72.08	0.08	73.01	1.01
72.5	68.75	-3.75	68.93	-3.57	69.88	-2.62	71.67	-0.83	72.47	-0.03	73.36	0.86
73	69.3	-3.7	69.48	-3.52	70.39	-2.61	72.1	-0.9	72.86	-0.14	73.71	0.71
73.5	69.86	-3.64	70.03	-3.47	70.89	-2.61	72.53	-0.97	73.25	-0.25	74.06	0.56
74	70.43	-3.57	70.58	-3.42	71.41	-2.59	72.96	-1.04	73.64	-0.36	74.41	0.41
74.5	70.99	-3.51	71.14	-3.36	71.92	-2.58	73.39	-1.11	74.03	-0.47	74.76	0.26
75	71.57	-3.43	71.7	-3.3	72.44	-2.56	73.82	-1.18	74.43	-0.57	75.11	0.11
75.5	72.14	-3.36	72.27	-3.23	72.96	-2.54	74.26	-1.24	74.83	-0.67	75.47	-0.03
76	72.72	-3.28	72.84	-3.16	73.49	-2.51	74.7	-1.3	75.23	-0.77	75.83	-0.17
76.5	73.3	-3.2	73.41	-3.09	74.02	-2.48	75.14	-1.36	75.64	-0.86	76.19	-0.31
77	73.89	-3.11	73.99	-3.01	74.55	-2.45	75.59	-1.41	76.05	-0.95	76.56	-0.44
77.5	74.48	-3.02	74.57	-2.93	75.09	-2.41	76.05	-1.45	76.47	-1.03	76.94	-0.56
78	75.07	-2.93	75.16	-2.84	75.63	-2.37	76.51	-1.49	76.9	-1.1	77.33	-0.67
78.5	75.66	-2.84	75.75	-2.75	76.18	-2.32	76.98	-1.52	77.33	-1.17	77.72	-0.78
79	76.26	-2.74	76.34	-2.66	76.73	-2.27	77.45	-1.55	77.77	-1.23	78.13	-0.87

Ideal	k=0		k=.0002		k=.0005k		k=.0008		k=.0009		k=.001	
Output	Output	error	Output	error	Output	error	Output	error	Output	error	Output	error
106	109.6	3.57	109.4	3.42	108.6	2.59	107	1.04	106.4	0.36	105.6	-0.41
106.5	110.1	3.64	110	3.47	109.1	2.61	107.5	0.97	106.8	0.25	105.9	-0.56
107	110.7	3.7	110.5	3.52	109.6	2.61	107.9	0.9	107.1	0.14	106.3	-0.71
107.5	111.3	3.75	111.1	3.57	110.1	2.62	108.3	0.83	107.5	0.03	106.6	-0.86
108	111.8	3.8	111.6	3.61	110.6	2.63	108.8	0.75	107.9	-0.08	107	-1.01
108.5	112.4	3.85	112.2	3.65	111.1	2.63	109.2	0.68	108.3	-0.18	107.3	-1.16
109	112.9	3.89	112.7	3.69	111.6	2.63	109.6	0.61	108.7	-0.29	107.7	-1.3
109.5	113.4	3.93	113.2	3.72	112.1	2.62	110	0.54	109.1	-0.39	108.1	-1.43
110	114	3.96	113.8	3.75	112.6	2.62	110.5	0.47	109.5	-0.48	108.4	-1.57
110.5	114.5	3.99	114.3	3.77	113.1	2.61	110.9	0.41	109.9	-0.58	108.8	-1.69
111	115	4.02	114.8	3.79	113.6	2.61	111.4	0.35	110.3	-0.66	109.2	-1.81
111.5	115.5	4.04	115.3	3.81	114.1	2.6	111.8	0.29	110.8	-0.74	109.6	-1.91
112	116.1	4.05	115.8	3.82	114.6	2.59	112.2	0.23	111.2	-0.82	110	-2.01
112.5	116.6	4.07	116.3	3.83	115.1	2.58	112.7	0.18	111.6	-0.89	110.4	-2.1
113	117.1	4.07	116.8	3.83	115.6	2.57	113.1	0.14	112.1	-0.95	110.8	-2.18
113.5	117.6	4.07	117.3	3.83	116.1	2.55	113.6	0.1	112.5	-1	111.3	-2.25
114	118.1	4.07	117.8	3.83	116.5	2.54	114.1	0.07	113	-1.04	111.7	-2.3
114.5	118.6	4.07	118.3	3.82	117	2.53	114.5	0.04	113.4	-1.08	112.2	-2.35
115	119.1	4.05	118.8	3.81	117.5	2.51	115	0.02	113.9	-1.1	112.6	-2.38
115.5	119.5	4.04	119.3	3.8	118	2.5	115.5	0	114.4	-1.12	113.1	-2.4
116	120	4.02	119.8	3.78	118.5	2.48	116	-0.01	114.9	-1.13	113.6	-2.41
116.5	120.5	3.99	120.3	3.75	119	2.46	116.5	-0.01	115.4	-1.13	114.1	-2.4
117	121	3.96	120.7	3.72	119.5	2.45	117	-0.01	115.9	-1.12	114.6	-2.38
117.5	121.4	3.93	121.2	3.69	119.9	2.43	117.5	0	116.4	-1.1	115.2	-2.35
118	121.9	3.89	121.7	3.66	120.4	2.41	118	0.01	116.9	-1.07	115.7	-2.3
118.5	122.4	3.85	122.1	3.62	120.9	2.39	118.5	0.03	117.5	-1.03	116.3	-2.24
119	122.8	3.8	122.6	3.57	121.4	2.37	119.1	0.06	118	-0.98	116.8	-2.17
119.5	123.3	3.75	123	3.53	121.9	2.35	119.6	0.09	118.6	-0.93	117.4	-2.09
120	123.7	3.69	123.5	3.48	122.3	2.33	120.1	0.13	119.1	-0.87	118	-2
120.5	124.1	3.63	123.9	3.42	122.8	2.31	120.7	0.17	119.7	-0.8	118.6	-1.9
121	124.6	3.56	124.4	3.36	123.3	2.28	121.2	0.21	120.3	-0.72	119.2	-1.79
121.5	125	3.49	124.8	3.3	123.8	2.26	121.8	0.26	120.9	-0.64	119.8	-1.67
122	125.4	3.42	125.2	3.23	124.2	2.23	122.3	0.31	121.4	-0.56	120.5	-1.54
122.5	125.8	3.34	125.7	3.16	124.7	2.2	122.9	0.36	122	-0.47	121.1	-1.41
123	126.3	3.25	126.1	3.08	125.2	2.17	123.4	0.41	122.6	-0.37	121.7	-1.27
123.5	126.7	3.17	126.5	3	125.6	2.13	124	0.47	123.2	-0.28	122.4	-1.13
124	127.1	3.07	126.9	2.92	126.1	2.1	124.5	0.52	123.8	-0.18	123	-0.98
124.5	127.5	2.98	127.3	2.83	126.6	2.06	125.1	0.58	124.4	-0.08	123.7	-0.83
125	127.9	2.87	127.7	2.74	127	2.01	125.6	0.63	125	0.02	124.3	-0.69
125.5	128.3	2.77	128.1	2.64	127.5	1.97	126.2	0.68	125.6	0.11	125	-0.54
126	128.7	2.66	128.5	2.54	127.9	1.92	126.7	0.73	126.2	0.2	125.6	-0.4
126.5	129.1	2.55	128.9	2.44	128.4	1.86	127.3	0.78	126.8	0.29	126.2	-0.26
127	129.4	2.43	129.3	2.33	128.8	1.81	127.8	0.82	127.4	0.38	126.9	-0.12
127.5	129.8	2.31	129.7	2.22	129.2	1.74	128.4	0.85	128	0.45	127.5	0
128	130.2	2.18	130.1	2.1	129.7	1.68	128.9	0.88	128.5	0.52	128.1	0.12
128.5	130.6	2.05	130.5	1.98	130.1	1.6	129.4	0.9	129.1	0.58	128.7	0.23
129	130.9	1.91	130.9	1.85	130.5	1.52	129.9	0.91	129.6	0.63	129.3	0.32
129.5	131.3	1.78	131.2	1.72	130.9	1.44	130.4	0.91	130.2	0.67	129.9	0.41
130	131.6	1.63	131.6	1.59	131.4	1.35	130.9	0.9	130.7	0.7	130.5	0.48
130.5	132	1.49	132	1.45	131.8	1.25	131.4	0.88	131.2	0.71	131	0.53
131	132.3	1.34	132.3	1.31	132.1	1.14	131.8	0.84	131.7	0.71	131.6	0.56
131.5	132.7	1.18	132.7	1.16	132.5	1.03	132.3	0.79	132.2	0.69	132.1	0.57
132	133	1.03	133	1.01	132.9	0.91	132.7	0.73	132.7	0.66	132.6	0.57

Ideal	k=0		k=.0002		k=.0005k		k=.0008		k=.0009		k=.001	
Output	Output	error	Output	error	Output	error	Output	error	Output	error	Output	error
132.5	133.4	0.86	133.4	0.85	133.3	0.78	133.2	0.66	133.1	0.6	133	0.54
133	133.7	0.7	133.7	0.69	133.7	0.65	133.6	0.56	133.5	0.53	133.5	0.49
133.5	134	0.53	134	0.52	134	0.5	134	0.45	133.9	0.43	133.9	0.41
134	134.4	0.36	134.4	0.35	134.3	0.34	134.3	0.32	134.3	0.31	134.3	0.3
134.5	134.7	0.18	134.7	0.18	134.7	0.18	134.7	0.17	134.7	0.17	134.7	0.17
135	135	0	135	0	135	0	135	0	135	0	135	0
135.5	135.3	-0.18	135.3	-0.18	135.3	-0.18	135.3	-0.17	135.3	-0.17	135.3	-0.17
136	135.6	-0.36	135.7	-0.35	135.7	-0.34	135.7	-0.32	135.7	-0.31	135.7	-0.3
136.5	136	-0.53	136	-0.52	136	-0.5	136.1	-0.45	136.1	-0.43	136.1	-0.41
137	136.3	-0.7	136.3	-0.69	136.4	-0.65	136.4	-0.56	136.5	-0.53	136.5	-0.49
137.5	136.6	-0.86	136.7	-0.85	136.7	-0.78	136.8	-0.66	136.9	-0.6	137	-0.54
138	137	-1.03	137	-1.01	137.1	-0.91	137.3	-0.73	137.3	-0.66	137.4	-0.57
138.5	137.3	-1.18	137.3	-1.16	137.5	-1.03	137.7	-0.79	137.8	-0.69	137.9	-0.57
139	137.7	-1.34	137.7	-1.31	137.9	-1.14	138.2	-0.84	138.3	-0.71	138.4	-0.56
139.5	138	-1.49	138.1	-1.45	138.3	-1.25	138.6	-0.88	138.8	-0.71	139	-0.53
140	138.4	-1.63	138.4	-1.59	138.7	-1.35	139.1	-0.9	139.3	-0.7	139.5	-0.48
140.5	138.7	-1.78	138.8	-1.72	139.1	-1.44	139.6	-0.91	139.8	-0.67	140.1	-0.41
141	139.1	-1.91	139.2	-1.85	139.5	-1.52	140.1	-0.91	140.4	-0.63	140.7	-0.32
141.5	139.5	-2.05	139.5	-1.98	139.9	-1.6	140.6	-0.9	140.9	-0.58	141.3	-0.23
142	139.8	-2.18	139.9	-2.1	140.3	-1.68	141.1	-0.88	141.5	-0.52	141.9	-0.12
142.5	140.2	-2.31	140.3	-2.22	140.8	-1.74	141.7	-0.85	142.1	-0.45	142.5	0
143	140.6	-2.43	140.7	-2.33	141.2	-1.81	142.2	-0.82	142.6	-0.38	143.1	0.12
143.5	141	-2.55	141.1	-2.44	141.6	-1.86	142.7	-0.78	143.2	-0.29	143.8	0.26
144	141.3	-2.66	141.5	-2.54	142.1	-1.92	143.3	-0.73	143.8	-0.2	144.4	0.4
144.5	141.7	-2.77	141.9	-2.64	142.5	-1.97	143.8	-0.68	144.4	-0.11	145	0.54
145	142.1	-2.87	142.3	-2.74	143	-2.01	144.4	-0.63	145	-0.02	145.7	0.69
145.5	142.5	-2.98	142.7	-2.83	143.4	-2.06	144.9	-0.58	145.6	0.08	146.3	0.83
146	142.9	-3.07	143.1	-2.92	143.9	-2.1	145.5	-0.52	146.2	0.18	147	0.98
146.5	143.3	-3.17	143.5	-3	144.4	-2.13	146	-0.47	146.8	0.28	147.6	1.13
147	143.8	-3.25	143.9	-3.08	144.8	-2.17	146.6	-0.41	147.4	0.37	148.3	1.27
147.5	144.2	-3.34	144.3	-3.16	145.3	-2.2	147.1	-0.36	148	0.47	148.9	1.41
148	144.6	-3.42	144.8	-3.23	145.8	-2.23	147.7	-0.31	148.6	0.56	149.5	1.54
148.5	145	-3.49	145.2	-3.3	146.2	-2.26	148.2	-0.26	149.1	0.64	150.2	1.67
149	145.4	-3.56	145.6	-3.36	146.7	-2.28	148.8	-0.21	149.7	0.72	150.8	1.79
149.5	145.9	-3.63	146.1	-3.42	147.2	-2.31	149.3	-0.17	150.3	0.8	151.4	1.9
150	146.3	-3.69	146.5	-3.48	147.7	-2.33	149.9	-0.13	150.9	0.87	152	2
150.5	146.8	-3.75	147	-3.53	148.2	-2.35	150.4	-0.09	151.4	0.93	152.6	2.09
151	147.2	-3.8	147.4	-3.57	148.6	-2.37	150.9	-0.06	152	0.98	153.2	2.17
151.5	147.7	-3.85	147.9	-3.62	149.1	-2.39	151.5	-0.03	152.5	1.03	153.7	2.24
152	148.1	-3.89	148.3	-3.66	149.6	-2.41	152	-0.01	153.1	1.07	154.3	2.3
152.5	148.6	-3.93	148.8	-3.69	150.1	-2.43	152.5	0	153.6	1.1	154.9	2.35
153	149	-3.96	149.3	-3.72	150.6	-2.45	153	0.01	154.1	1.12	155.4	2.38
153.5	149.5	-3.99	149.8	-3.75	151	-2.46	153.5	0.01	154.6	1.13	155.9	2.4
154	150	-4.02	150.2	-3.78	151.5	-2.48	154	0.01	155.1	1.13	156.4	2.41
154.5	150.5	-4.04	150.7	-3.8	152	-2.5	154.5	0	155.6	1.12	156.9	2.4
155	151	-4.05	151.2	-3.81	152.5	-2.51	155	-0.02	156.1	1.1	157.4	2.38
155.5	151.4	-4.07	151.7	-3.82	153	-2.53	155.5	-0.04	156.6	1.08	157.9	2.35
156	151.9	-4.07	152.2	-3.83	153.5	-2.54	155.9	-0.07	157	1.04	158.3	2.3
156.5	152.4	-4.07	152.7	-3.83	154	-2.55	156.4	-0.1	157.5	1	158.8	2.25
157	152.9	-4.07	153.2	-3.83	154.4	-2.57	156.9	-0.14	158	0.95	159.2	2.18
157.5	153.4	-4.07	153.7	-3.83	154.9	-2.58	157.3	-0.18	158.4	0.89	159.6	2.1
158	154	-4.05	154.2	-3.82	155.4	-2.59	157.8	-0.23	158.8	0.82	160	2.01
158.5	154.5	-4.04	154.7	-3.81	155.9	-2.6	158.2	-0.29	159.2	0.74	160.4	1.91

Ideal	k=0		k=.0002		k=.0005k		k=.0008		k=.0009		k=.001	
Output	Output	error	Output	error	Output	error	Output	error	Output	error	Output	error
159	155	-4.02	155.2	-3.79	156.4	-2.61	158.7	-0.35	159.7	0.66	160.8	1.81
159.5	155.5	-3.99	155.7	-3.77	156.9	-2.61	159.1	-0.41	160.1	0.58	161.2	1.69
160	156	-3.96	156.3	-3.75	157.4	-2.62	159.5	-0.47	160.5	0.48	161.6	1.57
160.5	156.6	-3.93	156.8	-3.72	157.9	-2.62	160	-0.54	160.9	0.39	161.9	1.43
161	157.1	-3.89	157.3	-3.69	158.4	-2.63	160.4	-0.61	161.3	0.29	162.3	1.3
161.5	157.7	-3.85	157.9	-3.65	158.9	-2.63	160.8	-0.68	161.7	0.18	162.7	1.16
162	158.2	-3.8	158.4	-3.61	159.4	-2.63	161.3	-0.75	162.1	0.08	163	1.01
162.5	158.8	-3.75	158.9	-3.57	159.9	-2.62	161.7	-0.83	162.5	-0.03	163.4	0.86
163	159.3	-3.7	159.5	-3.52	160.4	-2.61	162.1	-0.9	162.9	-0.14	163.7	0.71
163.5	159.9	-3.64	160	-3.47	160.9	-2.61	162.5	-0.97	163.3	-0.25	164.1	0.56
164	160.4	-3.57	160.6	-3.42	161.4	-2.59	163	-1.04	163.6	-0.36	164.4	0.41
164.5	161	-3.51	161.1	-3.36	161.9	-2.58	163.4	-1.11	164	-0.47	164.8	0.26
165	161.6	-3.43	161.7	-3.3	162.4	-2.56	163.8	-1.18	164.4	-0.57	165.1	0.11
165.5	162.1	-3.36	162.3	-3.23	163	-2.54	164.3	-1.24	164.8	-0.67	165.5	-0.03
166	162.7	-3.28	162.8	-3.16	163.5	-2.51	164.7	-1.3	165.2	-0.77	165.8	-0.17
166.5	163.3	-3.2	163.4	-3.09	164	-2.48	165.1	-1.36	165.6	-0.86	166.2	-0.31
167	163.9	-3.11	164	-3.01	164.6	-2.45	165.6	-1.41	166.1	-0.95	166.6	-0.44
167.5	164.5	-3.02	164.6	-2.93	165.1	-2.41	166.1	-1.45	166.5	-1.03	166.9	-0.56
168	165.1	-2.93	165.2	-2.84	165.6	-2.37	166.5	-1.49	166.9	-1.1	167.3	-0.67
168.5	165.7	-2.84	165.8	-2.75	166.2	-2.32	167	-1.52	167.3	-1.17	167.7	-0.78
169	166.3	-2.74	166.3	-2.66	166.7	-2.27	167.5	-1.55	167.8	-1.23	168.1	-0.87
169.5	166.9	-2.63	166.9	-2.57	167.3	-2.22	167.9	-1.56	168.2	-1.28	168.5	-0.96
170	167.5	-2.53	167.5	-2.47	167.8	-2.16	168.4	-1.57	168.7	-1.32	169	-1.03
170.5	168.1	-2.42	168.1	-2.37	168.4	-2.09	168.9	-1.58	169.2	-1.35	169.4	-1.1
171	168.7	-2.31	168.7	-2.26	169	-2.02	169.4	-1.57	169.6	-1.37	169.9	-1.15
171.5	169.3	-2.2	169.3	-2.16	169.6	-1.94	170	-1.55	170.1	-1.38	170.3	-1.19
172	169.9	-2.08	170	-2.05	170.1	-1.86	170.5	-1.53	170.6	-1.38	170.8	-1.21
172.5	170.5	-1.96	170.6	-1.93	170.7	-1.78	171	-1.49	171.1	-1.37	171.3	-1.23
173	171.2	-1.84	171.2	-1.82	171.3	-1.69	171.6	-1.45	171.7	-1.34	171.8	-1.23
173.5	171.8	-1.72	171.8	-1.7	171.9	-1.59	172.1	-1.39	172.2	-1.31	172.3	-1.21
174	172.4	-1.59	172.4	-1.58	172.5	-1.49	172.7	-1.33	172.7	-1.26	172.8	-1.18
174.5	173	-1.47	173	-1.46	173.1	-1.39	173.2	-1.26	173.3	-1.2	173.4	-1.14
175	173.7	-1.34	173.7	-1.33	173.7	-1.28	173.8	-1.18	173.9	-1.14	173.9	-1.09
175.5	174.3	-1.21	174.3	-1.2	174.3	-1.16	174.4	-1.09	174.4	-1.06	174.5	-1.02
176	174.9	-1.08	174.9	-1.07	175	-1.05	175	-0.99	175	-0.97	175.1	-0.94
176.5	175.6	-0.95	175.6	-0.94	175.6	-0.92	175.6	-0.89	175.6	-0.87	175.7	-0.85
177	176.2	-0.81	176.2	-0.81	176.2	-0.8	176.2	-0.78	176.2	-0.77	176.3	-0.75
177.5	176.8	-0.68	176.8	-0.68	176.8	-0.67	176.8	-0.66	176.9	-0.65	176.9	-0.64
178	177.5	-0.54	177.5	-0.54	177.5	-0.54	177.5	-0.53	177.5	-0.53	177.5	-0.53
178.5	178.1	-0.41	178.1	-0.41	178.1	-0.41	178.1	-0.4	178.1	-0.4	178.1	-0.4
179	178.7	-0.27	178.7	-0.27	178.7	-0.27	178.7	-0.27	178.7	-0.27	178.7	-0.27
179.5	179.4	-0.14	179.4	-0.14	179.4	-0.14	179.4	-0.14	179.4	-0.14	179.4	-0.14
180	180	0	180	0	180	0	180	0	180	0	180	0
180.5	180.6	0.14	180.6	0.14	180.6	0.14	180.6	0.14	180.6	0.14	180.6	0.14
181	181.3	0.27	181.3	0.27	181.3	0.27	181.3	0.27	181.3	0.27	181.3	0.27
181.5	181.9	0.41	181.9	0.41	181.9	0.41	181.9	0.4	181.9	0.4	181.9	0.4
182	182.5	0.54	182.5	0.54	182.5	0.54	182.5	0.53	182.5	0.53	182.5	0.53
182.5	183.2	0.68	183.2	0.68	183.2	0.67	183.2	0.66	183.2	0.65	183.1	0.64
183	183.8	0.81	183.8	0.81	183.8	0.8	183.8	0.78	183.8	0.77	183.8	0.75
183.5	184.5	0.95	184.4	0.94	184.4	0.92	184.4	0.89	184.4	0.87	184.4	0.85
184	185.1	1.08	185.1	1.07	185.1	1.05	185	0.99	185	0.97	184.9	0.94
184.5	185.7	1.21	185.7	1.2	185.7	1.16	185.6	1.09	185.6	1.06	185.5	1.02
185	186.3	1.34	186.3	1.33	186.3	1.28	186.2	1.18	186.1	1.14	186.1	1.09

Ideal	k=0		k=.0002		k=.0005k		k=.0008		k=.0009		k=.001	
Output	Output	error	Output	error	Output	error	Output	error	Output	error	Output	error
185.5	187	1.47	187	1.46	186.9	1.39	186.8	1.26	186.7	1.2	186.6	1.14
186	187.6	1.59	187.6	1.58	187.5	1.49	187.3	1.33	187.3	1.26	187.2	1.18
186.5	188.2	1.72	188.2	1.7	188.1	1.59	187.9	1.39	187.8	1.31	187.7	1.21
187	188.8	1.84	188.8	1.82	188.7	1.69	188.5	1.45	188.3	1.34	188.2	1.23
187.5	189.5	1.96	189.4	1.93	189.3	1.78	189	1.49	188.9	1.37	188.7	1.23
188	190.1	2.08	190.1	2.05	189.9	1.86	189.5	1.53	189.4	1.38	189.2	1.21
188.5	190.7	2.2	190.7	2.16	190.4	1.94	190.1	1.55	189.9	1.38	189.7	1.19
189	191.3	2.31	191.3	2.26	191	2.02	190.6	1.57	190.4	1.37	190.2	1.15
189.5	191.9	2.42	191.9	2.37	191.6	2.09	191.1	1.58	190.9	1.35	190.6	1.1
190	192.5	2.53	192.5	2.47	192.2	2.16	191.6	1.57	191.3	1.32	191	1.03
190.5	193.1	2.63	193.1	2.57	192.7	2.22	192.1	1.56	191.8	1.28	191.5	0.96
191	193.7	2.74	193.7	2.66	193.3	2.27	192.6	1.55	192.2	1.23	191.9	0.87
191.5	194.3	2.84	194.3	2.75	193.8	2.32	193	1.52	192.7	1.17	192.3	0.78
192	194.9	2.93	194.8	2.84	194.4	2.37	193.5	1.49	193.1	1.1	192.7	0.67
192.5	195.5	3.02	195.4	2.93	194.9	2.41	194	1.45	193.5	1.03	193.1	0.56
193	196.1	3.11	196	3.01	195.5	2.45	194.4	1.41	194	0.95	193.4	0.44
193.5	196.7	3.2	196.6	3.09	196	2.48	194.9	1.36	194.4	0.86	193.8	0.31
194	197.3	3.28	197.2	3.16	196.5	2.51	195.3	1.3	194.8	0.77	194.2	0.17
194.5	197.9	3.36	197.7	3.23	197	2.54	195.7	1.24	195.2	0.67	194.5	0.03
195	198.4	3.43	198.3	3.3	197.6	2.56	196.2	1.18	195.6	0.57	194.9	-0.11
195.5	199	3.51	198.9	3.36	198.1	2.58	196.6	1.11	196	0.47	195.2	-0.26
196	199.6	3.57	199.4	3.42	198.6	2.59	197	1.04	196.4	0.36	195.6	-0.41
196.5	200.1	3.64	200	3.47	199.1	2.61	197.5	0.97	196.8	0.25	195.9	-0.56
197	200.7	3.7	200.5	3.52	199.6	2.61	197.9	0.9	197.1	0.14	196.3	-0.71
197.5	201.3	3.75	201.1	3.57	200.1	2.62	198.3	0.83	197.5	0.03	196.6	-0.86
198	201.8	3.8	201.6	3.61	200.6	2.63	198.8	0.75	197.9	-0.08	197	-1.01
198.5	202.4	3.85	202.2	3.65	201.1	2.63	199.2	0.68	198.3	-0.18	197.3	-1.16
199	202.9	3.89	202.7	3.69	201.6	2.63	199.6	0.61	198.7	-0.29	197.7	-1.3
199.5	203.4	3.93	203.2	3.72	202.1	2.62	200	0.54	199.1	-0.39	198.1	-1.43
200	204	3.96	203.8	3.75	202.6	2.62	200.5	0.47	199.5	-0.48	198.4	-1.57
200.5	204.5	3.99	204.3	3.77	203.1	2.61	200.9	0.41	199.9	-0.58	198.8	-1.69
201	205	4.02	204.8	3.79	203.6	2.61	201.4	0.35	200.3	-0.66	199.2	-1.81
201.5	205.5	4.04	205.3	3.81	204.1	2.6	201.8	0.29	200.8	-0.74	199.6	-1.91
202	206.1	4.05	205.8	3.82	204.6	2.59	202.2	0.23	201.2	-0.82	200	-2.01
202.5	206.6	4.07	206.3	3.83	205.1	2.58	202.7	0.18	201.6	-0.89	200.4	-2.1
203	207.1	4.07	206.8	3.83	205.6	2.57	203.1	0.14	202.1	-0.95	200.8	-2.18
203.5	207.6	4.07	207.3	3.83	206.1	2.55	203.6	0.1	202.5	-1	201.3	-2.25
204	208.1	4.07	207.8	3.83	206.5	2.54	204.1	0.07	203	-1.04	201.7	-2.3
204.5	208.6	4.07	208.3	3.82	207	2.53	204.5	0.04	203.4	-1.08	202.2	-2.35
205	209.1	4.05	208.8	3.81	207.5	2.51	205	0.02	203.9	-1.1	202.6	-2.38
205.5	209.5	4.04	209.3	3.8	208	2.5	205.5	0	204.4	-1.12	203.1	-2.4
206	210	4.02	209.8	3.78	208.5	2.48	206	-0.01	204.9	-1.13	203.6	-2.41
206.5	210.5	3.99	210.3	3.75	209	2.46	206.5	-0.01	205.4	-1.13	204.1	-2.4
207	211	3.96	210.7	3.72	209.5	2.45	207	-0.01	205.9	-1.12	204.6	-2.38
207.5	211.4	3.93	211.2	3.69	209.9	2.43	207.5	0	206.4	-1.1	205.2	-2.35
208	211.9	3.89	211.7	3.66	210.4	2.41	208	0.01	206.9	-1.07	205.7	-2.3
208.5	212.4	3.85	212.1	3.62	210.9	2.39	208.5	0.03	207.5	-1.03	206.3	-2.24
209	212.8	3.8	212.6	3.57	211.4	2.37	209.1	0.06	208	-0.98	206.8	-2.17
209.5	213.3	3.75	213	3.53	211.9	2.35	209.6	0.09	208.6	-0.93	207.4	-2.09
210	213.7	3.69	213.5	3.48	212.3	2.33	210.1	0.13	209.1	-0.87	208	-2
210.5	214.1	3.63	213.9	3.42	212.8	2.31	210.7	0.17	209.7	-0.8	208.6	-1.9
211	214.6	3.56	214.4	3.36	213.3	2.28	211.2	0.21	210.3	-0.72	209.2	-1.79
211.5	215	3.49	214.8	3.3	213.8	2.26	211.8	0.26	210.9	-0.64	209.8	-1.67

Ideal	k=0		k=.0002		k=.0005k		k=.0008		k=.0009		k=.001	
Output	Output	error	Output	error	Output	error	Output	error	Output	error	Output	error
212	215.4	3.42	215.2	3.23	214.2	2.23	212.3	0.31	211.4	-0.56	210.5	-1.54
212.5	215.8	3.34	215.7	3.16	214.7	2.2	212.9	0.36	212	-0.47	211.1	-1.41
213	216.3	3.25	216.1	3.08	215.2	2.17	213.4	0.41	212.6	-0.37	211.7	-1.27
213.5	216.7	3.17	216.5	3	215.6	2.13	214	0.47	213.2	-0.28	212.4	-1.13
214	217.1	3.07	216.9	2.92	216.1	2.1	214.5	0.52	213.8	-0.18	213	-0.98
214.5	217.5	2.98	217.3	2.83	216.6	2.06	215.1	0.58	214.4	-0.08	213.7	-0.83
215	217.9	2.87	217.7	2.74	217	2.01	215.6	0.63	215	0.02	214.3	-0.69
215.5	218.3	2.77	218.1	2.64	217.5	1.97	216.2	0.68	215.6	0.11	215	-0.54
216	218.7	2.66	218.5	2.54	217.9	1.92	216.7	0.73	216.2	0.2	215.6	-0.4
216.5	219.1	2.55	218.9	2.44	218.4	1.86	217.3	0.78	216.8	0.29	216.2	-0.26
217	219.4	2.43	219.3	2.33	218.8	1.81	217.8	0.82	217.4	0.38	216.9	-0.12
217.5	219.8	2.31	219.7	2.22	219.2	1.74	218.4	0.85	218	0.45	217.5	0
218	220.2	2.18	220.1	2.1	219.7	1.68	218.9	0.88	218.5	0.52	218.1	0.12
218.5	220.6	2.05	220.5	1.98	220.1	1.6	219.4	0.9	219.1	0.58	218.7	0.23
219	220.9	1.91	220.9	1.85	220.5	1.52	219.9	0.91	219.6	0.63	219.3	0.32
219.5	221.3	1.78	221.2	1.72	220.9	1.44	220.4	0.91	220.2	0.67	219.9	0.41
220	221.6	1.63	221.6	1.59	221.4	1.35	220.9	0.9	220.7	0.7	220.5	0.48
220.5	222	1.49	222	1.45	221.8	1.25	221.4	0.88	221.2	0.71	221	0.53
221	222.3	1.34	222.3	1.31	222.1	1.14	221.8	0.84	221.7	0.71	221.6	0.56
221.5	222.7	1.18	222.7	1.16	222.5	1.03	222.3	0.79	222.2	0.69	222.1	0.57
222	223	1.03	223	1.01	222.9	0.91	222.7	0.73	222.7	0.66	222.6	0.57
222.5	223.4	0.86	223.4	0.85	223.3	0.78	223.2	0.66	223.1	0.6	223	0.54
223	223.7	0.7	223.7	0.69	223.7	0.65	223.6	0.56	223.5	0.53	223.5	0.49
223.5	224	0.53	224	0.52	224	0.5	224	0.45	223.9	0.43	223.9	0.41
224	224.4	0.36	224.4	0.35	224.3	0.34	224.3	0.32	224.3	0.31	224.3	0.3
224.5	224.7	0.18	224.7	0.18	224.7	0.18	224.7	0.17	224.7	0.17	224.7	0.17
225	225	0	225	0	225	0	225	0	225	0	225	0
225.5	225.3	-0.18	225.3	-0.18	225.3	-0.18	225.3	-0.17	225.3	-0.17	225.3	-0.17
226	225.6	-0.36	225.7	-0.35	225.7	-0.34	225.7	-0.32	225.7	-0.31	225.7	-0.3
226.5	226	-0.53	226	-0.52	226	-0.5	226.1	-0.45	226.1	-0.43	226.1	-0.41
227	226.3	-0.7	226.3	-0.69	226.4	-0.65	226.4	-0.56	226.5	-0.53	226.5	-0.49
227.5	226.6	-0.86	226.7	-0.85	226.7	-0.78	226.8	-0.66	226.9	-0.6	227	-0.54
228	227	-1.03	227	-1.01	227.1	-0.91	227.3	-0.73	227.3	-0.66	227.4	-0.57
228.5	227.3	-1.18	227.3	-1.16	227.5	-1.03	227.7	-0.79	227.8	-0.69	227.9	-0.57
229	227.7	-1.34	227.7	-1.31	227.9	-1.14	228.2	-0.84	228.3	-0.71	228.4	-0.56
229.5	228	-1.49	228.1	-1.45	228.3	-1.25	228.6	-0.88	228.8	-0.71	229	-0.53
230	228.4	-1.63	228.4	-1.59	228.7	-1.35	229.1	-0.9	229.3	-0.7	229.5	-0.48
230.5	228.7	-1.78	228.8	-1.72	229.1	-1.44	229.6	-0.91	229.8	-0.67	230.1	-0.41
231	229.1	-1.91	229.2	-1.85	229.5	-1.52	230.1	-0.91	230.4	-0.63	230.7	-0.32
231.5	229.5	-2.05	229.5	-1.98	229.9	-1.6	230.6	-0.9	230.9	-0.58	231.3	-0.23
232	229.8	-2.18	229.9	-2.1	230.3	-1.68	231.1	-0.88	231.5	-0.52	231.9	-0.12
232.5	230.2	-2.31	230.3	-2.22	230.8	-1.74	231.7	-0.85	232.1	-0.45	232.5	0
233	230.6	-2.43	230.7	-2.33	231.2	-1.81	232.2	-0.82	232.6	-0.38	233.1	0.12
233.5	231	-2.55	231.1	-2.44	231.6	-1.86	232.7	-0.78	233.2	-0.29	233.8	0.26
234	231.3	-2.66	231.5	-2.54	232.1	-1.92	233.3	-0.73	233.8	-0.2	234.4	0.4
234.5	231.7	-2.77	231.9	-2.64	232.5	-1.97	233.8	-0.68	234.4	-0.11	235	0.54
235	232.1	-2.87	232.3	-2.74	233	-2.01	234.4	-0.63	235	-0.02	235.7	0.69
235.5	232.5	-2.98	232.7	-2.83	233.4	-2.06	234.9	-0.58	235.6	0.08	236.3	0.83
236	232.9	-3.07	233.1	-2.92	233.9	-2.1	235.5	-0.52	236.2	0.18	237	0.98
236.5	233.3	-3.17	233.5	-3	234.4	-2.13	236	-0.47	236.8	0.28	237.6	1.13
237	233.8	-3.25	233.9	-3.08	234.8	-2.17	236.6	-0.41	237.4	0.37	238.3	1.27
237.5	234.2	-3.34	234.3	-3.16	235.3	-2.2	237.1	-0.36	238	0.47	238.9	1.41
238	234.6	-3.42	234.8	-3.23	235.8	-2.23	237.7	-0.31	238.6	0.56	239.5	1.54

deal	k=0		k=.0002		k=.0005k		k=.0008		k=.0009		k=.001	
Output	Output	error	Output	error	Output	error	Output	error	Output	error	Output	error
238.5	235	-3.49	235.2	-3.3	236.2	-2.26	238.2	-0.26	239.1	0.64	240.2	1.67
239	235.4	-3.56	235.6	-3.36	236.7	-2.28	238.8	-0.21	239.7	0.72	240.8	1.79
239.5	235.9	-3.63	236.1	-3.42	237.2	-2.31	239.3	-0.17	240.3	0.8	241.4	1.9
240	236.3	-3.69	236.5	-3.48	237.7	-2.33	239.9	-0.13	240.9	0.87	242	2
240.5	236.8	-3.75	237	-3.53	238.2	-2.35	240.4	-0.09	241.4	0.93	242.6	2.09
241	237.2	-3.8	237.4	-3.57	238.6	-2.37	240.9	-0.06	242	0.98	243.2	2.17
241.5	237.7	-3.85	237.9	-3.62	239.1	-2.39	241.5	-0.03	242.5	1.03	243.7	2.24
242	238.1	-3.89	238.3	-3.66	239.6	-2.41	242	-0.01	243.1	1.07	244.3	2.3
242.5	238.6	-3.93	238.8	-3.69	240.1	-2.43	242.5	0	243.6	1.1	244.9	2.35
243	239	-3.96	239.3	-3.72	240.6	-2.45	243	0.01	244.1	1.12	245.4	2.38
243.5	239.5	-3.99	239.8	-3.75	241	-2.46	243.5	0.01	244.6	1.13	245.9	2.4
244	240	-4.02	240.2	-3.78	241.5	-2.48	244	0.01	245.1	1.13	246.4	2.41
244.5	240.5	-4.04	240.7	-3.8	242	-2.5	244.5	0	245.6	1.12	246.9	2.4
245	241	-4.05	241.2	-3.81	242.5	-2.51	245	-0.02	246.1	1.1	247.4	2.38
245.5	241.4	-4.07	241.7	-3.82	243	-2.53	245.5	-0.04	246.6	1.08	247.9	2.35
246	241.9	-4.07	242.2	-3.83	243.5	-2.54	245.9	-0.07	247	1.04	248.3	2.3
246.5	242.4	-4.07	242.7	-3.83	244	-2.55	246.4	-0.1	247.5	1	248.8	2.25
247	242.9	-4.07	243.2	-3.83	244.4	-2.57	246.9	-0.14	248	0.95	249.2	2.18
247.5	243.4	-4.07	243.7	-3.83	244.9	-2.58	247.3	-0.18	248.4	0.89	249.6	2.1
248	244	-4.05	244.2	-3.82	245.4	-2.59	247.8	-0.23	248.8	0.82	250	2.01
248.5	244.5	-4.04	244.7	-3.81	245.9	-2.6	248.2	-0.29	249.2	0.74	250.4	1.91
249	245	-4.02	245.2	-3.79	246.4	-2.61	248.7	-0.35	249.7	0.66	250.8	1.81
249.5	245.5	-3.99	245.7	-3.77	246.9	-2.61	249.1	-0.41	250.1	0.58	251.2	1.69
250	246	-3.96	246.3	-3.75	247.4	-2.62	249.5	-0.47	250.5	0.48	251.6	1.57
250.5	246.6	-3.93	246.8	-3.72	247.9	-2.62	250	-0.54	250.9	0.39	251.9	1.43
251	247.1	-3.89	247.3	-3.69	248.4	-2.63	250.4	-0.61	251.3	0.29	252.3	1.3
251.5	247.7	-3.85	247.9	-3.65	248.9	-2.63	250.8	-0.68	251.7	0.18	252.7	1.16
252	248.2	-3.8	248.4	-3.61	249.4	-2.63	251.3	-0.75	252.1	0.08	253	1.01
252.5	248.8	-3.75	248.9	-3.57	249.9	-2.62	251.7	-0.83	252.5	-0.03	253.4	0.86
253	249.3	-3.7	249.5	-3.52	250.4	-2.61	252.1	-0.9	252.9	-0.14	253.7	0.71
253.5	249.9	-3.64	250	-3.47	250.9	-2.61	252.5	-0.97	253.3	-0.25	254.1	0.56
254	250.4	-3.57	250.6	-3.42	251.4	-2.59	253	-1.04	253.6	-0.36	254.4	0.41
254.5	251	-3.51	251.1	-3.36	251.9	-2.58	253.4	-1.11	254	-0.47	254.8	0.26
255	251.6	-3.43	251.7	-3.3	252.4	-2.56	253.8	-1.18	254.4	-0.57	255.1	0.11
255.5	252.1	-3.36	252.3	-3.23	253	-2.54	254.3	-1.24	254.8	-0.67	255.5	-0.03
256	252.7	-3.28	252.8	-3.16	253.5	-2.51	254.7	-1.3	255.2	-0.77	255.8	-0.17
256.5	253.3	-3.2	253.4	-3.09	254	-2.48	255.1	-1.36	255.6	-0.86	256.2	-0.31
257	253.9	-3.11	254	-3.01	254.6	-2.45	255.6	-1.41	256.1	-0.95	256.6	-0.44
257.5	254.5	-3.02	254.6	-2.93	255.1	-2.41	256.1	-1.45	256.5	-1.03	256.9	-0.56
258	255.1	-2.93	255.2	-2.84	255.6	-2.37	256.5	-1.49	256.9	-1.1	257.3	-0.67
258.5	255.7	-2.84	255.8	-2.75	256.2	-2.32	257	-1.52	257.3	-1.17	257.7	-0.78
259	256.3	-2.74	256.3	-2.66	256.7	-2.27	257.5	-1.55	257.8	-1.23	258.1	-0.87
259.5	256.9	-2.63	256.9	-2.57	257.3	-2.22	257.9	-1.56	258.2	-1.28	258.5	-0.96
260	257.5	-2.53	257.5	-2.47	257.8	-2.16	258.4	-1.57	258.7	-1.32	259	-1.03
260.5	258.1	-2.42	258.1	-2.37	258.4	-2.09	258.9	-1.58	259.2	-1.35	259.4	-1.1
261	258.7	-2.31	258.7	-2.26	259	-2.02	259.4	-1.57	259.6	-1.37	259.9	-1.15
261.5	259.3	-2.2	259.3	-2.16	259.6	-1.94	260	-1.55	260.1	-1.38	260.3	-1.19
262	259.9	-2.08	260	-2.05	260.1	-1.86	260.5	-1.53	260.6	-1.38	260.8	-1.21
262.5	260.5	-1.96	260.6	-1.93	260.7	-1.78	261	-1.49	261.1	-1.37	261.3	-1.23
263	261.2	-1.84	261.2	-1.82	261.3	-1.69	261.6	-1.45	261.7	-1.34	261.8	-1.23
263.5	261.8	-1.72	261.8	-1.7	261.9	-1.59	262.1	-1.39	262.2	-1.31	262.3	-1.21
264	262.4	-1.59	262.4	-1.58	262.5	-1.49	262.7	-1.33	262.7	-1.26	262.8	-1.18
264.5	263	-1.47	263	-1.46	263.1	-1.39	263.2	-1.26	263.3	-1.2	263.4	-1.14

Ideal	k=0		k=.0002		k=.0005k		k=.0008		k=.0009		k=.001	
Output	Output	error	Output	error	Output	error	Output	error	Output	error	Output	error
265	263.7	-1.34	263.7	-1.33	263.7	-1.28	263.8	-1.18	263.9	-1.14	263.9	-1.09
265.5	264.3	-1.21	264.3	-1.2	264.3	-1.16	264.4	-1.09	264.4	-1.06	264.5	-1.02
266	264.9	-1.08	264.9	-1.07	265	-1.05	265	-0.99	265	-0.97	265.1	-0.94
266.5	265.6	-0.95	265.6	-0.94	265.6	-0.92	265.6	-0.89	265.6	-0.87	265.7	-0.85
267	266.2	-0.81	266.2	-0.81	266.2	-0.8	266.2	-0.78	266.2	-0.77	266.3	-0.75
267.5	266.8	-0.68	266.8	-0.68	266.8	-0.67	266.8	-0.66	266.9	-0.65	266.9	-0.64
268	267.5	-0.54	267.5	-0.54	267.5	-0.54	267.5	-0.53	267.5	-0.53	267.5	-0.53
268.5	268.1	-0.41	268.1	-0.41	268.1	-0.41	268.1	-0.4	268.1	-0.4	268.1	-0.4
269	268.7	-0.27	268.7	-0.27	268.7	-0.27	268.7	-0.27	268.7	-0.27	268.7	-0.27
269.5	269.4	-0.14	269.4	-0.14	269.4	-0.14	269.4	-0.14	269.4	-0.14	269.4	-0.14
270	270	0	270	0	270	0	270	0	270	0	270	0
270.5	270.6	0.14	270.6	0.14	270.6	0.14	270.6	0.14	270.6	0.14	270.6	0.14
271	271.3	0.27	271.3	0.27	271.3	0.27	271.3	0.27	271.3	0.27	271.3	0.27
271.5	271.9	0.41	271.9	0.41	271.9	0.41	271.9	0.4	271.9	0.4	271.9	0.4
272	272.5	0.54	272.5	0.54	272.5	0.54	272.5	0.53	272.5	0.53	272.5	0.53
272.5	273.2	0.68	273.2	0.68	273.2	0.67	273.2	0.66	273.2	0.65	273.1	0.64
273	273.8	0.81	273.8	0.81	273.8	0.8	273.8	0.78	273.8	0.77	273.8	0.75
273.5	274.5	0.95	274.4	0.94	274.4	0.92	274.4	0.89	274.4	0.87	274.4	0.85
274	275.1	1.08	275.1	1.07	275.1	1.05	275	0.99	275	0.97	274.9	0.94
274.5	275.7	1.21	275.7	1.2	275.7	1.16	275.6	1.09	275.6	1.06	275.5	1.02
275	276.3	1.34	276.3	1.33	276.3	1.28	276.2	1.18	276.1	1.14	276.1	1.09
275.5	277	1.47	277	1.46	276.9	1.39	276.8	1.26	276.7	1.2	276.6	1.14
276	277.6	1.59	277.6	1.58	277.5	1.49	277.3	1.33	277.3	1.26	277.2	1.18
276.5	278.2	1.72	278.2	1.7	278.1	1.59	277.9	1.39	277.8	1.31	277.7	1.21
277	278.8	1.84	278.8	1.82	278.7	1.69	278.5	1.45	278.3	1.34	278.2	1.23
277.5	279.5	1.96	279.4	1.93	279.3	1.78	279	1.49	278.9	1.37	278.7	1.23
278	280.1	2.08	280.1	2.05	279.9	1.86	279.5	1.53	279.4	1.38	279.2	1.21
278.5	280.7	2.2	280.7	2.16	280.4	1.94	280.1	1.55	279.9	1.38	279.7	1.19
279	281.3	2.31	281.3	2.26	281	2.02	280.6	1.57	280.4	1.37	280.2	1.15
279.5	281.9	2.42	281.9	2.37	281.6	2.09	281.1	1.58	280.9	1.35	280.6	1.1
280	282.5	2.53	282.5	2.47	282.2	2.16	281.6	1.57	281.3	1.32	281	1.03
280.5	283.1	2.63	283.1	2.57	282.7	2.22	282.1	1.56	281.8	1.28	281.5	0.96
281	283.7	2.74	283.7	2.66	283.3	2.27	282.6	1.55	282.2	1.23	281.9	0.87
281.5	284.3	2.84	284.3	2.75	283.8	2.32	283	1.52	282.7	1.17	282.3	0.78
282	284.9	2.93	284.8	2.84	284.4	2.37	283.5	1.49	283.1	1.1	282.7	0.67
282.5	285.5	3.02	285.4	2.93	284.9	2.41	284	1.45	283.5	1.03	283.1	0.56
283	286.1	3.11	286	3.01	285.5	2.45	284.4	1.41	284	0.95	283.4	0.44
283.5	286.7	3.2	286.6	3.09	286	2.48	284.9	1.36	284.4	0.86	283.8	0.31
284	287.3	3.28	287.2	3.16	286.5	2.51	285.3	1.3	284.8	0.77	284.2	0.17
284.5	287.9	3.36	287.7	3.23	287	2.54	285.7	1.24	285.2	0.67	284.5	0.03
285	288.4	3.43	288.3	3.3	287.6	2.56	286.2	1.18	285.6	0.57	284.9	-0.11
285.5	289	3.51	288.9	3.36	288.1	2.58	286.6	1.11	286	0.47	285.2	-0.26
286	289.6	3.57	289.4	3.42	288.6	2.59	287	1.04	286.4	0.36	285.6	-0.41
286.5	290.1	3.64	290	3.47	289.1	2.61	287.5	0.97	286.8	0.25	285.9	-0.56
287	290.7	3.7	290.5	3.52	289.6	2.61	287.9	0.9	287.1	0.14	286.3	-0.71
287.5	291.3	3.75	291.1	3.57	290.1	2.62	288.3	0.83	287.5	0.03	286.6	-0.86
288	291.8	3.8	291.6	3.61	290.6	2.63	288.8	0.75	287.9	-0.08	287	-1.01
288.5	292.4	3.85	292.2	3.65	291.1	2.63	289.2	0.68	288.3	-0.18	287.3	-1.16
289	292.9	3.89	292.7	3.69	291.6	2.63	289.6	0.61	288.7	-0.29	287.7	-1.3
289.5	293.4	3.93	293.2	3.72	292.1	2.62	290	0.54	289.1	-0.39	288.1	-1.43
290	294	3.96	293.8	3.75	292.6	2.62	290.5	0.47	289.5	-0.48	288.4	-1.57
290.5	294.5	3.99	294.3	3.77	293.1	2.61	290.9	0.41	289.9	-0.58	288.8	-1.69
291	295	4.02	294.8	3.79	293.6	2.61	291.4	0.35	290.3	-0.66	289.2	-1.81

Ideal	k=0		k=.0002		k=.0005k		k=.0008		k=.0009		k=.001	
Output	Output	error	Output	error	Output	error	Output	error	Output	error	Output	error
291.5	295.5	4.04	295.3	3.81	294.1	2.6	291.8	0.29	290.8	-0.74	289.6	-1.91
292	296.1	4.05	295.8	3.82	294.6	2.59	292.2	0.23	291.2	-0.82	290	-2.01
292.5	296.6	4.07	296.3	3.83	295.1	2.58	292.7	0.18	291.6	-0.89	290.4	-2.1
293	297.1	4.07	296.8	3.83	295.6	2.57	293.1	0.14	292.1	-0.95	290.8	-2.18
293.5	297.6	4.07	297.3	3.83	296.1	2.55	293.6	0.1	292.5	-1	291.3	-2.25
294	298.1	4.07	297.8	3.83	296.5	2.54	294.1	0.07	293	-1.04	291.7	-2.3
294.5	298.6	4.07	298.3	3.82	297	2.53	294.5	0.04	293.4	-1.08	292.2	-2.35
295	299.1	4.05	298.8	3.81	297.5	2.51	295	0.02	293.9	-1.1	292.6	-2.38
295.5	299.5	4.04	299.3	3.8	298	2.5	295.5	0	294.4	-1.12	293.1	-2.4
296	300	4.02	299.8	3.78	298.5	2.48	296	-0.01	294.9	-1.13	293.6	-2.41
296.5	300.5	3.99	300.3	3.75	299	2.46	296.5	-0.01	295.4	-1.13	294.1	-2.4
297	301	3.96	300.7	3.72	299.5	2.45	297	-0.01	295.9	-1.12	294.6	-2.38
297.5	301.4	3.93	301.2	3.69	299.9	2.43	297.5	0	296.4	-1.1	295.2	-2.35
298	301.9	3.89	301.7	3.66	300.4	2.41	298	0.01	296.9	-1.07	295.7	-2.3
298.5	302.4	3.85	302.1	3.62	300.9	2.39	298.5	0.03	297.5	-1.03	296.3	-2.24
299	302.8	3.8	302.6	3.57	301.4	2.37	299.1	0.06	298	-0.98	296.8	-2.17
299.5	303.3	3.75	303	3.53	301.9	2.35	299.6	0.09	298.6	-0.93	297.4	-2.09
300	303.7	3.69	303.5	3.48	302.3	2.33	300.1	0.13	299.1	-0.87	298	-2
300.5	304.1	3.63	303.9	3.42	302.8	2.31	300.7	0.17	299.7	-0.8	298.6	-1.9
301	304.6	3.56	304.4	3.36	303.3	2.28	301.2	0.21	300.3	-0.72	299.2	-1.79
301.5	305	3.49	304.8	3.3	303.8	2.26	301.8	0.26	300.9	-0.64	299.8	-1.67
302	305.4	3.42	305.2	3.23	304.2	2.23	302.3	0.31	301.4	-0.56	300.5	-1.54
302.5	305.8	3.34	305.7	3.16	304.7	2.2	302.9	0.36	302	-0.47	301.1	-1.41
303	306.3	3.25	306.1	3.08	305.2	2.17	303.4	0.41	302.6	-0.37	301.7	-1.27
303.5	306.7	3.17	306.5	3	305.6	2.13	304	0.47	303.2	-0.28	302.4	-1.13
304	307.1	3.07	306.9	2.92	306.1	2.1	304.5	0.52	303.8	-0.18	303	-0.98
304.5	307.5	2.98	307.3	2.83	306.6	2.06	305.1	0.58	304.4	-0.08	303.7	-0.83
305	307.9	2.87	307.7	2.74	307	2.01	305.6	0.63	305	0.02	304.3	-0.69
305.5	308.3	2.77	308.1	2.64	307.5	1.97	306.2	0.68	305.6	0.11	305	-0.54
306	308.7	2.66	308.5	2.54	307.9	1.92	306.7	0.73	306.2	0.2	305.6	-0.4
306.5	309.1	2.55	308.9	2.44	308.4	1.86	307.3	0.78	306.8	0.29	306.2	-0.26
307	309.4	2.43	309.3	2.33	308.8	1.81	307.8	0.82	307.4	0.38	306.9	-0.12
307.5	309.8	2.31	309.7	2.22	309.2	1.74	308.4	0.85	308	0.45	307.5	0
308	310.2	2.18	310.1	2.1	309.7	1.68	308.9	0.88	308.5	0.52	308.1	0.12
308.5	310.6	2.05	310.5	1.98	310.1	1.6	309.4	0.9	309.1	0.58	308.7	0.23
309	310.9	1.91	310.9	1.85	310.5	1.52	309.9	0.91	309.6	0.63	309.3	0.32
309.5	311.3	1.78	311.2	1.72	310.9	1.44	310.4	0.91	310.2	0.67	309.9	0.41
310	311.6	1.63	311.6	1.59	311.4	1.35	310.9	0.9	310.7	0.7	310.5	0.48
310.5	312	1.49	312	1.45	311.8	1.25	311.4	0.88	311.2	0.71	311	0.53
311	312.3	1.34	312.3	1.31	312.1	1.14	311.8	0.84	311.7	0.71	311.6	0.56
311.5	312.7	1.18	312.7	1.16	312.5	1.03	312.3	0.79	312.2	0.69	312.1	0.57
312	313	1.03	313	1.01	312.9	0.91	312.7	0.73	312.7	0.66	312.6	0.57
312.5	313.4	0.86	313.4	0.85	313.3	0.78	313.2	0.66	313.1	0.6	313	0.54
313	313.7	0.7	313.7	0.69	313.7	0.65	313.6	0.56	313.5	0.53	313.5	0.49
313.5	314	0.53	314	0.52	314	0.5	314	0.45	313.9	0.43	313.9	0.41
314	314.4	0.36	314.4	0.35	314.3	0.34	314.3	0.32	314.3	0.31	314.3	0.3
314.5	314.7	0.18	314.7	0.18	314.7	0.18	314.7	0.17	314.7	0.17	314.7	0.17
315	315	0	315	0	315	0	315	0	315	0	315	0
315.5	315.3	-0.18	315.3	-0.18	315.3	-0.18	315.3	-0.17	315.3	-0.17	315.3	-0.17
316	315.6	-0.36	315.7	-0.35	315.7	-0.34	315.7	-0.32	315.7	-0.31	315.7	-0.3
316.5	316	-0.53	316	-0.52	316	-0.5	316.1	-0.45	316.1	-0.43	316.1	-0.41
317	316.3	-0.7	316.3	-0.69	316.4	-0.65	316.4	-0.56	316.5	-0.53	316.5	-0.49
317.5	316.6	-0.86	316.7	-0.85	316.7	-0.78	316.8	-0.66	316.9	-0.6	317	-0.54

Ideal	k=0		k=.0002		k=.0005k		k=.0008		k=.0009		k=.001	
Output	Output	error	Output	error	Output	error	Output	error	Output	error	Output	error
318	317	-1.03	317	-1.01	317.1	-0.91	317.3	-0.73	317.3	-0.66	317.4	-0.57
318.5	317.3	-1.18	317.3	-1.16	317.5	-1.03	317.7	-0.79	317.8	-0.69	317.9	-0.57
319	317.7	-1.34	317.7	-1.31	317.9	-1.14	318.2	-0.84	318.3	-0.71	318.4	-0.56
319.5	318	-1.49	318.1	-1.45	318.3	-1.25	318.6	-0.88	318.8	-0.71	319	-0.53
320	318.4	-1.63	318.4	-1.59	318.7	-1.35	319.1	-0.9	319.3	-0.7	319.5	-0.48
320.5	318.7	-1.78	318.8	-1.72	319.1	-1.44	319.6	-0.91	319.8	-0.67	320.1	-0.41
321	319.1	-1.91	319.2	-1.85	319.5	-1.52	320.1	-0.91	320.4	-0.63	320.7	-0.32
321.5	319.5	-2.05	319.5	-1.98	319.9	-1.6	320.6	-0.9	320.9	-0.58	321.3	-0.23
322	319.8	-2.18	319.9	-2.1	320.3	-1.68	321.1	-0.88	321.5	-0.52	321.9	-0.12
322.5	320.2	-2.31	320.3	-2.22	320.8	-1.74	321.7	-0.85	322.1	-0.45	322.5	0
323	320.6	-2.43	320.7	-2.33	321.2	-1.81	322.2	-0.82	322.6	-0.38	323.1	0.12
323.5	321	-2.55	321.1	-2.44	321.6	-1.86	322.7	-0.78	323.2	-0.29	323.8	0.26
324	321.3	-2.66	321.5	-2.54	322.1	-1.92	323.3	-0.73	323.8	-0.2	324.4	0.4
324.5	321.7	-2.77	321.9	-2.64	322.5	-1.97	323.8	-0.68	324.4	-0.11	325	0.54
325	322.1	-2.87	322.3	-2.74	323	-2.01	324.4	-0.63	325	-0.02	325.7	0.69
325.5	322.5	-2.98	322.7	-2.83	323.4	-2.06	324.9	-0.58	325.6	0.08	326.3	0.83
326	322.9	-3.07	323.1	-2.92	323.9	-2.1	325.5	-0.52	326.2	0.18	327	0.98
326.5	323.3	-3.17	323.5	-3	324.4	-2.13	326	-0.47	326.8	0.28	327.6	1.13
327	323.8	-3.25	323.9	-3.08	324.8	-2.17	326.6	-0.41	327.4	0.37	328.3	1.27
327.5	324.2	-3.34	324.3	-3.16	325.3	-2.2	327.1	-0.36	328	0.47	328.9	1.41
328	324.6	-3.42	324.8	-3.23	325.8	-2.23	327.7	-0.31	328.6	0.56	329.5	1.54
328.5	325	-3.49	325.2	-3.3	326.2	-2.26	328.2	-0.26	329.1	0.64	330.2	1.67
329	325.4	-3.56	325.6	-3.36	326.7	-2.28	328.8	-0.21	329.7	0.72	330.8	1.79
329.5	325.9	-3.63	326.1	-3.42	327.2	-2.31	329.3	-0.17	330.3	0.8	331.4	1.9
330	326.3	-3.69	326.5	-3.48	327.7	-2.33	329.9	-0.13	330.9	0.87	332	2
330.5	326.8	-3.75	327	-3.53	328.2	-2.35	330.4	-0.09	331.4	0.93	332.6	2.09
331	327.2	-3.8	327.4	-3.57	328.6	-2.37	330.9	-0.06	332	0.98	333.2	2.17
331.5	327.7	-3.85	327.9	-3.62	329.1	-2.39	331.5	-0.03	332.5	1.03	333.7	2.24
332	328.1	-3.89	328.3	-3.66	329.6	-2.41	332	-0.01	333.1	1.07	334.3	2.3
332.5	328.6	-3.93	328.8	-3.69	330.1	-2.43	332.5	0	333.6	1.1	334.9	2.35
333	329	-3.96	329.3	-3.72	330.6	-2.45	333	0.01	334.1	1.12	335.4	2.38
333.5	329.5	-3.99	329.8	-3.75	331	-2.46	333.5	0.01	334.6	1.13	335.9	2.4
334	330	-4.02	330.2	-3.78	331.5	-2.48	334	0.01	335.1	1.13	336.4	2.41
334.5	330.5	-4.04	330.7	-3.8	332	-2.5	334.5	0	335.6	1.12	336.9	2.4
335	331	-4.05	331.2	-3.81	332.5	-2.51	335	-0.02	336.1	1.1	337.4	2.38
335.5	331.4	-4.07	331.7	-3.82	333	-2.53	335.5	-0.04	336.6	1.08	337.9	2.35
336	331.9	-4.07	332.2	-3.83	333.5	-2.54	335.9	-0.07	337	1.04	338.3	2.3
336.5	332.4	-4.07	332.7	-3.83	334	-2.55	336.4	-0.1	337.5	1	338.8	2.25
337	332.9	-4.07	333.2	-3.83	334.4	-2.57	336.9	-0.14	338	0.95	339.2	2.18
337.5	333.4	-4.07	333.7	-3.83	334.9	-2.58	337.3	-0.18	338.4	0.89	339.6	2.1
338	334	-4.05	334.2	-3.82	335.4	-2.59	337.8	-0.23	338.8	0.82	340	2.01
338.5	334.5	-4.04	334.7	-3.81	335.9	-2.6	338.2	-0.29	339.2	0.74	340.4	1.91
339	335	-4.02	335.2	-3.79	336.4	-2.61	338.7	-0.35	339.7	0.66	340.8	1.81
339.5	335.5	-3.99	335.7	-3.77	336.9	-2.61	339.1	-0.41	340.1	0.58	341.2	1.69
340	336	-3.96	336.3	-3.75	337.4	-2.62	339.5	-0.47	340.5	0.48	341.6	1.57
340.5	336.6	-3.93	336.8	-3.72	337.9	-2.62	340	-0.54	340.9	0.39	341.9	1.43
341	337.1	-3.89	337.3	-3.69	338.4	-2.63	340.4	-0.61	341.3	0.29	342.3	1.3
341.5	337.7	-3.85	337.9	-3.65	338.9	-2.63	340.8	-0.68	341.7	0.18	342.7	1.16
342	338.2	-3.8	338.4	-3.61	339.4	-2.63	341.3	-0.75	342.1	0.08	343	1.01
342.5	338.8	-3.75	338.9	-3.57	339.9	-2.62	341.7	-0.83	342.5	-0.03	343.4	0.86
343	339.3	-3.7	339.5	-3.52	340.4	-2.61	342.1	-0.9	342.9	-0.14	343.7	0.71
343.5	339.9	-3.64	340	-3.47	340.9	-2.61	342.5	-0.97	343.3	-0.25	344.1	0.56
344	340.4	-3.57	340.6	-3.42	341.4	-2.59	343	-1.04	343.6	-0.36	344.4	0.41

Ideal	k=0		k=.0002		k=.0005k		k=.0008		k=.0009		k=.001	
Output	Output	error	Output	error	Output	error	Output	error	Output	error	Output	error
344.5	341	-3.51	341.1	-3.36	341.9	-2.58	343.4	-1.11	344	-0.47	344.8	0.26
345	341.6	-3.43	341.7	-3.3	342.4	-2.56	343.8	-1.18	344.4	-0.57	345.1	0.11
345.5	342.1	-3.36	342.3	-3.23	343	-2.54	344.3	-1.24	344.8	-0.67	345.5	-0.03
346	342.7	-3.28	342.8	-3.16	343.5	-2.51	344.7	-1.3	345.2	-0.77	345.8	-0.17
346.5	343.3	-3.2	343.4	-3.09	344	-2.48	345.1	-1.36	345.6	-0.86	346.2	-0.31
347	343.9	-3.11	344	-3.01	344.6	-2.45	345.6	-1.41	346.1	-0.95	346.6	-0.44
347.5	344.5	-3.02	344.6	-2.93	345.1	-2.41	346.1	-1.45	346.5	-1.03	346.9	-0.56
348	345.1	-2.93	345.2	-2.84	345.6	-2.37	346.5	-1.49	346.9	-1.1	347.3	-0.67
348.5	345.7	-2.84	345.8	-2.75	346.2	-2.32	347	-1.52	347.3	-1.17	347.7	-0.78
349	346.3	-2.74	346.3	-2.66	346.7	-2.27	347.5	-1.55	347.8	-1.23	348.1	-0.87
349.5	346.9	-2.63	346.9	-2.57	347.3	-2.22	347.9	-1.56	348.2	-1.28	348.5	-0.96
350	347.5	-2.53	347.5	-2.47	347.8	-2.16	348.4	-1.57	348.7	-1.32	349	-1.03
350.5	348.1	-2.42	348.1	-2.37	348.4	-2.09	348.9	-1.58	349.2	-1.35	349.4	-1.1
351	348.7	-2.31	348.7	-2.26	349	-2.02	349.4	-1.57	349.6	-1.37	349.9	-1.15
351.5	349.3	-2.2	349.3	-2.16	349.6	-1.94	350	-1.55	350.1	-1.38	350.3	-1.19
352	349.9	-2.08	350	-2.05	350.1	-1.86	350.5	-1.53	350.6	-1.38	350.8	-1.21
352.5	350.5	-1.96	350.6	-1.93	350.7	-1.78	351	-1.49	351.1	-1.37	351.3	-1.23
353	351.2	-1.84	351.2	-1.82	351.3	-1.69	351.6	-1.45	351.7	-1.34	351.8	-1.23
353.5	351.8	-1.72	351.8	-1.7	351.9	-1.59	352.1	-1.39	352.2	-1.31	352.3	-1.21
354	352.4	-1.59	352.4	-1.58	352.5	-1.49	352.7	-1.33	352.7	-1.26	352.8	-1.18
354.5	353	-1.47	353	-1.46	353.1	-1.39	353.2	-1.26	353.3	-1.2	353.4	-1.14
355	353.7	-1.34	353.7	-1.33	353.7	-1.28	353.8	-1.18	353.9	-1.14	353.9	-1.09
355.5	354.3	-1.21	354.3	-1.2	354.3	-1.16	354.4	-1.09	354.4	-1.06	354.5	-1.02
356	354.9	-1.08	354.9	-1.07	355	-1.05	355	-0.99	355	-0.97	355.1	-0.94
356.5	355.6	-0.95	355.6	-0.94	355.6	-0.92	355.6	-0.89	355.6	-0.87	355.7	-0.85
357	356.2	-0.81	356.2	-0.81	356.2	-0.8	356.2	-0.78	356.2	-0.77	356.3	-0.75
357.5	356.8	-0.68	356.8	-0.68	356.8	-0.67	356.8	-0.66	356.9	-0.65	356.9	-0.64
358	357.5	-0.54	357.5	-0.54	357.5	-0.54	357.5	-0.53	357.5	-0.53	357.5	-0.53
358.5	358.1	-0.41	358.1	-0.41	358.1	-0.41	358.1	-0.4	358.1	-0.4	358.1	-0.4
359	358.7	-0.27	358.7	-0.27	358.7	-0.27	358.7	-0.27	358.7	-0.27	358.7	-0.27
359.5	359.4	-0.14	359.4	-0.14	359.4	-0.14	359.4	-0.14	359.4	-0.14	359.4	-0.14
360	360	0	360	0	360	0	360	0	360	0	360	0